Supporting Information

Evaluation of the pharmacophoric role of the O-O bond in synthetic anti-leishmanial compounds: comparison between 1,2-dioxanes and tetrahydropyrans

Margherita Ortalli,[a] Stefania Varani,[a,b] Giorgia Cimato,[a] Ruben Veronesi,[c] Arianna Quintavalla,*[,c,d] Marco Lombardo,*[,c,d] Magda Monari,[c] Claudio Trombini[c,d]

[a] Unit of Clinical Microbiology, Regional Reference Centre for Microbiological Emergencies (CRREM), St. Orsola-Malpighi University Hospital, Via Massarenti 9, 40138 Bologna, Italy.

[b] Alma Mater Studiorum - University of Bologna, Department of Experimental, Diagnostic and Specialty Medicine, Via Massarenti 9, 40138 Bologna, Italy.

[c] Alma Mater Studiorum - University of Bologna, Department of Chemistry "G. Ciamician", Via Selmi 2, 40126 Bologna, Italy.

[d] Centro Interuniversitario di Ricerca sulla Malaria (CIRM) - Italian Malaria Network (IMN), University of Milan, 20100 Milan, Italy.

Corresponding Authors:

*E-mail: arianna.quintavalla@unibo.it

*E-mail: marco.lombardo@unibo.it

List of contents:

X-ray crystallography	S3
Cis-stereopreference in tetrahydropyrans **9**	S5
Susceptibility test on *Leishmania* promastigotes with 10% FBS in the HOMEM assay medium	S6
Cytotoxicity in THP-1 cell line	S7
Effect of iron chelator DFO on bioactivity of **2b** and **3b**	S8
Effect of iron chelator DFP on bioactivity of **2a** and **3a**	S10
Calculated LogP	S12
NMR spectra	S17
HLPC analyses	S45
References	S52

X-ray crystallography

The X-ray intensity data were measured on a Bruker Apex II CCD diffractometer. Cell dimensions, and the orientation matrix were initially determined from a least-squares refinement on reflections measured in three sets of 20 exposures, collected in three different ω regions, and eventually refined against all data. A full sphere of reciprocal space was scanned by 0.3° ω steps. The software SMART[1] was used for collecting frames of data, indexing reflections and determination of lattice parameters. The collected frames were then processed for integration by the SAINT program,[1] and an empirical absorption correction was applied using SADABS.[2] The structures were solved by direct methods (SIR 2014)[3] and subsequent Fourier syntheses and refined by full-matrix least-squares on F^2 (SHELXTL),[4] using anisotropic thermal parameters for all non-hydrogen atoms. The aromatic, methylene, methine and methyl hydrogen atoms were placed in calculated positions, refined with isotropic thermal parameters *U(H)* = 1.2 *Ueq*(C) or *U(H)* = 1.5 *Ueq*(C_{methyl}) and allowed to ride on their carrier carbons. Molecular drawings were generated using Mercury.[5]

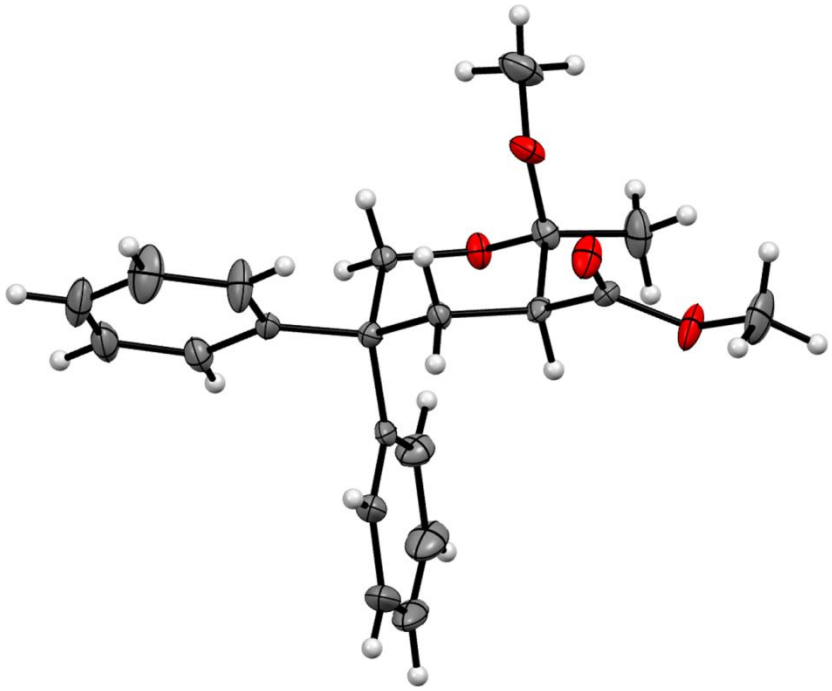

Figure S1. Determination of the relative stereochemistry of 2-methoxy tetrahydropyran **9b** through X-ray crystallographic analysis (thermal ellipsoids are drawn at 30% of the probability level).

Table S1. Crystal data and structure refinement for compound **9b**.

Compound	**9b**
Formula	$C_{21}H_{24}O_4$
Fw	340.40
T, K	296
λ, Å	0.71073
Crystal symmetry	Monoclinic
Space group	$P2_1/c$
a, Å	7.8520(7)
b, Å	19.4333(19)
c, Å	12.8156(13)
α	90
β	106.256(3)
γ	90
Cell volume, Å^3	1877.4(3)
Z	4
D_c, Mg m^{-3}	1.204
μ(Mo-K_α), mm^{-1}	0.082
F(000)	728
Crystal size/ mm	0.20 x 0.15 x 0.10
θ limits, °	1.959 - 24.999
Reflections collected	16176
Unique obs. Reflections [$F_o > 4\sigma(F_o)$]	3143 [R(int) = 0.1289]
Goodness-of-fit-on F^2	1.072
R_1 (F)[a], wR_2 (F^2)[b] [$I > 2\sigma(I)$]	0.0978, 0.2296
Largest diff. peak and hole, e. Å^{-3}	0.287 and -0.378

[a] $R_1 = \Sigma||F_o|-|F_c||/\Sigma|F_o|$.

[b] $wR_2 = [\Sigma w(F_o^2-F_c^2)^2/\Sigma w(F_o^2)^2]^{1/2}$ where $w = 1/[\sigma^2(F_o^2) + (aP)^2 + bP]$ where $P = (F_o^2 + F_c^2)/3$.

Cis-stereopreference in tetrahydropyrans 9

The favored *cis* relative stereochemistry established by X-ray crystallographic analysis for product **9b** was extended to the other tetrahydropyrans **9a** and **9c** obtained using the same stereoselective synthetic approach (Scheme S1).

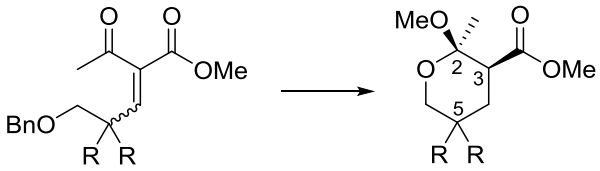

8a, R = Bu
8b, R = Ph
8c, R = Me

9a, R = Bu
9b, R = Ph
9c, R = Me

Scheme S1. Reagents and conditions: Pd/C (20% w/w), H_2 (filled balloon), MeOH, rt, 12-16 h.

In Scheme S2 we present a hypothesis which could explain the *cis*-stereopreference in the construction of tetrahydropyrans **9**.

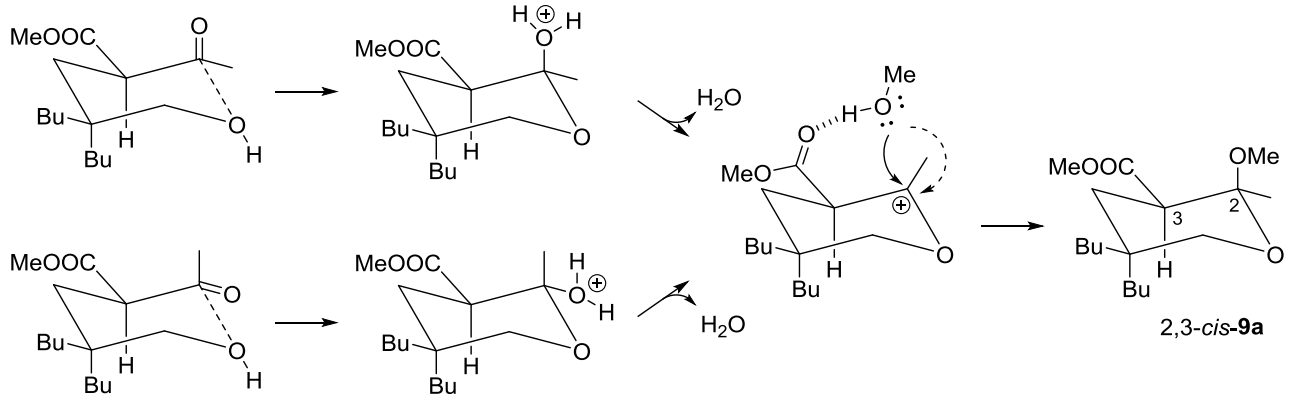

Scheme S2. Hypothesis justifying the *cis*-stereoselective synthesis of tetrahydropyran **9a**.

Susceptibility test on *Leishmania* promastigotes with 10% FBS in the HOMEM assay medium

As the 20% FBS that is employed in the assay medium is a very nutrient- and antioxidant-rich environment, which could potentially prevent a stronger activation of endoperoxides **2** in comparison to the non-peroxidic analogs **3**, we performed additional susceptibility tests for selected compounds by employing *L. donovani* cultures in HOMEM 10% FBS and we compared the results with those obtained by employing 20% FBS.

We observed a slight reduction of the IC_{50} of all the tested compounds with 10% FBS in the assay medium as compared to 20% FBS. However, the bioactivities of endoperoxides **2** and tetrahydropyrans **3** remained comparable, suggesting a not significant pharmacophoric role of the O-O bond also under these bioassay-conditions. The antioxidant-rich environment (ie 20% FBS) does not appear to play a significant role in blocking the activation of endoperoxides. We can speculate that the increased antileishmanial activity of both peroxides and tetrahydropyrans in the presence of 10% FBS can be caused by a decreased parasite vitality with lower FBS concentration.

Table S2. Inhibitory activity of tetrahydropyrans **3** and endoperoxides **2** against promastigotes of *L. donovani* in the presence of 20% FBS and 10% FBS, respectively, in the medium.

Compound	IC_{50} 20% FBS	IC_{50} 10% FBS
3a	3.4	1.9
2a	7.5	2.7
3b	5.8	3.2
2b	6.3	1.2

Cytotoxicity in THP-1 cell line

We performed additional cytotoxicity tests employing THP-1 cell line. We also calculated the corresponding selectivity indexes, as the ratio between CC_{50} of THP-1 cell line and IC_{50} on amastigotes of *L. donovani*.

We found that three compounds **3a**, **3d** and **2d** showed a slightly higher cytotoxic effect on THP-1 cells than on VERO cells. On the other hand, compounds **2a**, **3b** and **2b** showed a lower cytotoxic effect on THP-1 cells than on VERO cells; thus showing a not significant variance of selectivity index.

Table S3. Inhibitory activity of tetrahydropyrans **3** and endoperoxides **2** against amastigotes of *L. donovani*, cytotoxicity in human acute monocytic leukemia cell line (THP-1) and selectivity index (SI).

Tetrahydropyran **3**[a]	**IC_{50} (μM)**[b]	**CC_{50} (μM)**[c]	**SI**[d]	**Endoperoxide** **2**[a]	**IC_{50} (μM)**[b]	**CC_{50} (μM)**[c]	**SI**[d]
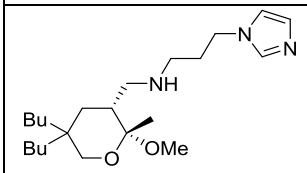 **3a**	3.4 ±0.6	26.0	7.6	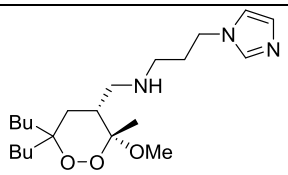 **2a**	12.2 ±1.2	86.0	7.0
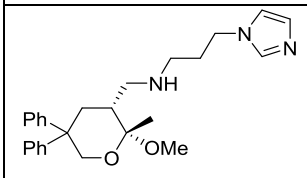 **3b**	3.2 ±0.9	50.0	15.6	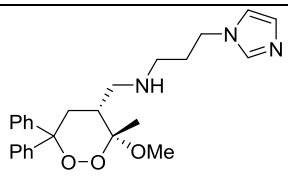 **2b**	5.0 ±1.0	52.5	10.5
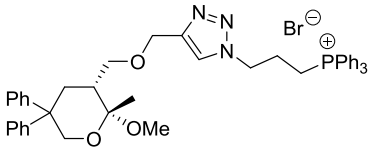 **3d**	2.8 ±0.7	64.1	22.9	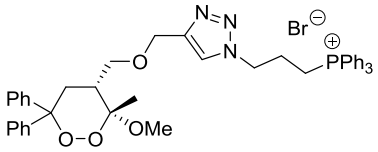 **2d**	16.5 ±1.5	142.5	8.6

[a] Compounds tested as racemates. [b] IC_{50} represents the concentration of a compound that causes 50% growth inhibition. Results represent the mean (± standard deviation, SD) of three independent experiments performed in duplicate. [c] CC_{50} represents 50% cytotoxic concentration on THP-1 cells. [d] Selectivity index (SI) = CC_{50}/IC_{50}.

Effect of iron chelator DFO on bioactivity of 2b and 3b

As for compounds **2a** and **3a,** we evaluated the bioactivity of tetrahydropyran **3b** and endoperoxide **2b** against promastigotes of *L. donovani* in the presence of the iron chelator DFO to investigate whether the IC_{50} values of these compounds were affected by the presence of DFO. The investigation was performed by co-incubating **2b** and **3b** with DFO at different concentrations (100 μM, 50 μM, 25 μM, 15 μM). Table S4 shows how the different doses of DFO don't adduct visible variation of IC_{50} of the compounds, thus confirming a scarce influence of the iron on the compound bioactivity, confirming the same behavior observed for **2a** and **3a**.

Table S4. Inhibitory activity of tetrahydropyran **3b** and endoperoxide **2b** against promastigotes of *L. donovani* in the presence or absence of the iron chelator DFO.

Compound[a]	**DFO (μM)**	**IC_{50} (μM)**[b]
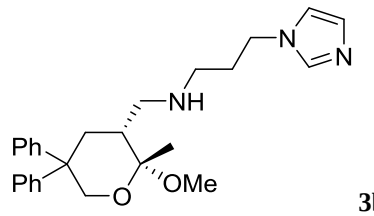 **3b**	-	6.6
	100	4.9
	50	6.6
	25	7.5
	15	7.5
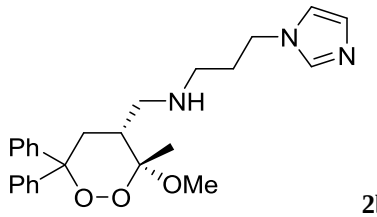 **2b**	-	7.5
	100	5.1
	50	5.5
	25	5.3
	15	6.0

[a] Compounds tested as racemates. [b] IC_{50} represents the concentration of a compound that causes 50% growth inhibition. DFO = desferrioxamine.

The isobole technique depicts synergistic (FIC values < 0.5) or antagonistic (FIC values > 4.0) interactions between DFO and the two tested compounds. Has shown in Figure S2, combination of DFO with **2b** or **3b** resulted in additive effects, since no antagonism or synergism was observed. The same trend of compounds **2a** and **3a** was confirmed.

A) **B)**

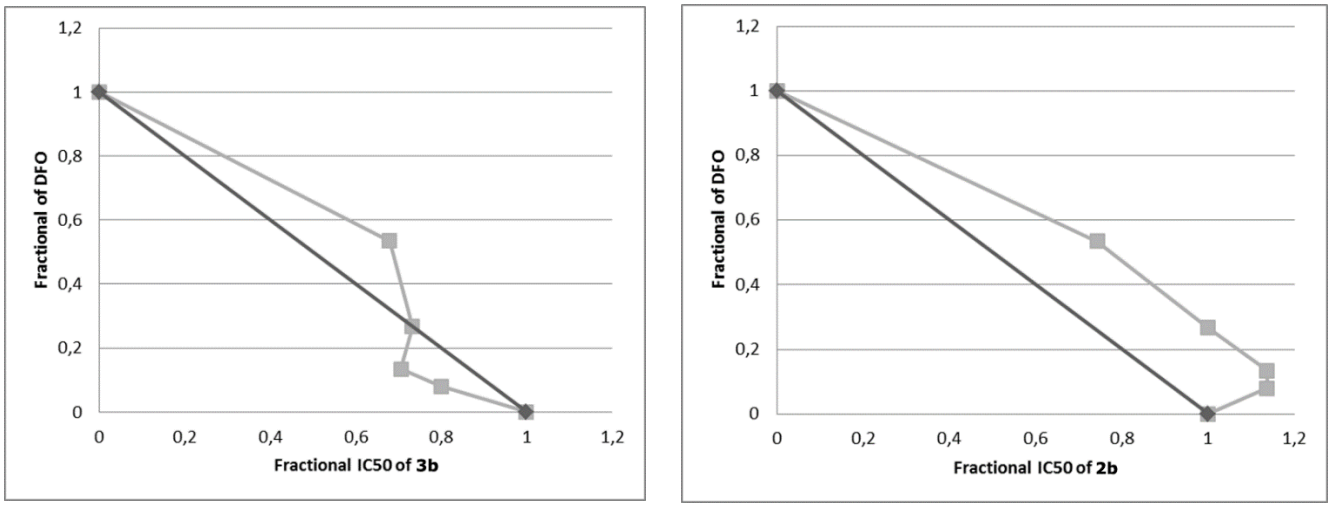

Figure S2. Isobolograms depicting the interaction of: **A**) tetrahydropyran **3b** with iron chelator DFO; **B**) endoperoxide **2b** with iron chelator DFO. Dark grey line is line of additivity. X axes depict the fractional inhibitory concentration (FIC; FIC = IC_{50} of the drug in the combination/IC_{50} of the drug when tested alone). Y axes depict the fractional of DFO. Square in the figure indicates Σ FIC values from each drug combination.

Effect of the iron chelator DFP on bioactivity of 2a and 3a

To investigate the role of iron in the activation of compounds **2a** and **3a**, we also tested these compounds against promastigotes of *L. donovani* in the presence of the iron chelator Deferiprone (DFP), which is a more lipophilic iron-chelator than DFO.

IC_{50} (DFP) = 219 μM; CC_{50} (DFP) = 143 μM.

Table S5. Inhibitory activity of tetrahydropyran **3a** and endoperoxide **2a** against promastigotes of *L. donovani* in the presence or absence of the iron chelator DFP.

Compound[a]	DFP (μM)	IC_{50} (μM)[b]
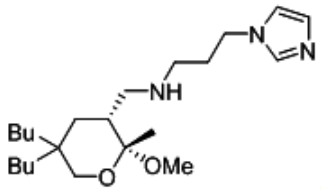 **3a**	-	3.4
	200	4
	100	6.2
	50	6.5
	25	6.1
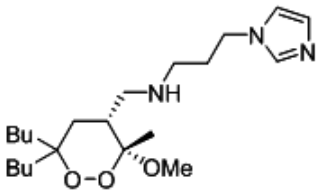 **2a**	-	7.5
	200	7.1
	100	15
	50	13.2
	25	13

[a] Compounds tested as racemates. [b] IC_{50} represents the concentration of a compound that causes 50% growth inhibition. DFP = deferiprone.

Also in this case, we observed a not significant variation of the IC_{50} values when the concentration of the iron-chelator was modified. At the highest concentration of the iron-chelator, the lowest IC_{50} was recorded, confirming the activity of these compounds even in the absence of low molecular weight iron-species.

As shown in isobolograms depicted in Figure S3, we observed a not significant variation of the IC_{50} values when the concentration of the iron-chelator increased. FIC values for both compounds are > 0.5 and < 4, therefore no antagonism or synergism was observed.

A) **B)**

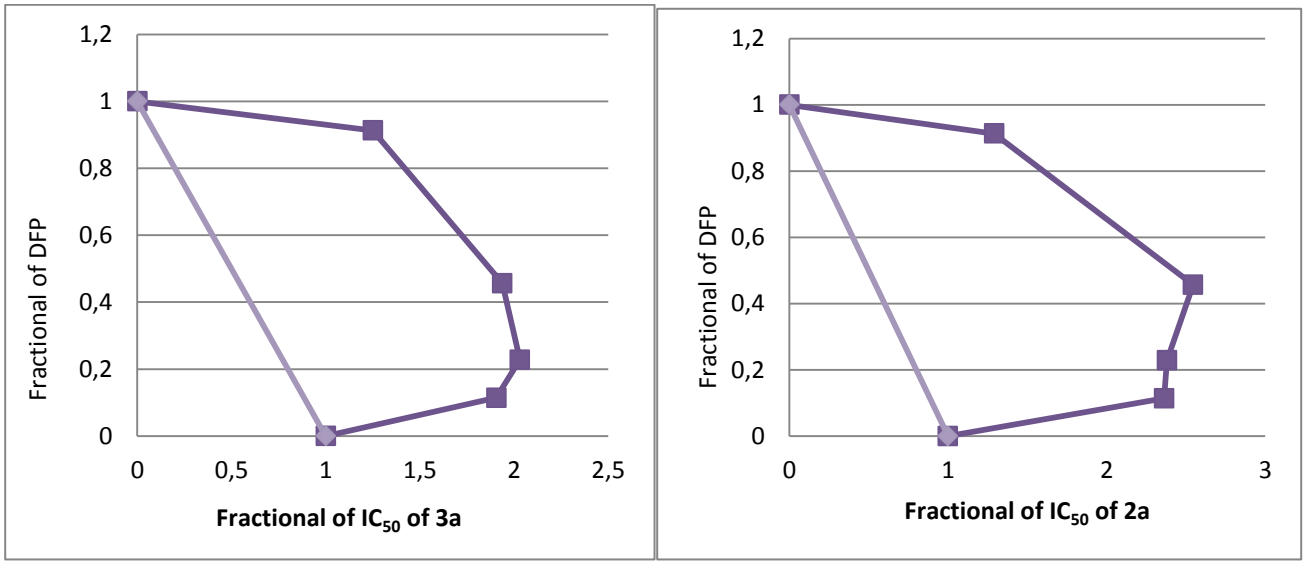

Figure S3 Isobolograms depicting the interaction of: **A**) tetrahydropyran **3a** with iron chelator DFP; **B**) endoperoxide **2a** with iron chelator DFP. Light purple line is line of additivity. X axes depict the fractional inhibitory concentration (FIC; FIC = IC_{50} of the drug in the combination/IC_{50} of the drug when tested alone). Y axes depict the fractional of DFP. Square in the figure indicates Σ FIC values from each drug combination.

Calculated LogP

The LogP values of the compounds tested on *L. donovani* promastigotes were calculated using the software ChemDraw Professional 15.0.

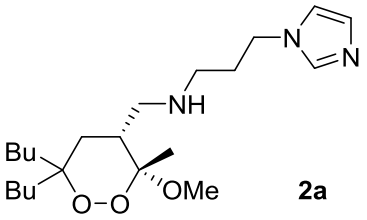

2a

```
tPSA: 55.32
CLogP: 4.2224
CMR: 11.033
LogS: -4.823
pKa: 8.677
```

```
**********************************************************************
 Estimation of logarithm of Partition Coefficient [n-Octanol/Water] Log(p)
**********************************************************************

Log(p)........:     3.48
St..deviation.:     0.47
by Crippen's fragmentation: J.Chem.Inf.Comput.Sci.,27,21(1987).

Log(p)........:     3.38
St..deviation.:     0.49
by Viswanadhan's fragmentation: J.Chem.Inf.Comput.Sci.,29,163(1989).
```

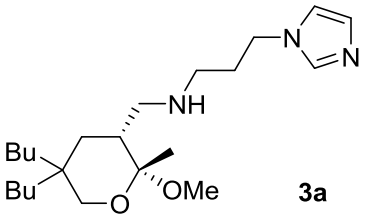

3a

```
tPSA: 46.09
CLogP: 4.5434
CMR: 11.2167
LogS: -5.023
pKa: 9.165
```

```
**********************************************************************
 Estimation of logarithm of Partition Coefficient [n-Octanol/Water] Log(p)
**********************************************************************

Log(p)........:     3.81
St..deviation.:     0.47
by Crippen's fragmentation: J.Chem.Inf.Comput.Sci.,27,21(1987).

Log(p)........:     3.68
St..deviation.:     0.49
by Viswanadhan's fragmentation: J.Chem.Inf.Comput.Sci.,29,163(1989).
```

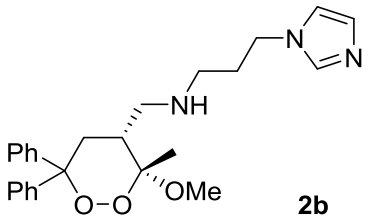

2b

tPSA: 55.32

CLogP: 3.1264

CMR: 12.345

LogS: -5.604

pKa: 8.584

```
*********************************************************************************
 Estimation of logarithm of Partition Coefficient [n-Octanol/Water] Log(p)
*********************************************************************************

Log(p)........:     3.63
St..deviation.:     0.47
by Crippen's fragmentation: J.Chem.Inf.Comput.Sci.,27,21(1987).

Log(p)........:     3.73
St..deviation.:     0.49
by Viswanadhan's fragmentation: J.Chem.Inf.Comput.Sci.,29,163(1989).
```

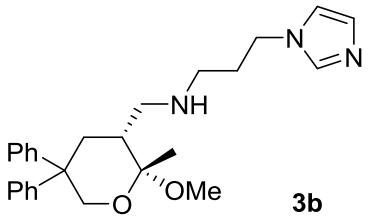

3b

tPSA: 46.09

CLogP: 3.4474

CMR: 12.5287

LogS: -5.546

pKa: 9.079

```
*********************************************************************************
 Estimation of logarithm of Partition Coefficient [n-Octanol/Water] Log(p)
*********************************************************************************

Log(p)........:     3.69
St..deviation.:     0.47
by Crippen's fragmentation: J.Chem.Inf.Comput.Sci.,27,21(1987).

Log(p)........:     3.74
St..deviation.:     0.49
by Viswanadhan's fragmentation: J.Chem.Inf.Comput.Sci.,29,163(1989).
```

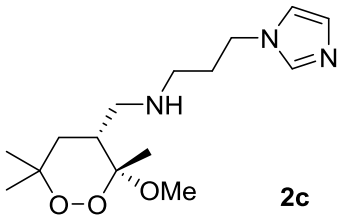

2c

tPSA: 55.32

CLogP: 1.0484

CMR: 8.2502

LogS: -2.624

pKa: 8.669

```
*********************************************************************************
 Estimation of logarithm of Partition Coefficient [n-Octanol/Water] Log(p)
*********************************************************************************

Log(p).........:     0.84
St..deviation.:      0.47
by Crippen's fragmentation: J.Chem.Inf.Comput.Sci.,27,21(1987).

Log(p).........:     0.86
St..deviation.:      0.49
by Viswanadhan's fragmentation: J.Chem.Inf.Comput.Sci.,29,163(1989).
```

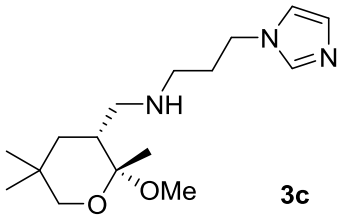

3c

tPSA: 46.09

CLogP: 1.3694

CMR: 8.4339

LogS: -2.521

pKa: 9.157

```
*********************************************************************************
 Estimation of logarithm of Partition Coefficient [n-Octanol/Water] Log(p)
*********************************************************************************

Log(p).........:     1.31
St..deviation.:      0.47
by Crippen's fragmentation: J.Chem.Inf.Comput.Sci.,27,21(1987).

Log(p).........:     1.30
St..deviation.:      0.49
by Viswanadhan's fragmentation: J.Chem.Inf.Comput.Sci.,29,163(1989).
```

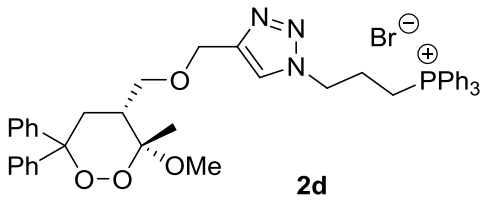

2d

tPSA: 64.88
CLogP: 8.7696
CMR: 20.95
LogS: -11.27
pKa: N/A

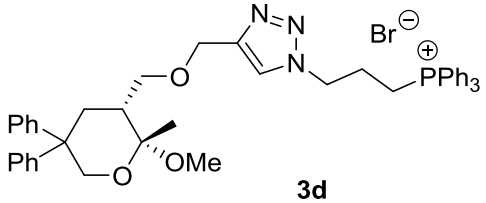

3d

tPSA: 55.65
CLogP: 9.0906
CMR: 21.1337
LogS: -11.2
pKa: N/A

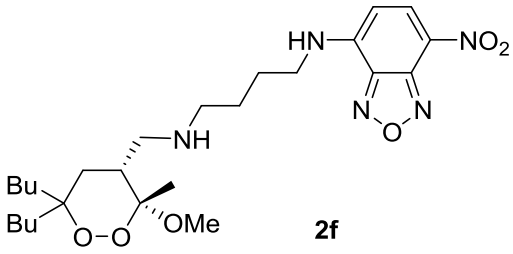

2f

tPSA: 137.51
CLogP: 6.3691
CMR: 13.7383
LogS: -7.214
pKa: 9.039

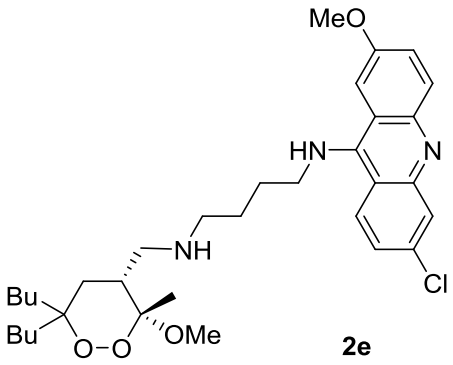

2e

tPSA: 73.34

CLogP: 9.25217

CMR: 16.9203

LogS: -9.049

pKa: 9.029

```
**********************************************************************************
 Estimation of logarithm of Partition Coefficient [n-Octanol/Water] Log(p)
**********************************************************************************

Log(p).........:     7.83
St..deviation.:      0.47
by Crippen's fragmentation: J.Chem.Inf.Comput.Sci.,27,21(1987).

Log(p).........:     7.68
St..deviation.:      0.49
by Viswanadhan's fragmentation: J.Chem.Inf.Comput.Sci.,29,163(1989).
```

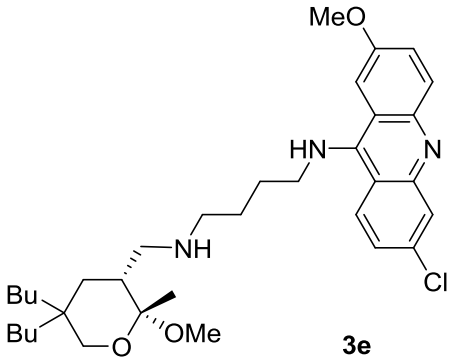

3e

tPSA: 64.11

CLogP: 9.57317

CMR: 17.104

LogS: -9.212

pKa: 9.518

```
**********************************************************************************
 Estimation of logarithm of Partition Coefficient [n-Octanol/Water] Log(p)
**********************************************************************************

Log(p).........:     8.16
St..deviation.:      0.47
by Crippen's fragmentation: J.Chem.Inf.Comput.Sci.,27,21(1987).

Log(p).........:     7.97
St..deviation.:      0.49
by Viswanadhan's fragmentation: J.Chem.Inf.Comput.Sci.,29,163(1989).
```

NMR spectra

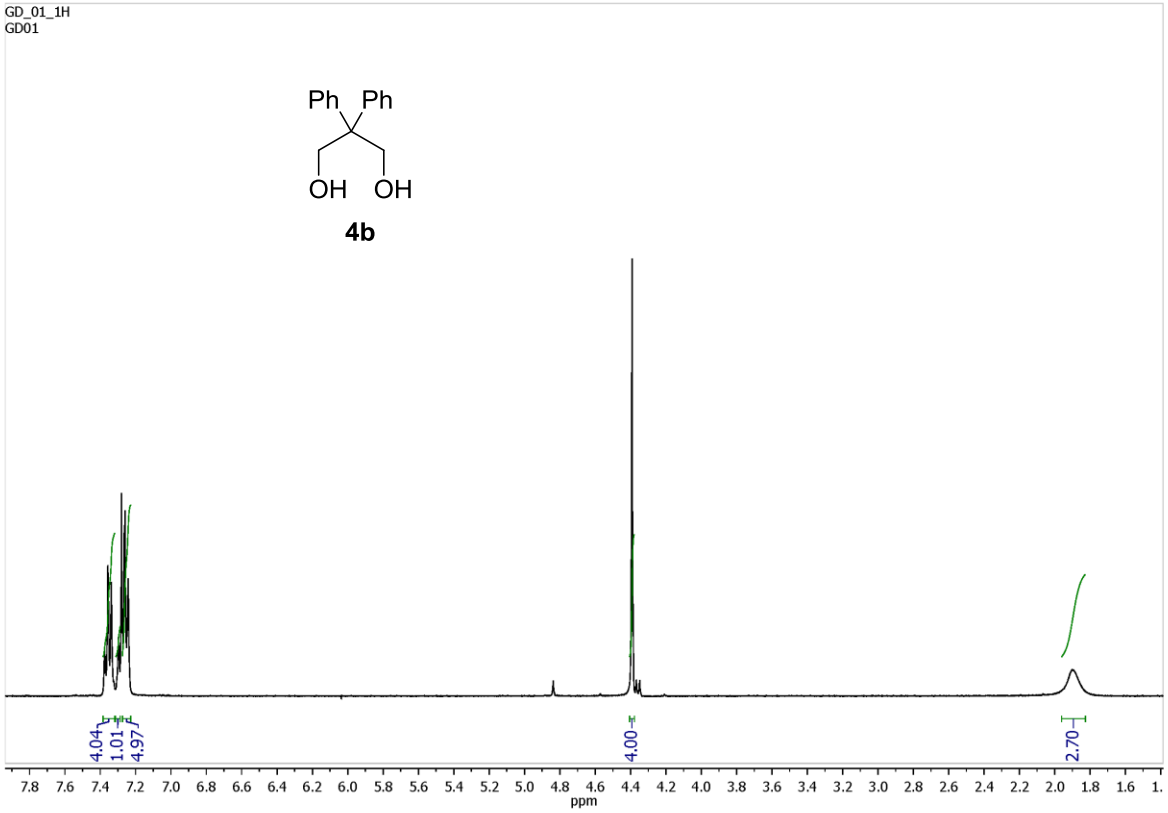
GD_01_1H
GD01
Ph Ph
OH OH
4b
4.04
1.01
4.97
4.00
2.70
ppm

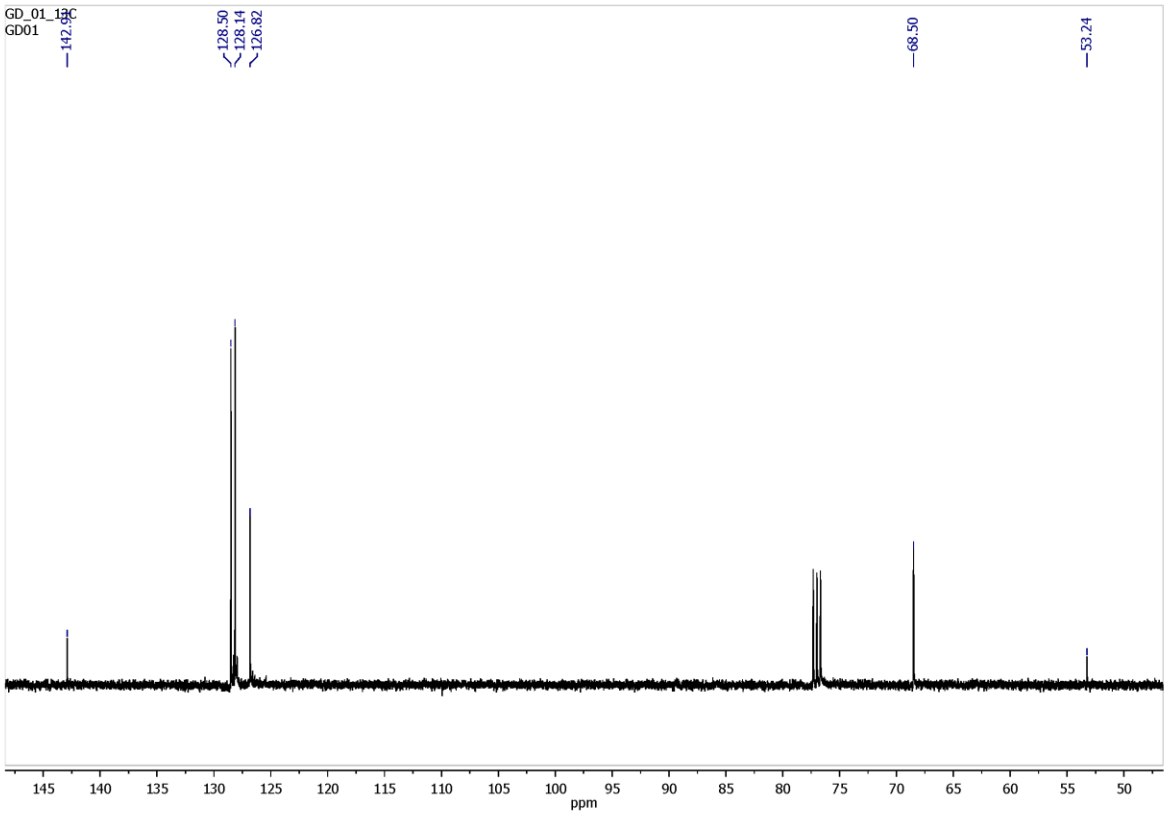
GD_01_13C
GD01
142.96
128.50
128.14
126.82
68.50
53.24
ppm

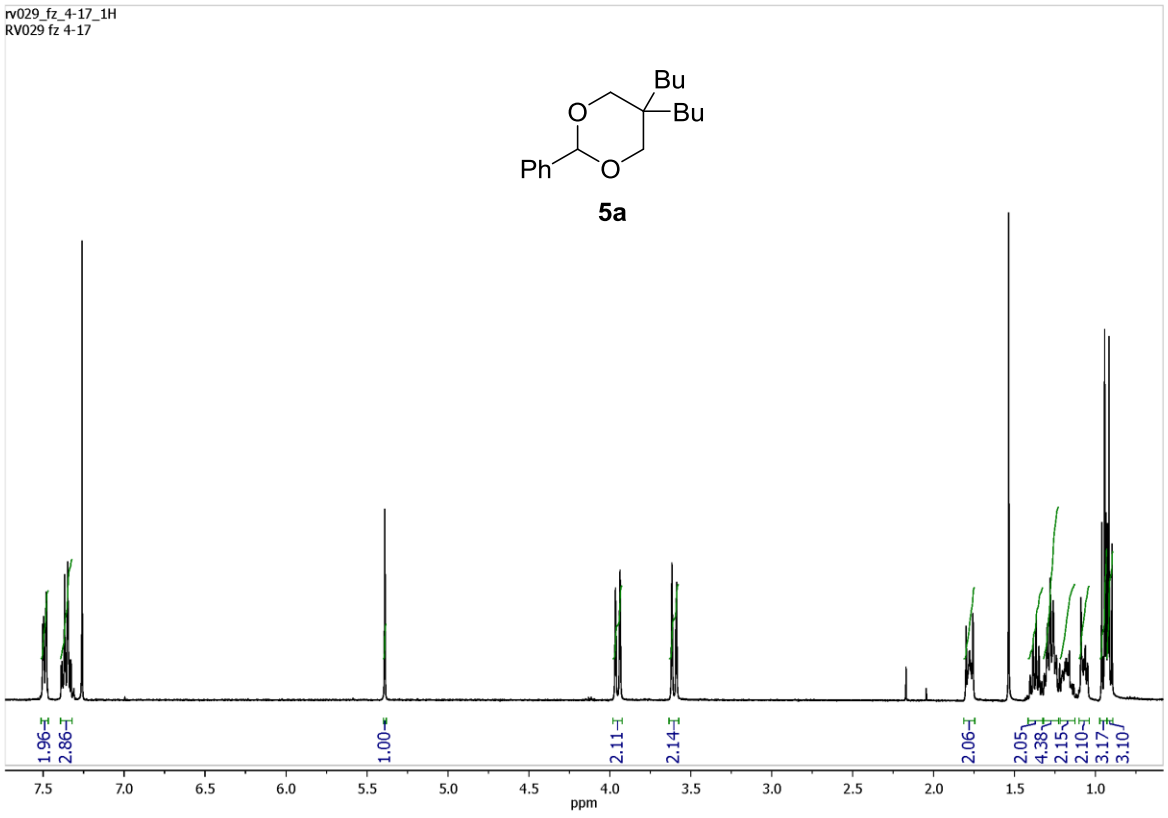
rv029_fz_4-17_1H
RV029 fz 4-17
Bu
Bu
O
O
Ph
5a
1.96
2.86
1.00
2.11
2.14
2.06
2.05
4.38
2.15
2.10
3.17
3.10
7.5
7.0
6.5
6.0
5.5
5.0
4.5
4.0
3.5
3.0
2.5
2.0
1.5
1.0
ppm

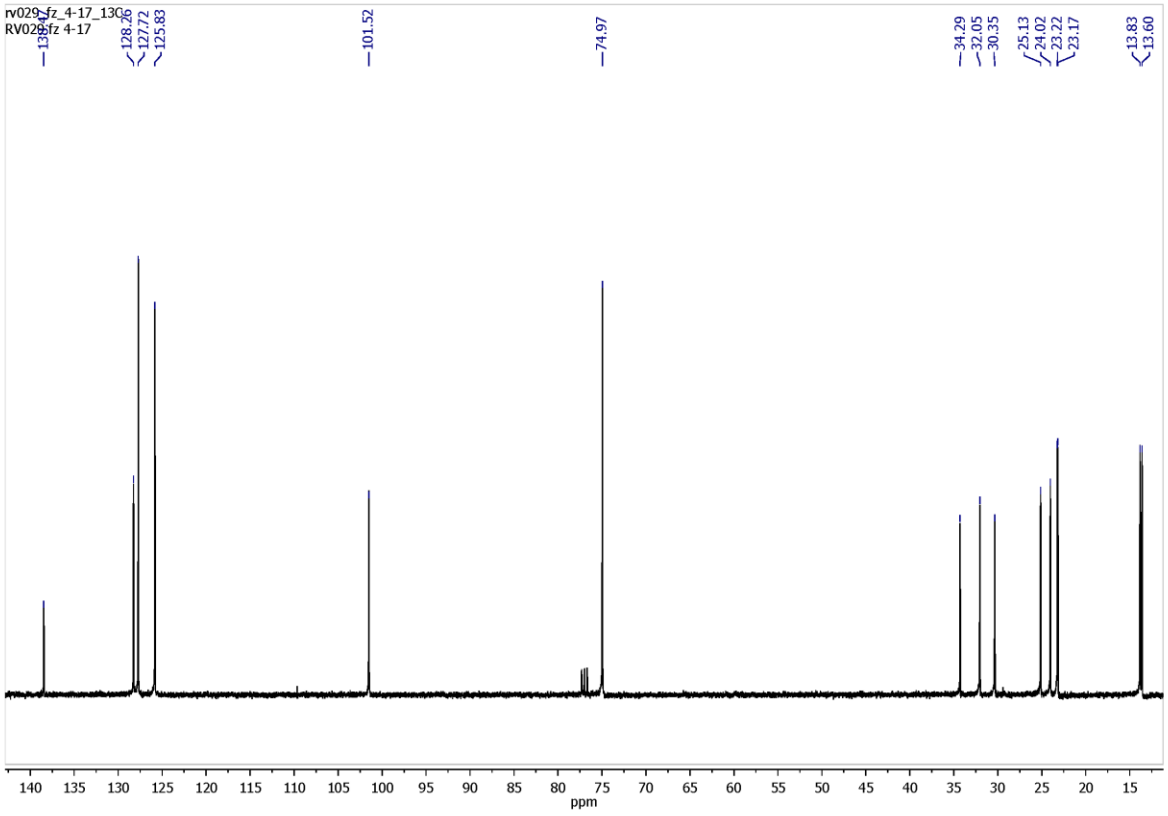
rv029_fz_4-17_13C
RV029 fz 4-17
138.47
128.26
127.72
125.83
101.52
74.97
34.29
32.05
30.35
25.13
24.02
23.22
23.17
13.83
13.60
140
135
130
125
120
115
110
105
100
95
90
85
80
75
70
65
60
55
50
45
40
35
30
25
20
15
ppm

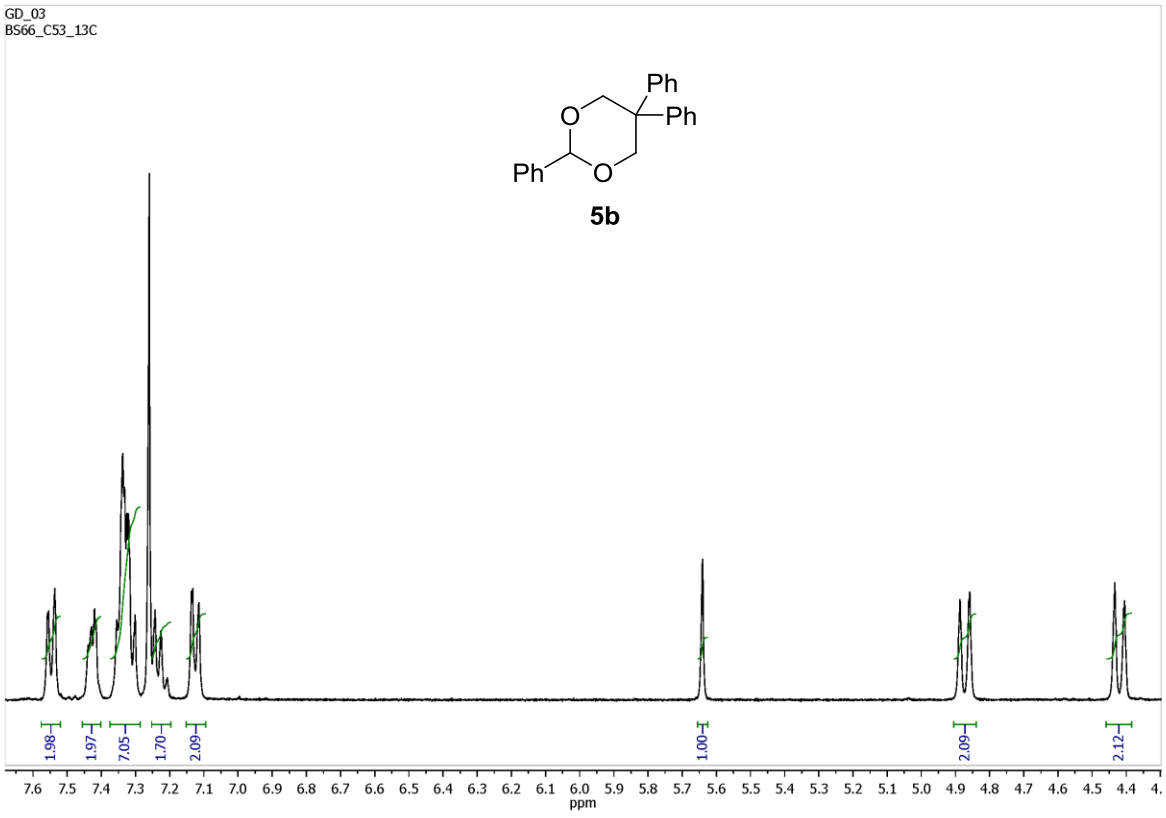
GD_03
BS66_C53_13C
Ph
O
Ph
Ph
O
1.98
1.97
7.05
1.70
2.09
1.00
2.09
2.12
ppm

5b

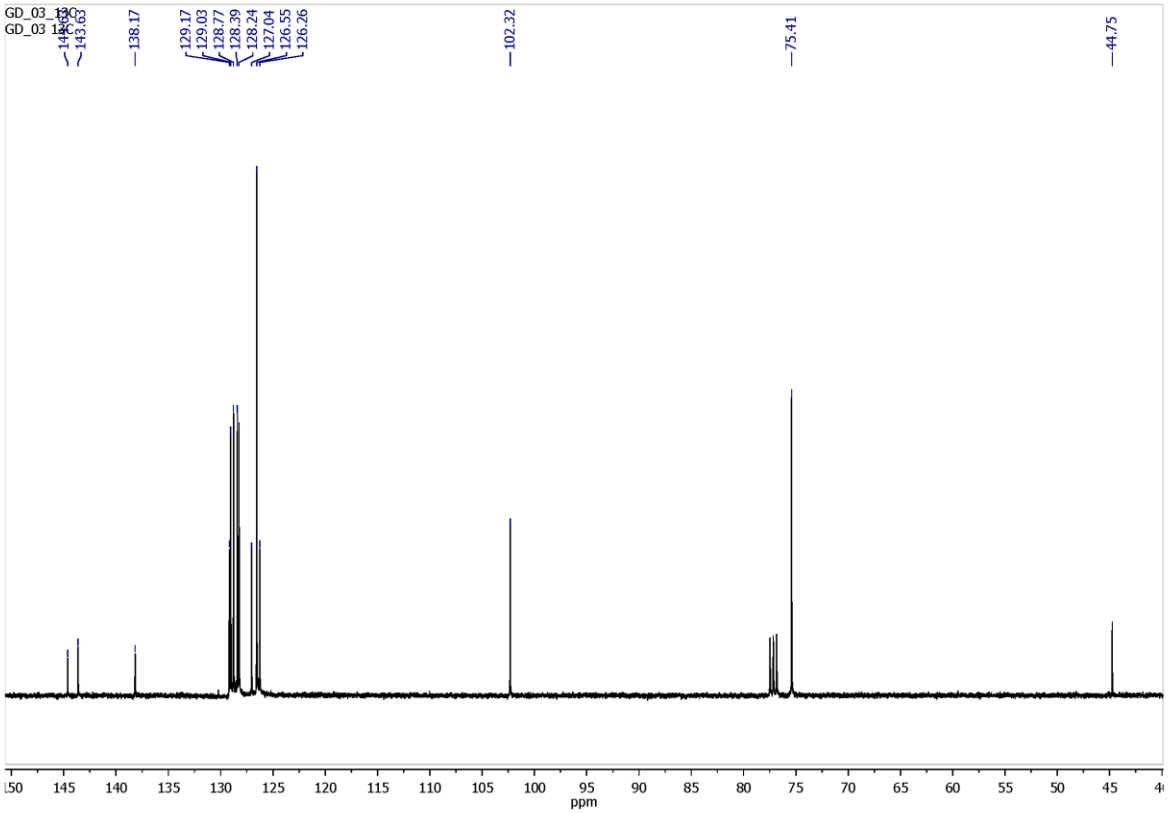
GD_03_13C
GD_03_13C
143.63
138.17
129.17
129.03
128.77
128.39
128.24
127.04
126.55
126.26
102.32
75.41
44.75
ppm

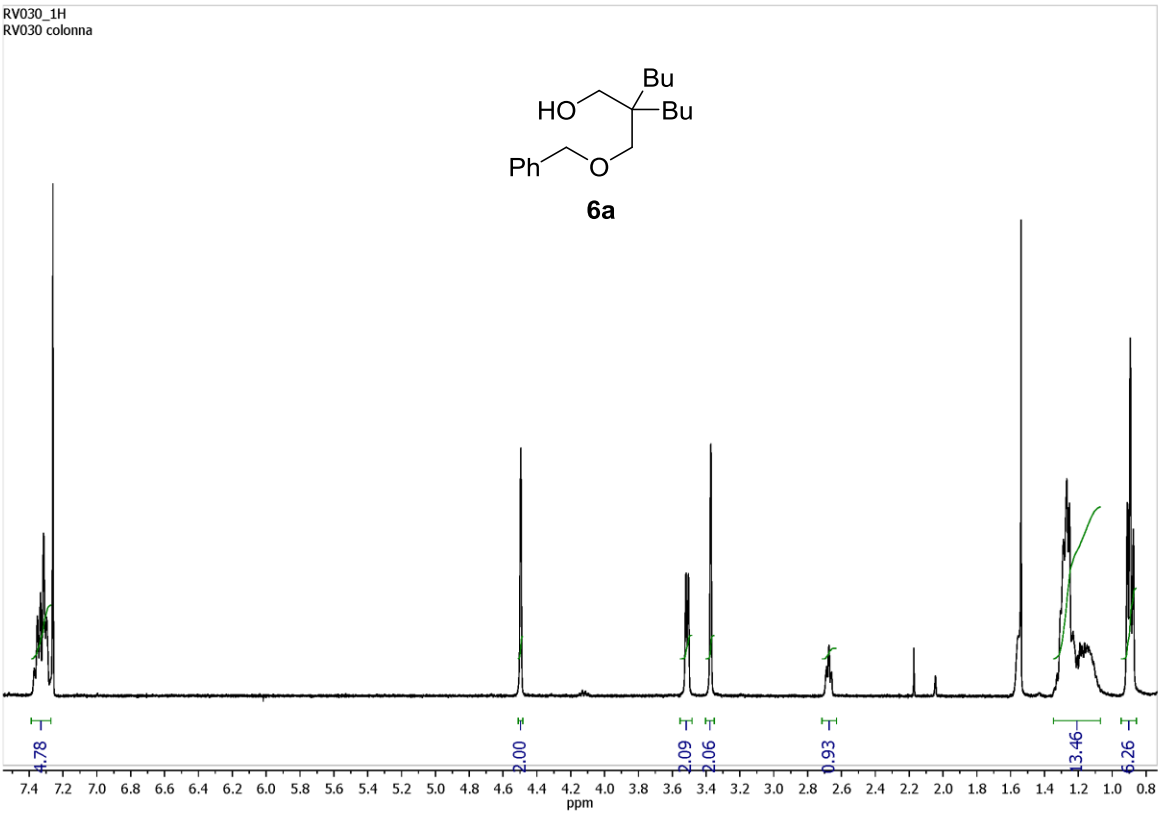
RV030_1H
RV030 colonna
Bu
HO
Bu
Ph
O
6a
4.78
2.00
2.09
2.06
0.93
13.46
6.26
ppm

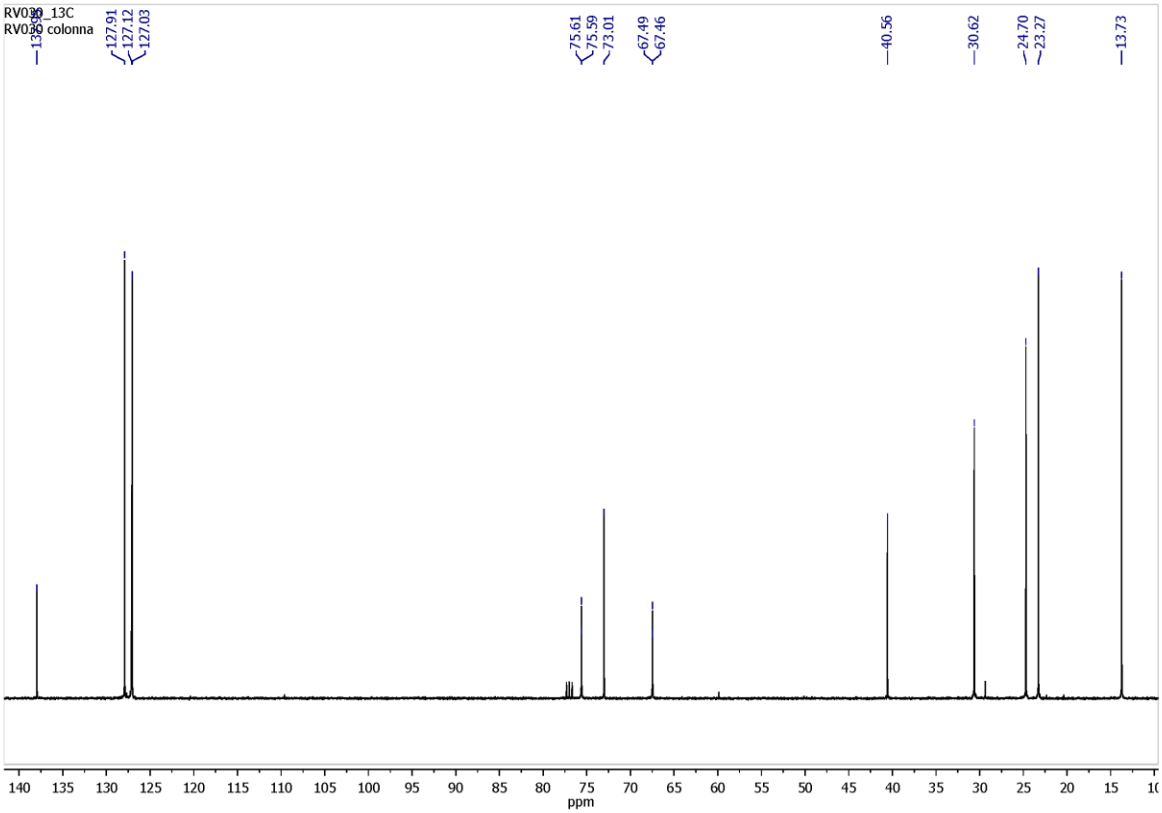
RV030_13C
RV030 colonna
127.91
127.12
127.03
75.61
75.59
73.01
67.49
67.46
40.56
30.62
24.70
23.27
13.73
ppm

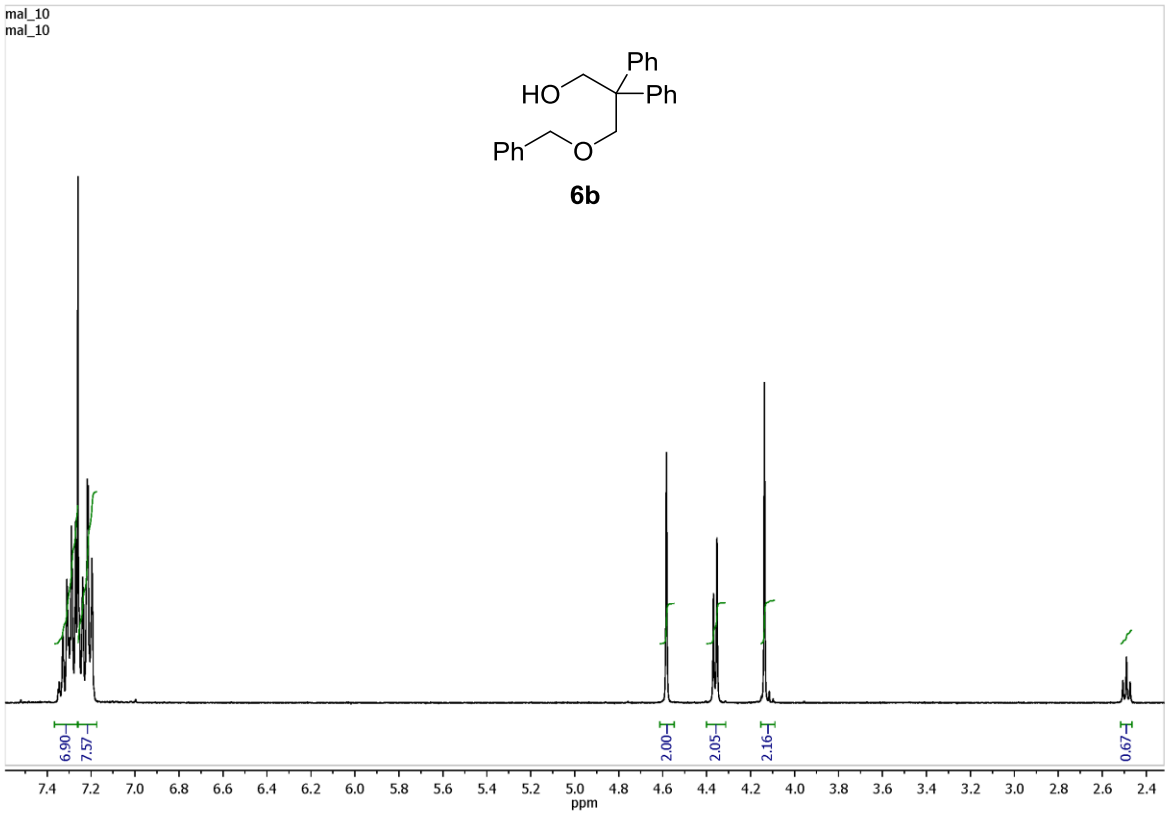
mal_10
mal_10
HO
Ph
Ph
Ph
O
6b
6.90
7.57
2.00
2.05
2.16
0.67
ppm

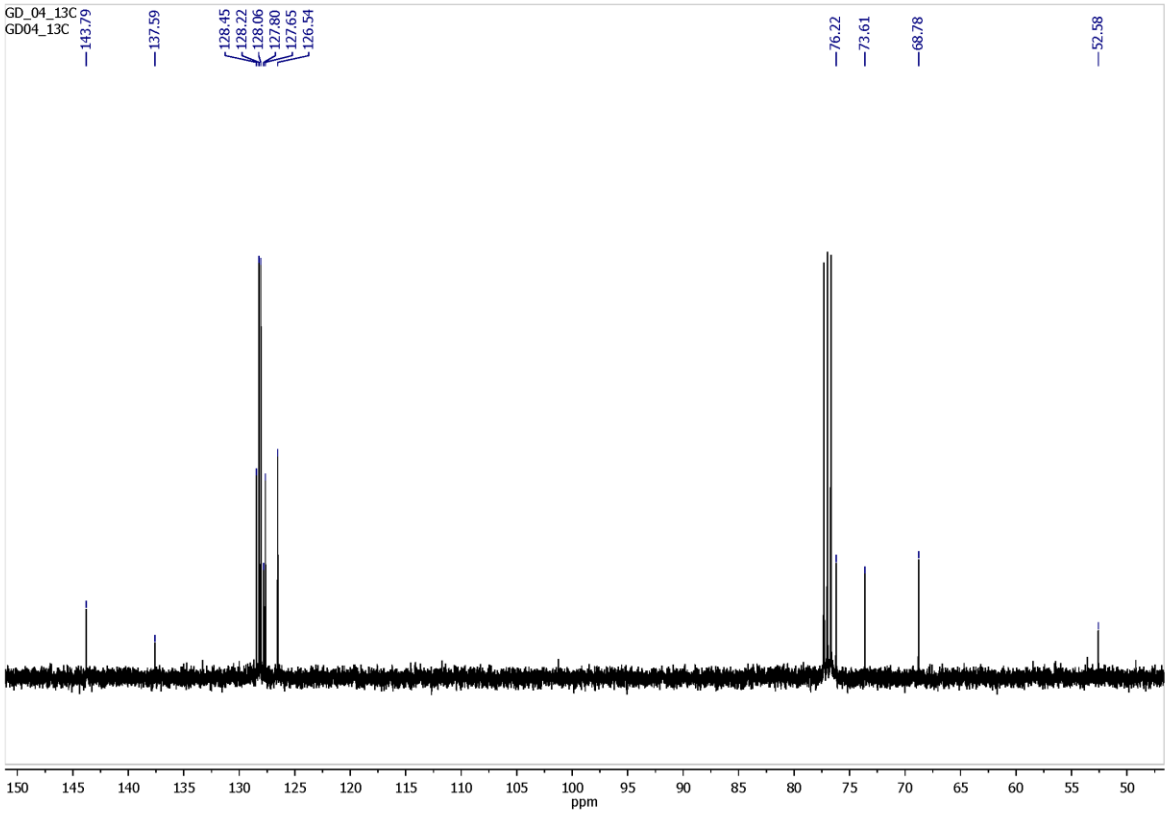
GD_04_13C
GD04_13C
143.79
137.59
128.45
128.22
128.06
127.80
127.65
126.54
76.22
73.61
68.78
52.58
ppm

RV031_colo_1h
RV031_colo_1H

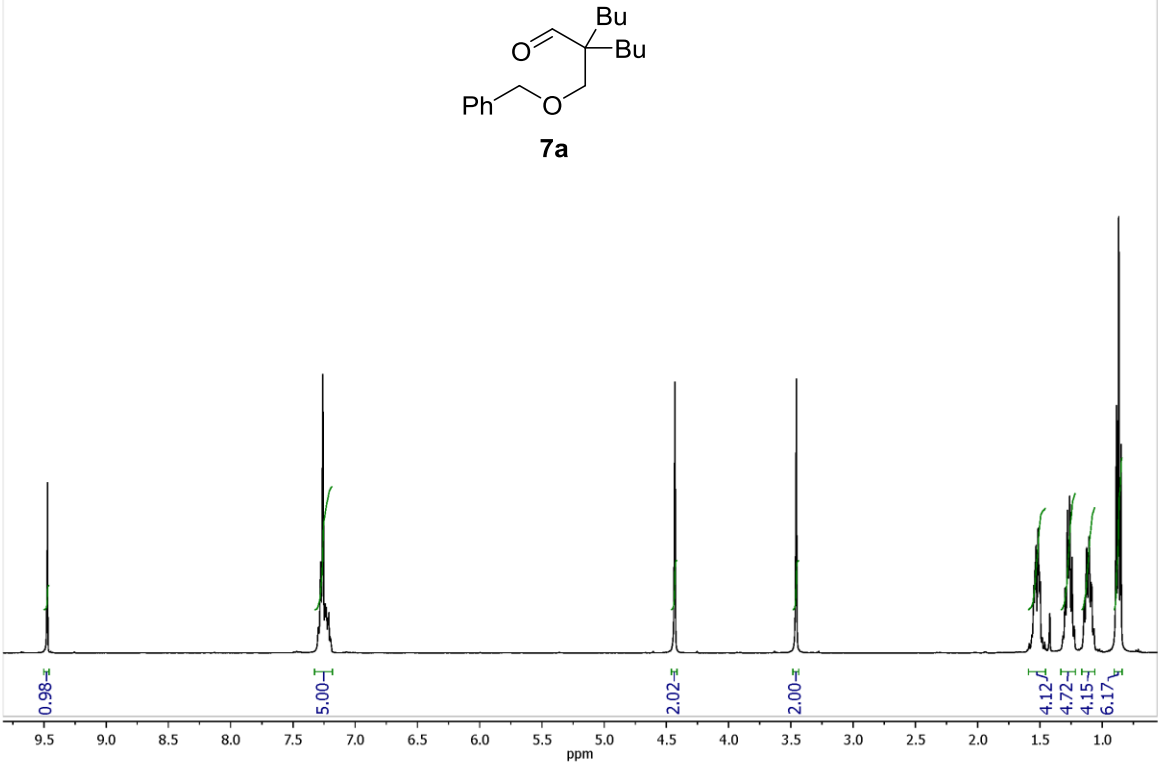

7a

RV031_colo_13C
RV031_colo_13C

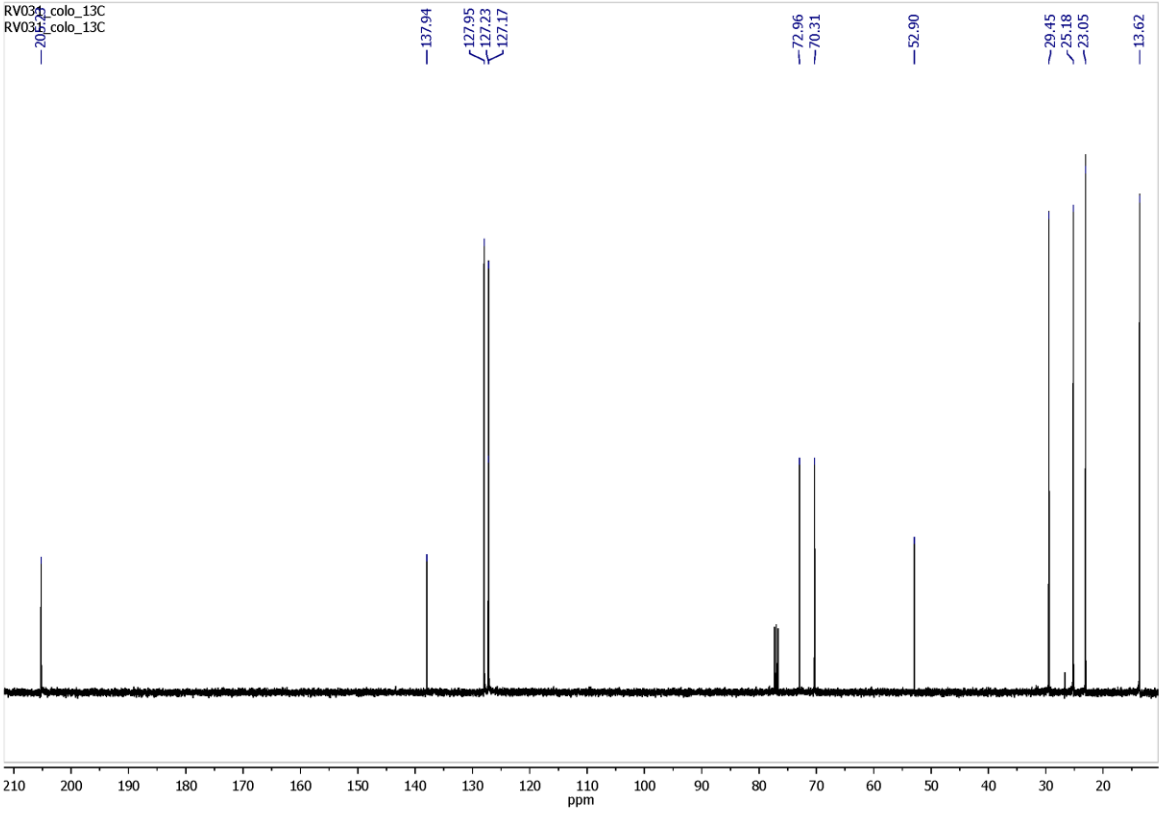

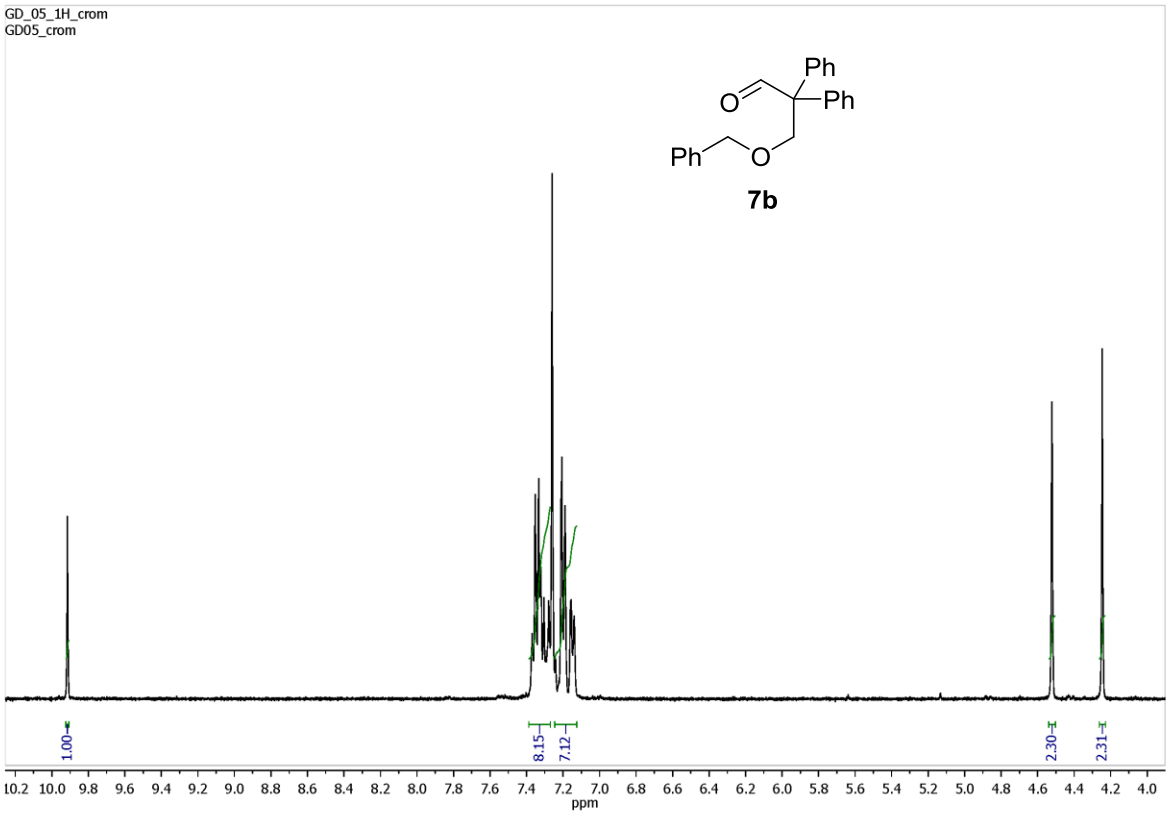
GD_05_1H_crom
GD05_crom
Ph
Ph
O
Ph
O
7b
1.00
8.15
7.12
2.30
2.31
ppm

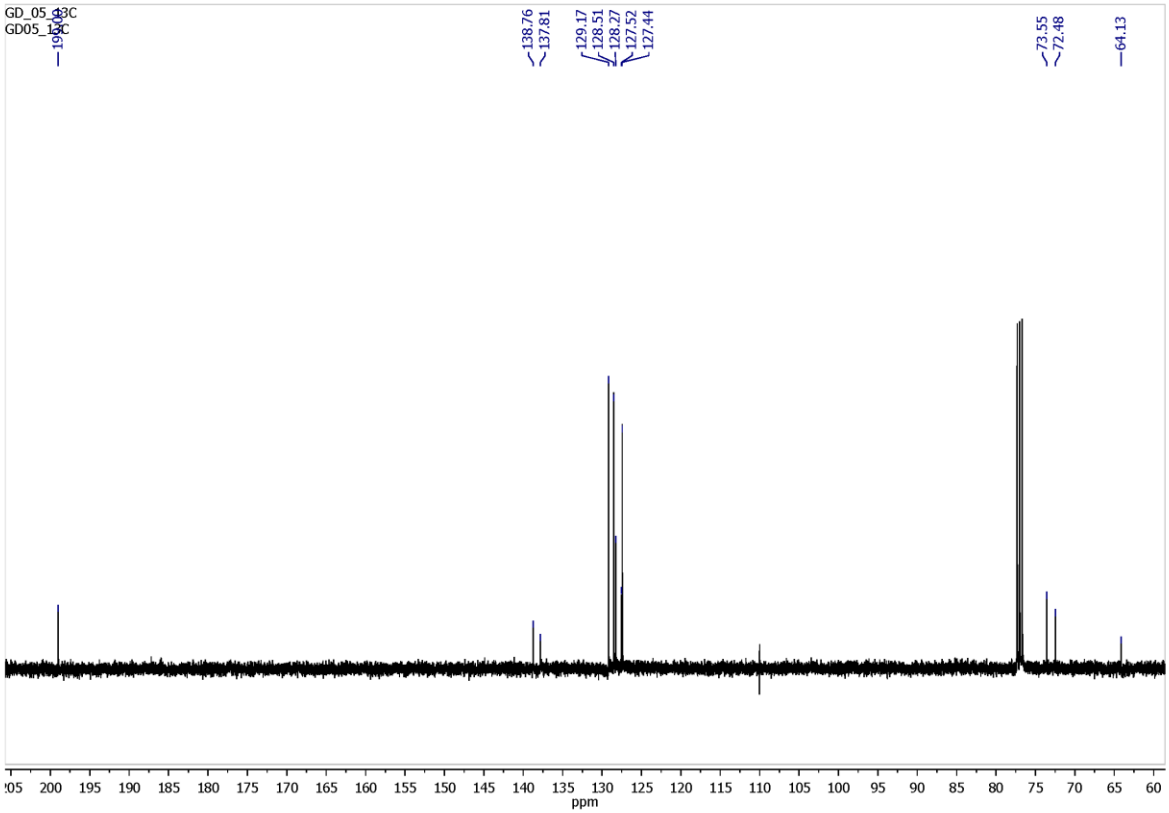
GD_05_13C
GD05_13C
138.76
137.81
129.17
128.51
128.27
127.52
127.44
73.55
72.48
64.13
ppm

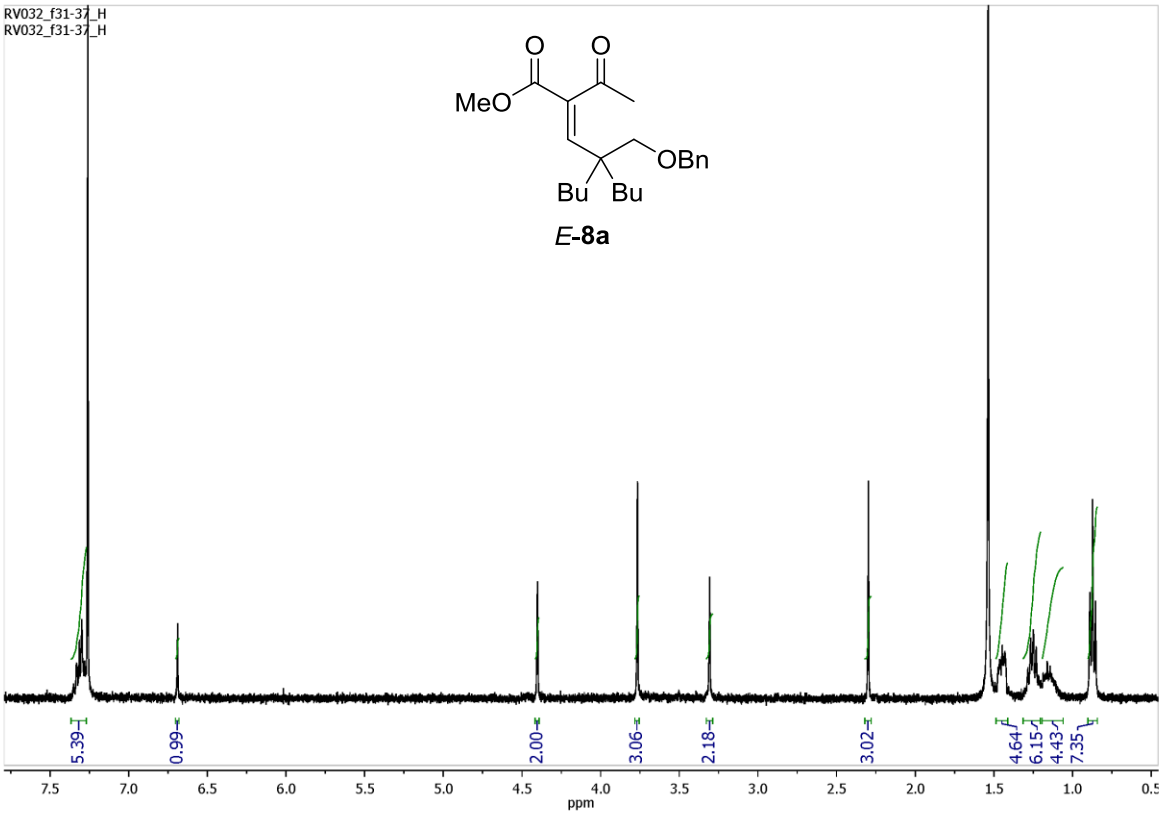
RV032_f31-37_H
RV032_f31-37_H
O
O
MeO
OBn
Bu
Bu
5.39
0.99
2.00
3.06
2.18
3.02
4.64
6.15
4.43
7.35
7.5
7.0
6.5
6.0
5.5
5.0
4.5
4.0
3.5
3.0
2.5
2.0
1.5
1.0
0.5
ppm

E-**8a**

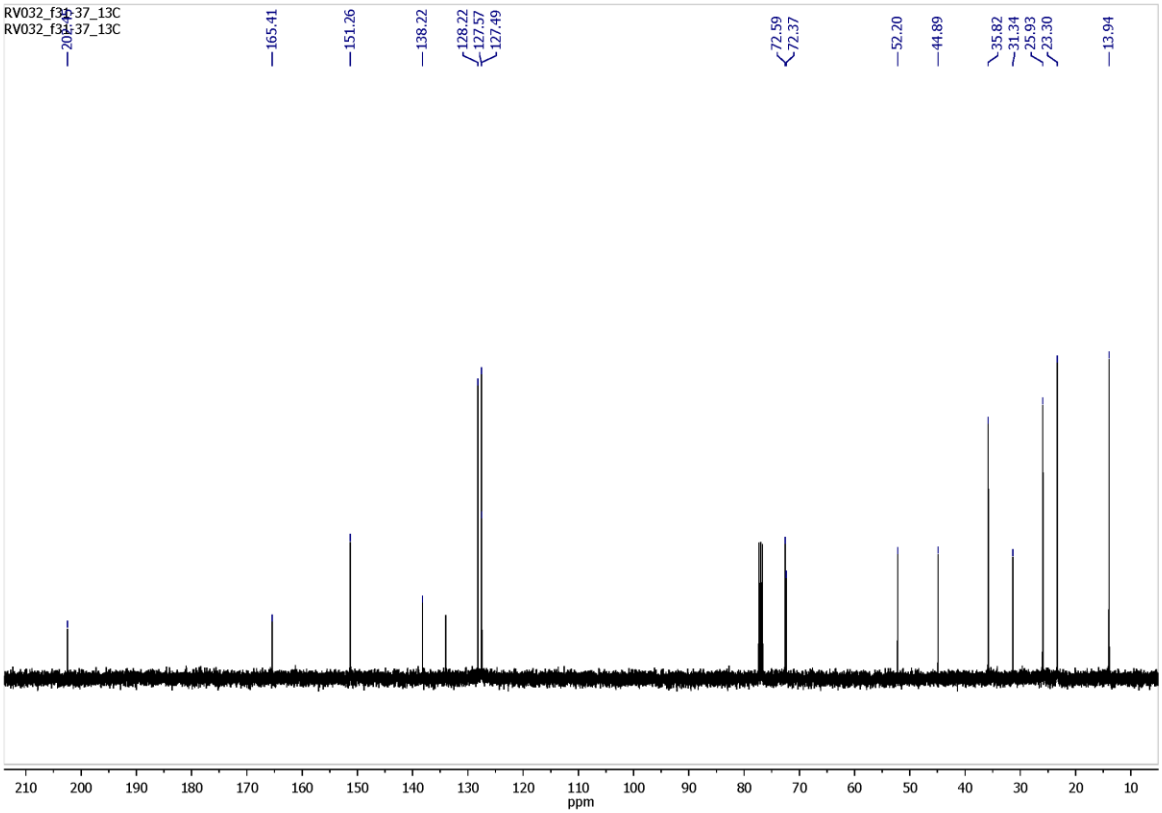
RV032_f31-37_13C
RV032_f31-37_13C
165.41
151.26
138.22
128.22
127.57
127.49
72.59
72.37
52.20
44.89
35.82
31.34
25.93
23.30
13.94
210
200
190
180
170
160
150
140
130
120
110
100
90
80
70
60
50
40
30
20
10
ppm

^{1}H NOEDIFF NMR analysis.

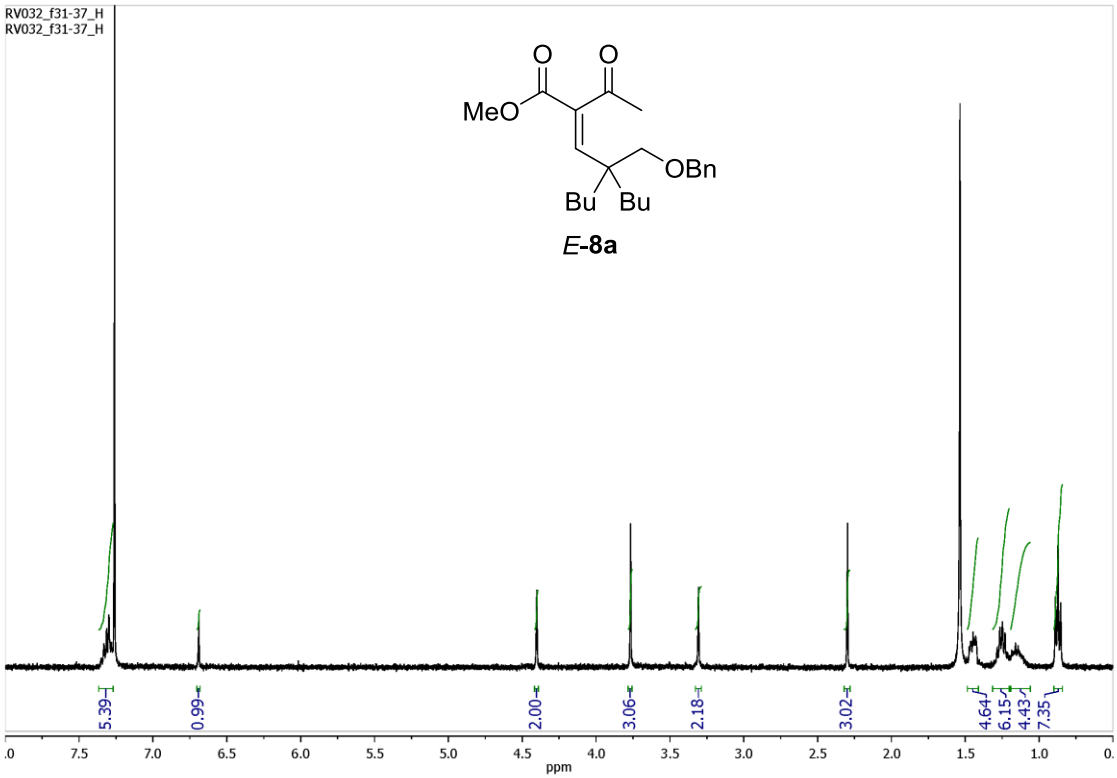

E-**8a**

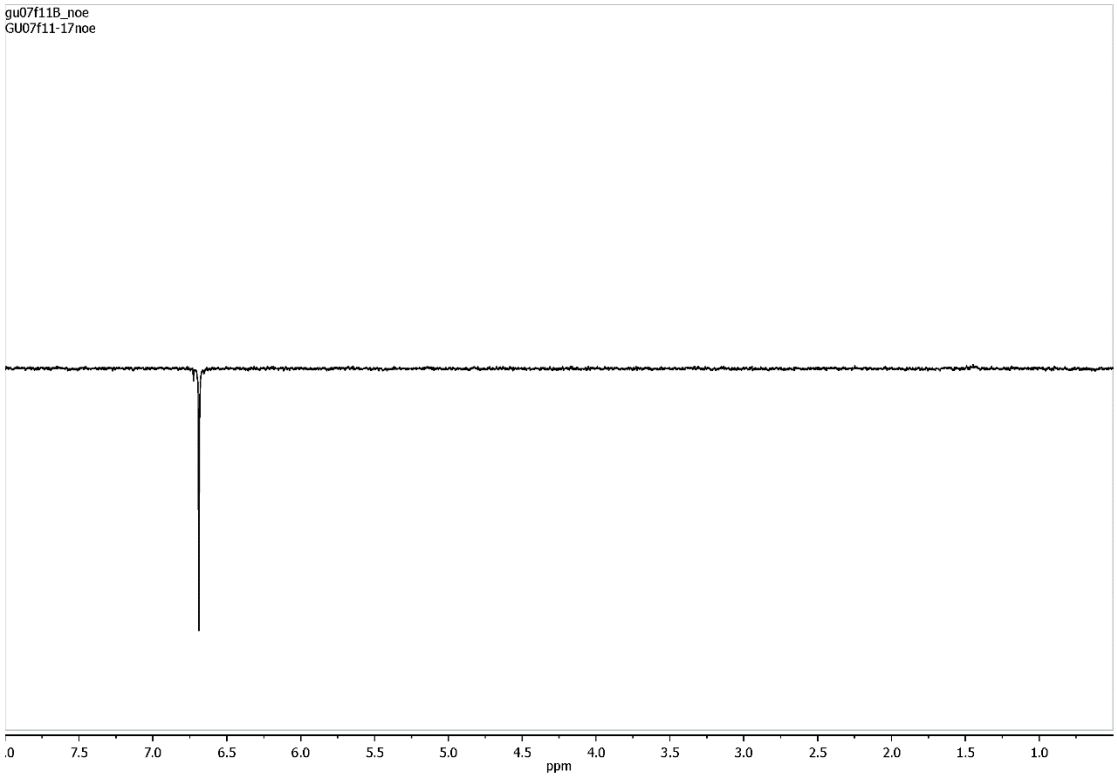

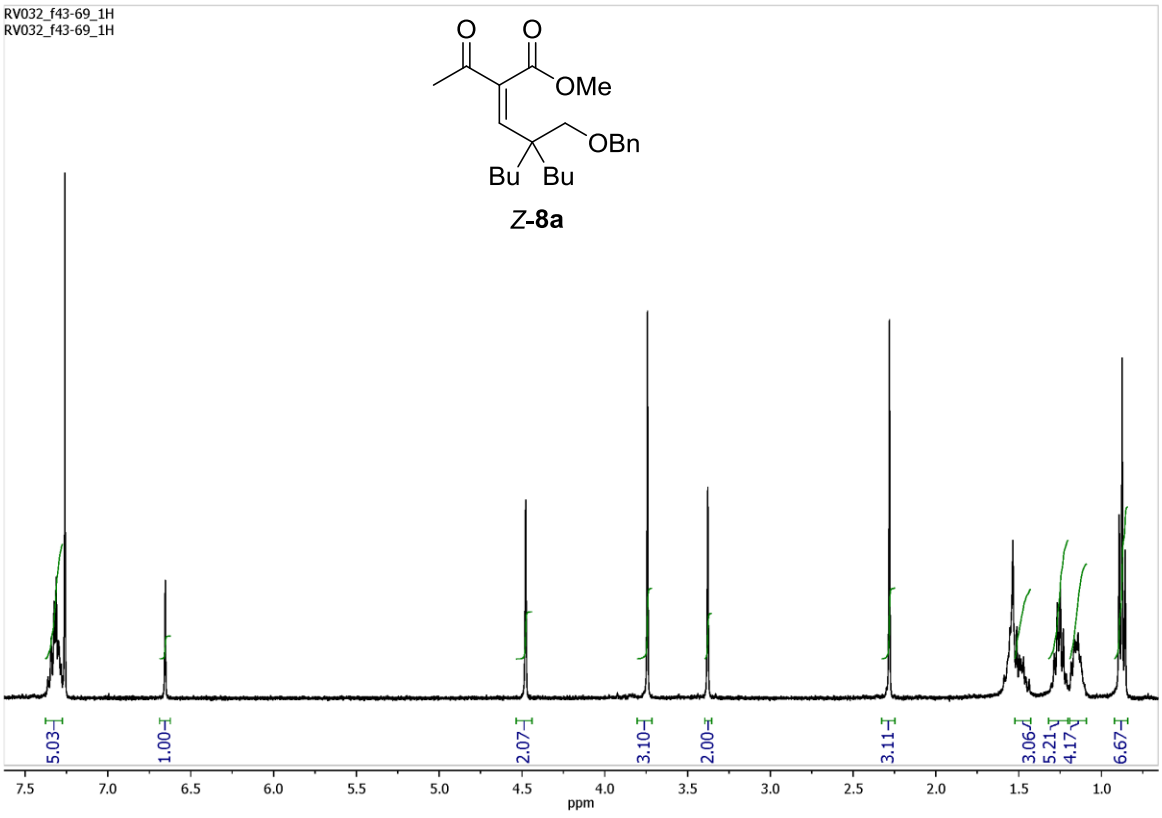
RV032_f43-69_1H
RV032_f43-69_1H
O
O
OMe
OBn
Bu
Bu
5.03
1.00
2.07
3.10
2.00
3.11
3.06
5.21
4.17
6.67
7.5
7.0
6.5
6.0
5.5
5.0
4.5
4.0
3.5
3.0
2.5
2.0
1.5
1.0
ppm

Z-**8a**

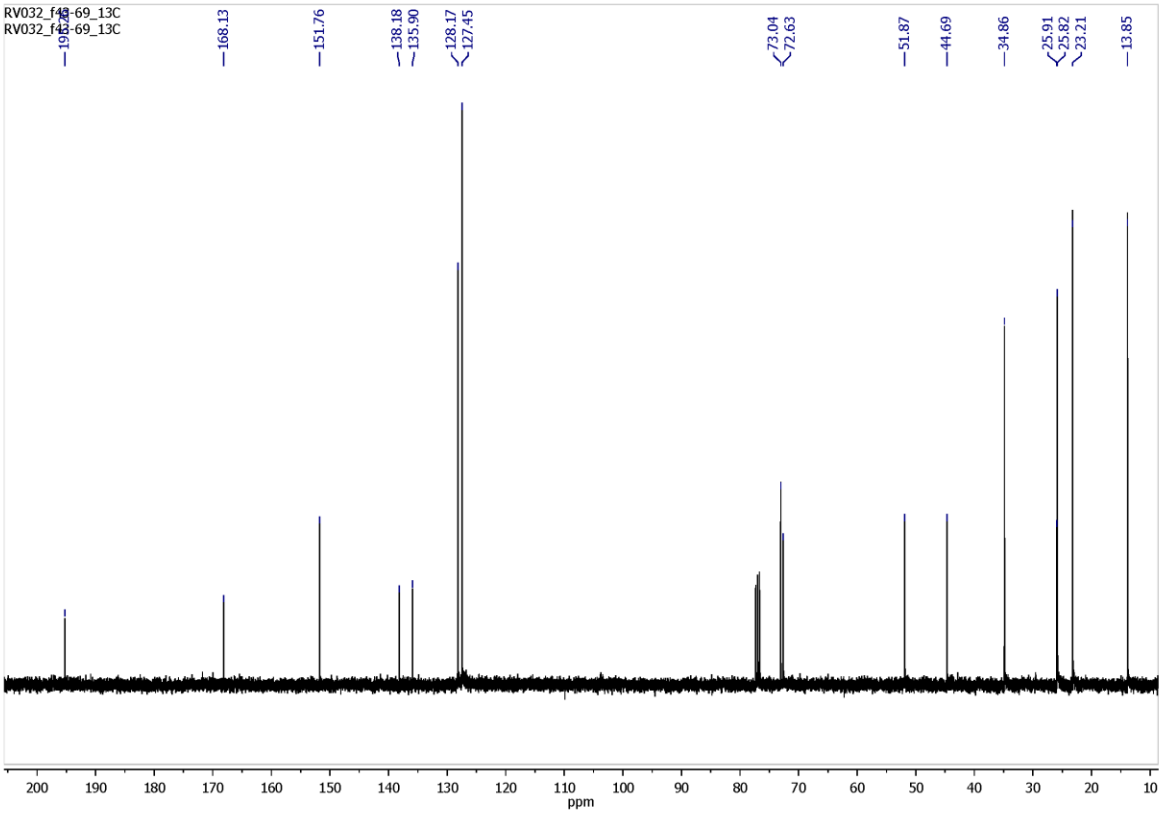
RV032_f43-69_13C
RV032_f43-69_13C
168.13
151.76
138.18
135.90
128.17
127.45
73.04
72.63
51.87
44.69
34.86
25.91
25.82
23.21
13.85
200
190
180
170
160
150
140
130
120
110
100
90
80
70
60
50
40
30
20
10
ppm

^{1}H NOEDIFF NMR analysis.

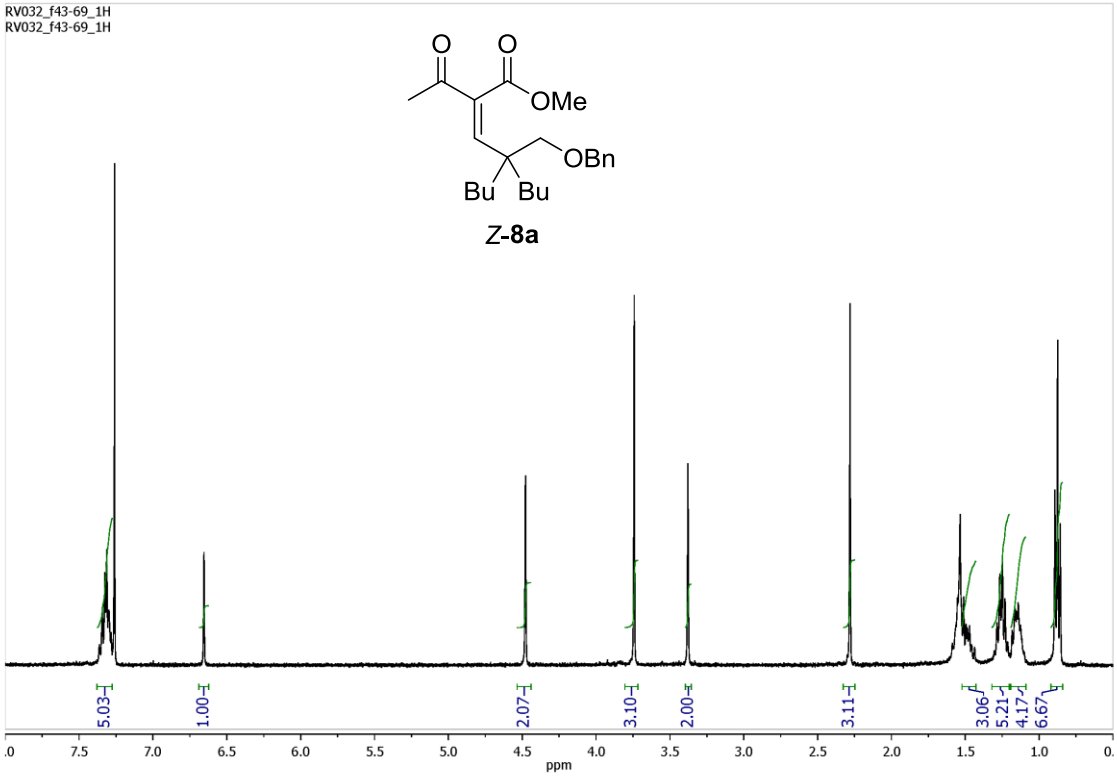

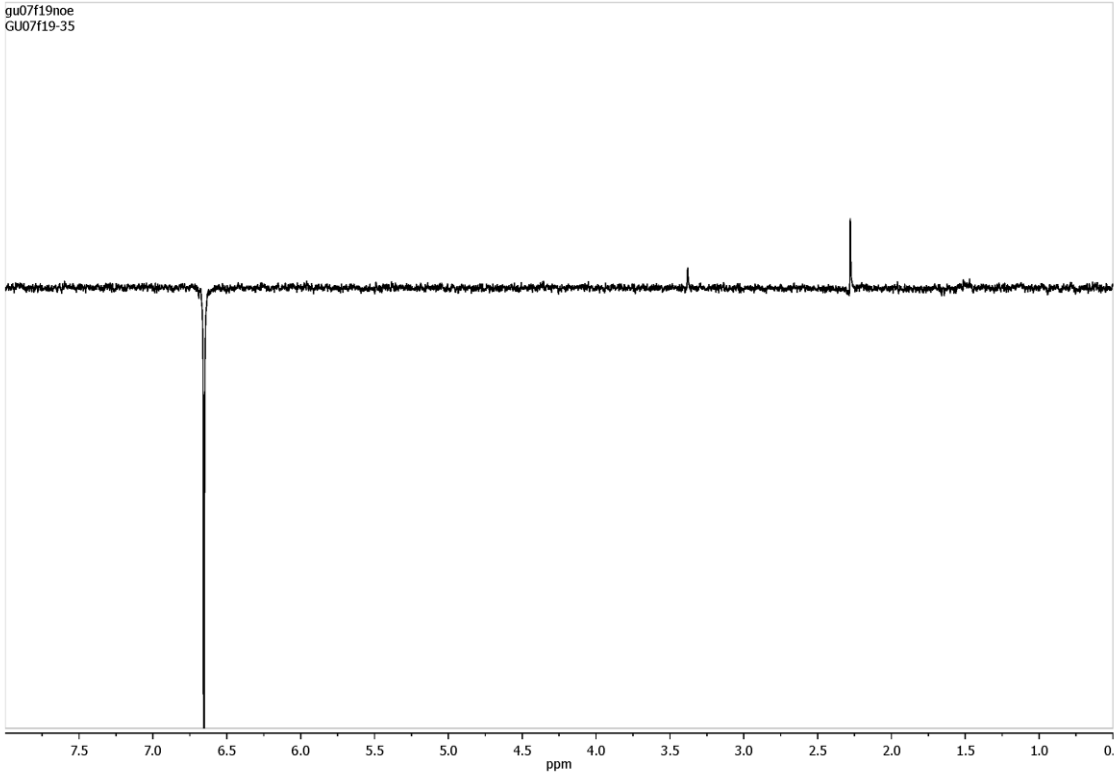

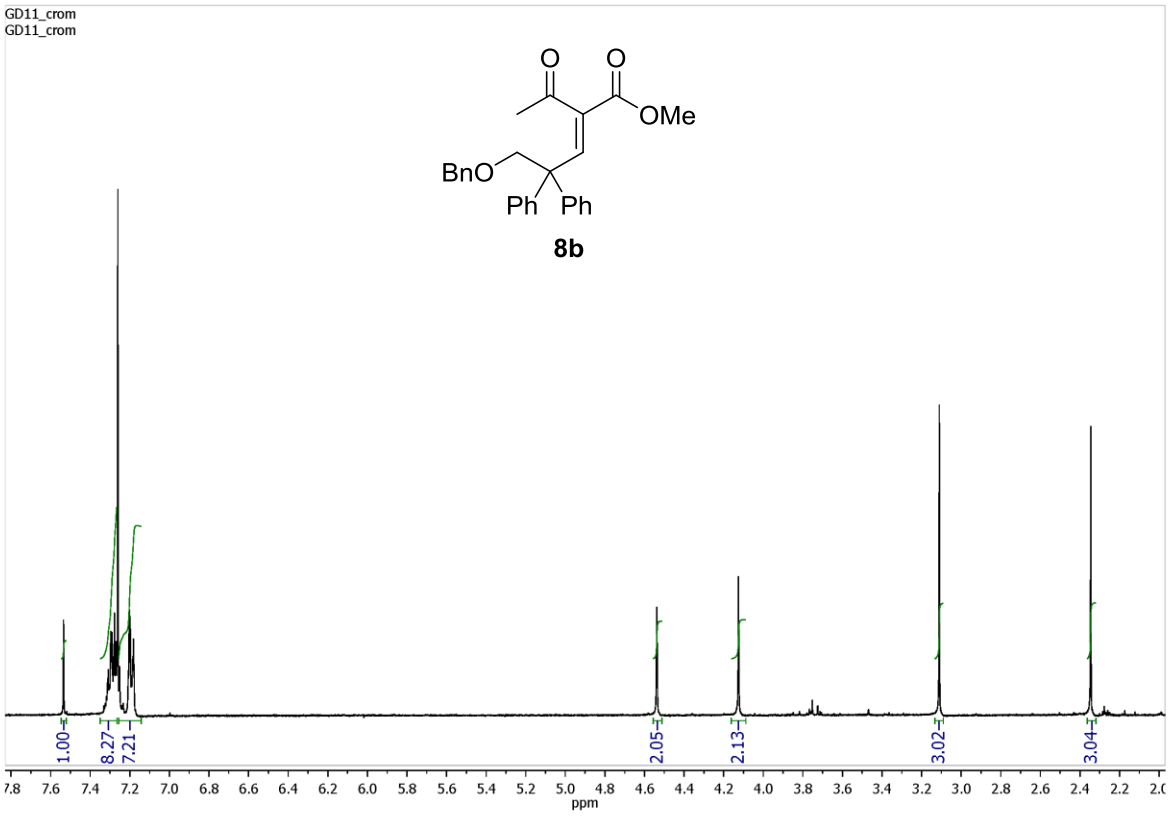
GD11_crom
GD11_crom
O
O
OMe
BnO
Ph
Ph
1.00
8.27
7.21
2.05
2.13
3.02
3.04
ppm

8b

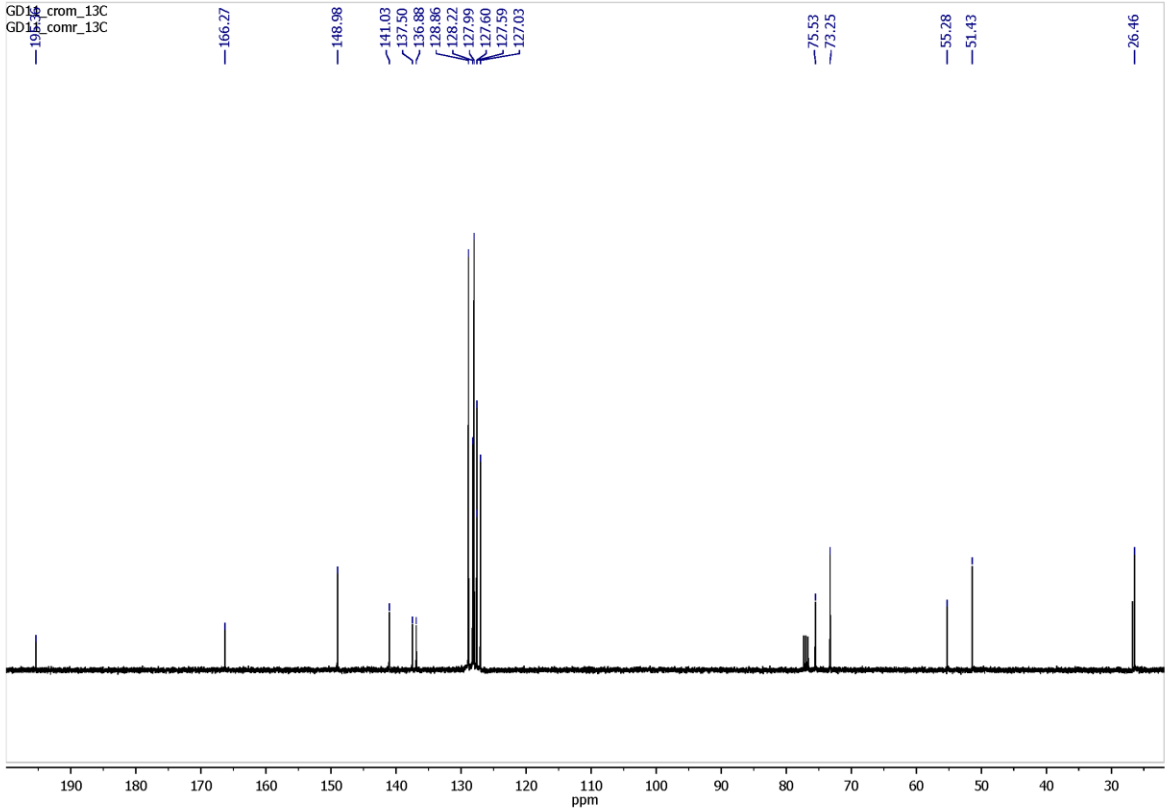
GD11_crom_13C
GD11_comr_13C
166.27
148.98
141.03
137.50
136.88
128.86
128.22
127.99
127.60
127.59
127.03
75.53
73.25
55.28
51.43
26.46
ppm

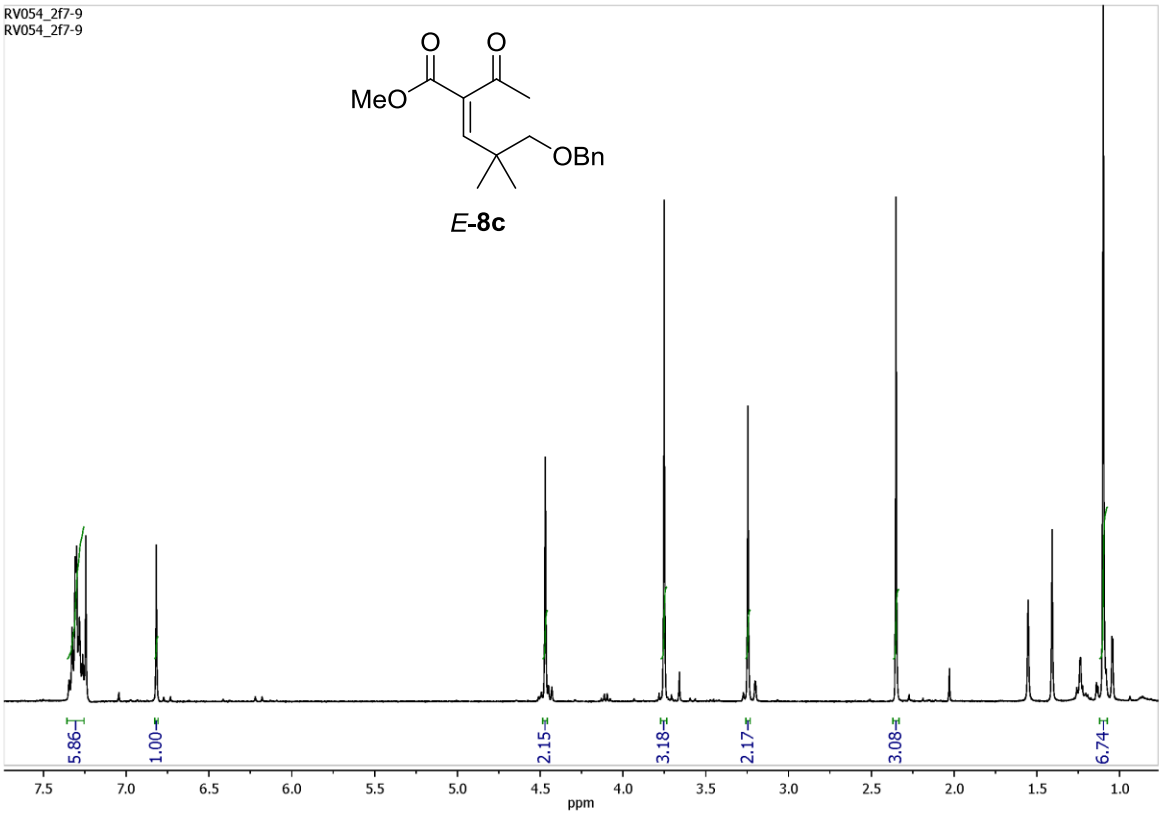
RV054_2f7-9
RV054_2f7-9
MeO
O
O
OBn
5.86
1.00
2.15
3.18
2.17
3.08
6.74
7.5
7.0
6.5
6.0
5.5
5.0
4.5
4.0
3.5
3.0
2.5
2.0
1.5
1.0
ppm

E-**8c**

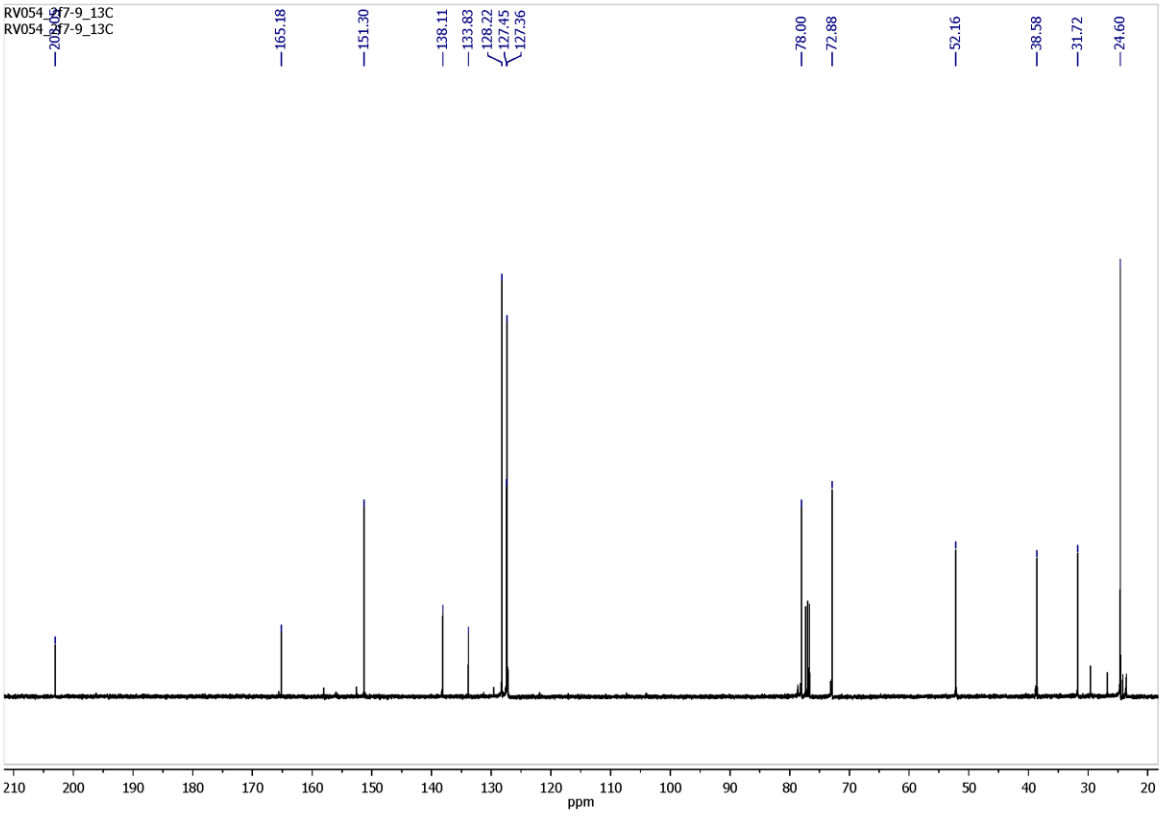
RV054_2f7-9_13C
RV054_2f7-9_13C
165.18
151.30
138.11
133.83
128.22
127.45
127.36
78.00
72.88
52.16
38.58
31.72
24.60
210
200
190
180
170
160
150
140
130
120
110
100
90
80
70
60
50
40
30
20
ppm

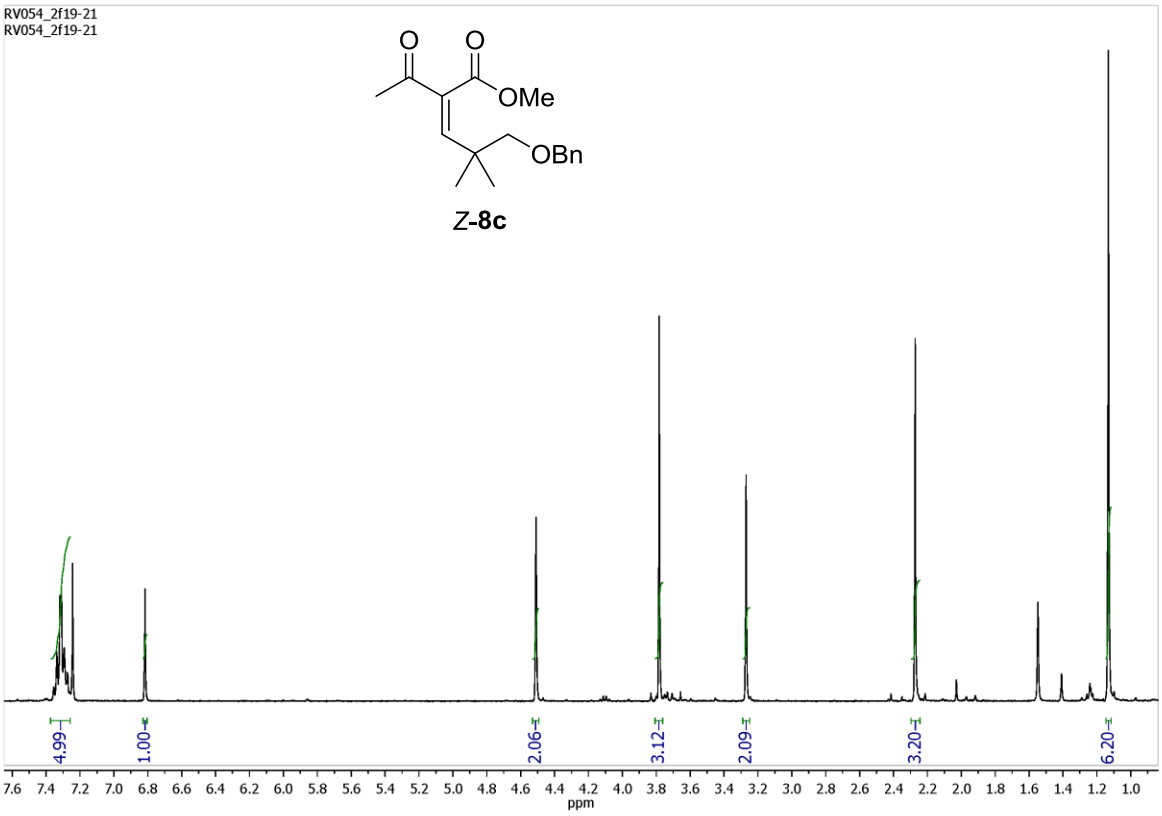
RV054_2f19-21
RV054_2f19-21
O
O
OMe
OBn
4.99
1.00
2.06
3.12
2.09
3.20
6.20
ppm

Z-**8c**

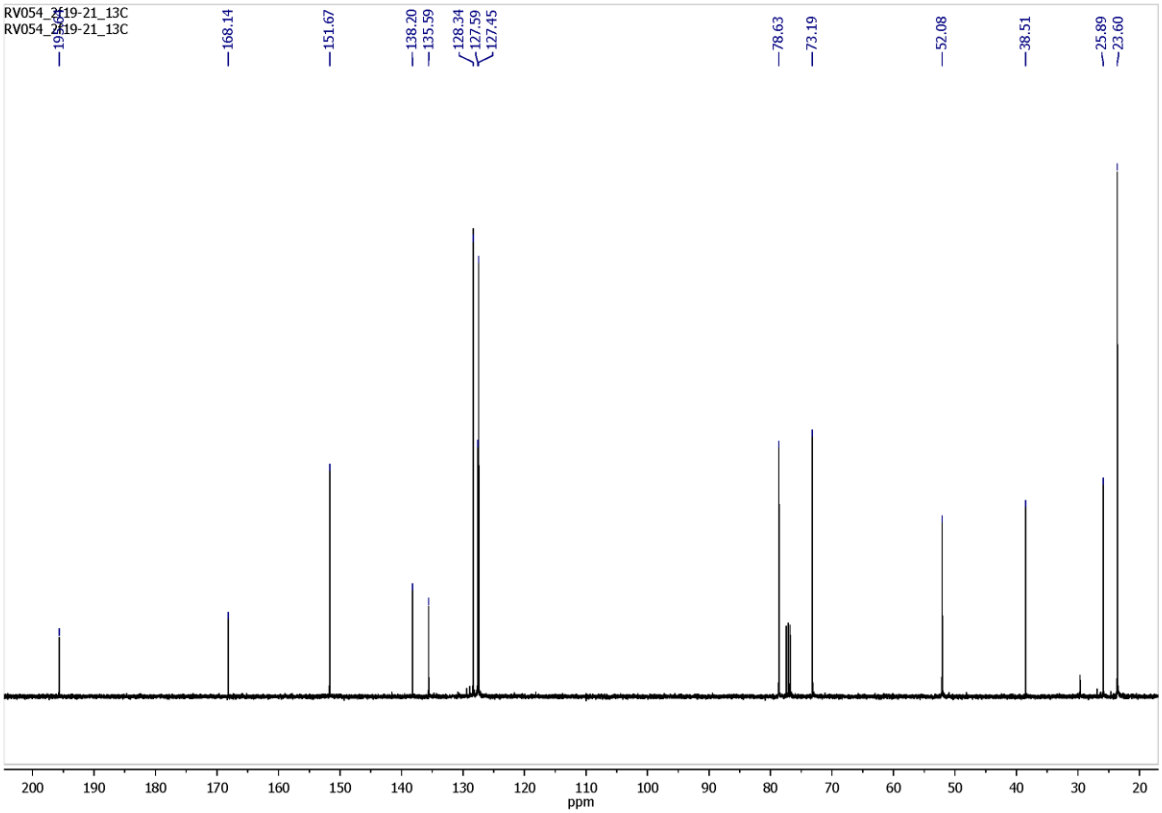
RV054_2f19-21_13C
RV054_2f19-21_13C
168.14
151.67
138.20
135.59
128.34
127.59
127.45
78.63
73.19
52.08
38.51
25.89
23.60
ppm

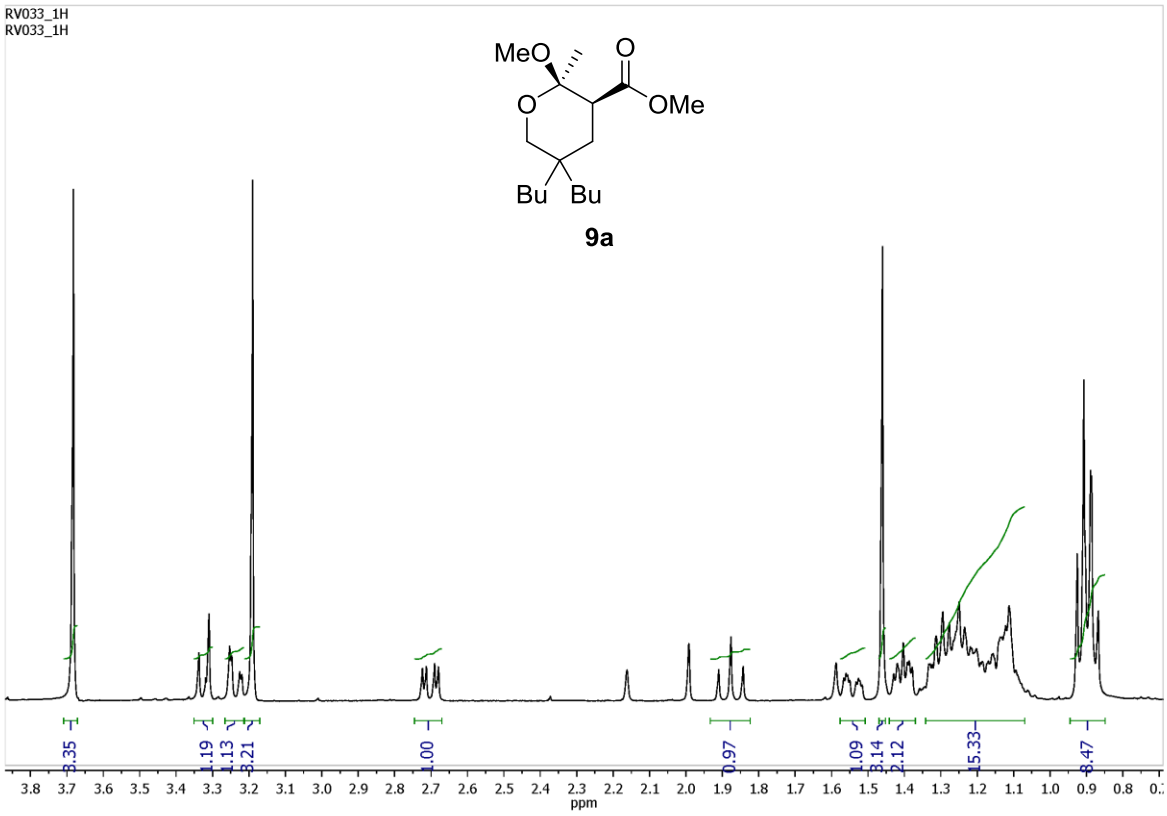
RV033_1H
RV033_1H
MeO
O
O
OMe
Bu
Bu
9a
3.35
1.19
1.13
3.21
1.00
0.97
1.09
3.14
2.12
15.33
8.47
ppm

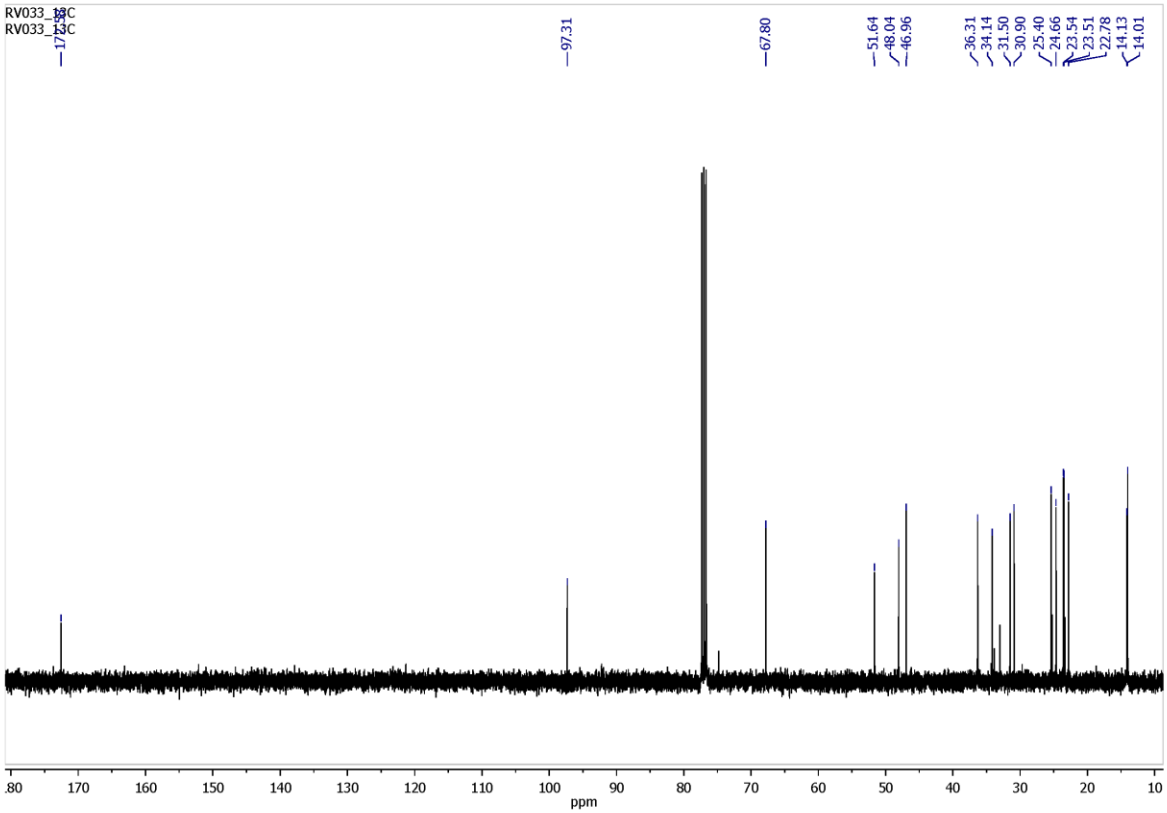
RV033_13C
RV033_13C
97.31
67.80
51.64
48.04
46.96
36.31
34.14
31.50
30.90
25.40
24.66
23.54
23.51
22.78
14.13
14.01
ppm

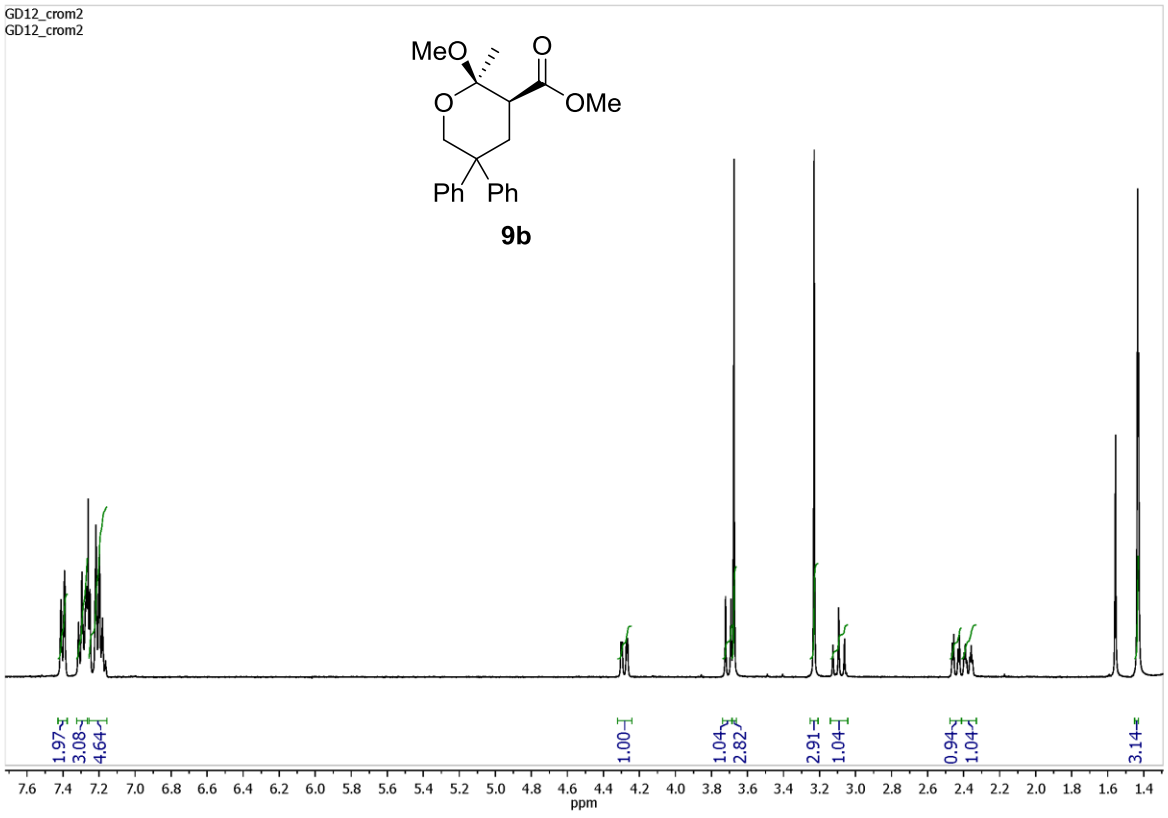
GD12_crom2
GD12_crom2
MeO
O
O
OMe
Ph
Ph
1.97
3.08
4.64
1.00
1.04
2.82
2.91
1.04
0.94
1.04
3.14
ppm

9b

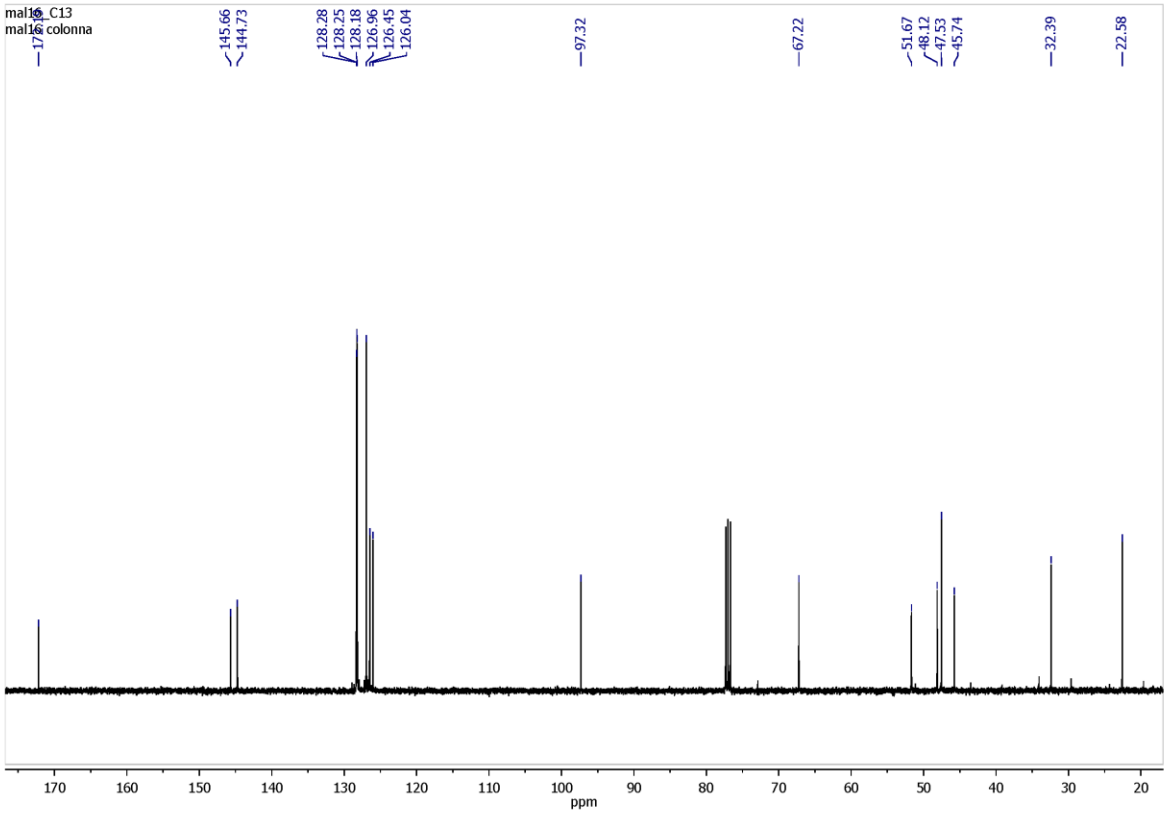
mal16_C13
mal16 colonna
145.66
144.73
128.28
128.25
128.18
126.96
126.45
126.04
97.32
67.22
51.67
48.12
47.53
45.74
32.39
22.58
ppm

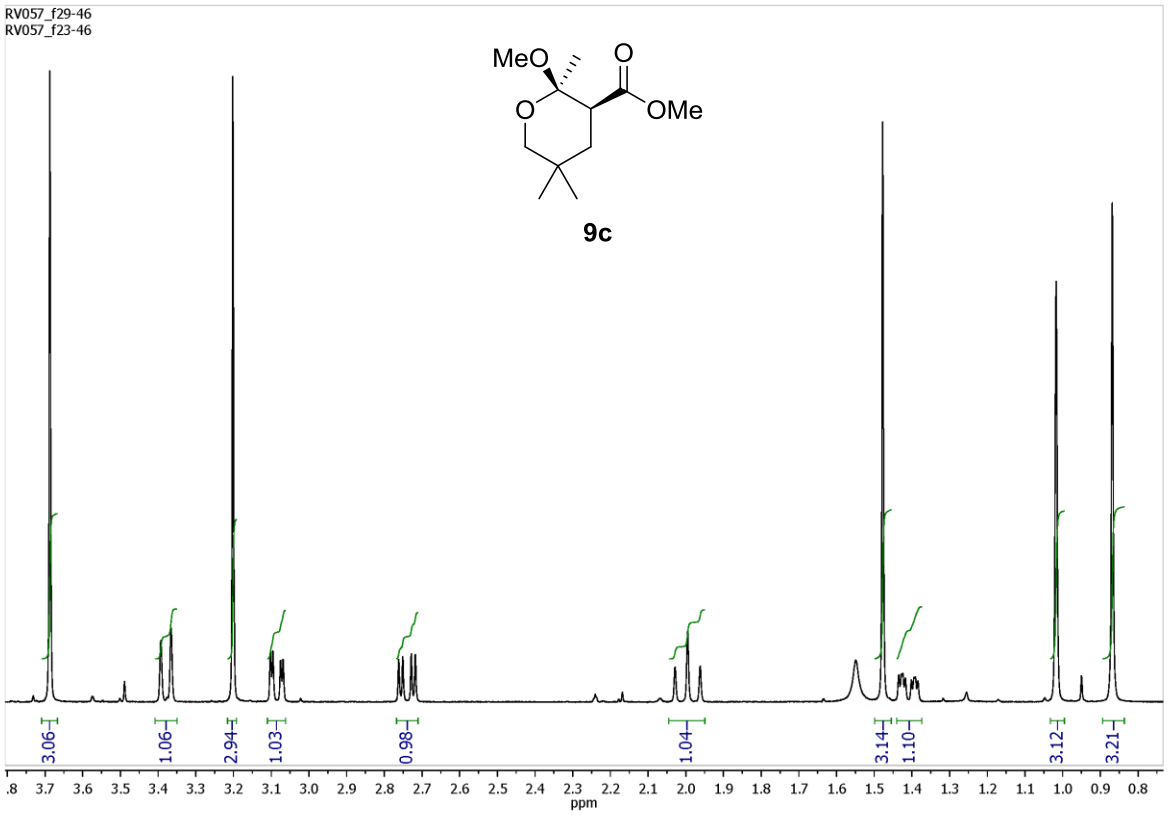
RV057_f29-46
RV057_f23-46
MeO
O
O
OMe
9c
3.06
1.06
2.94
1.03
0.98
1.04
3.14
1.10
3.12
3.21
ppm

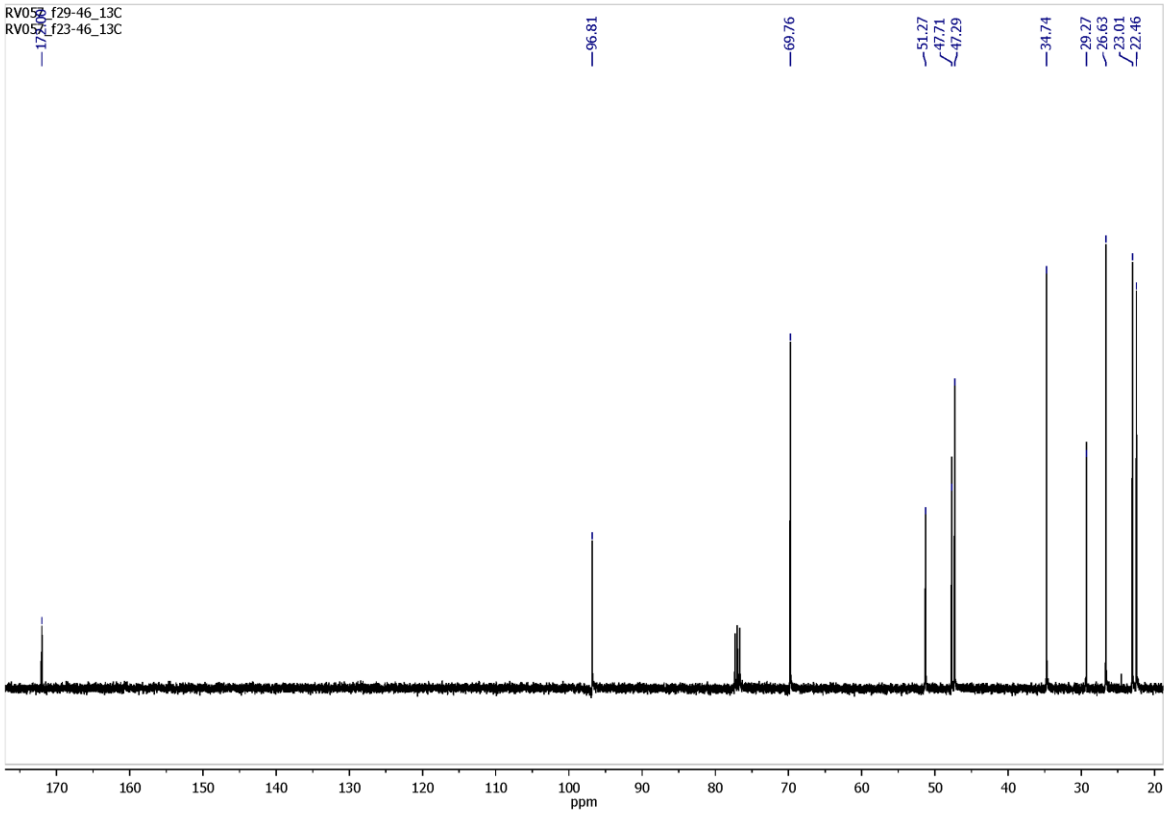
RV057_f29-46_13C
RV057_f23-46_13C
174.70
96.81
69.76
51.27
47.71
47.29
34.74
29.27
26.63
23.01
22.46
ppm

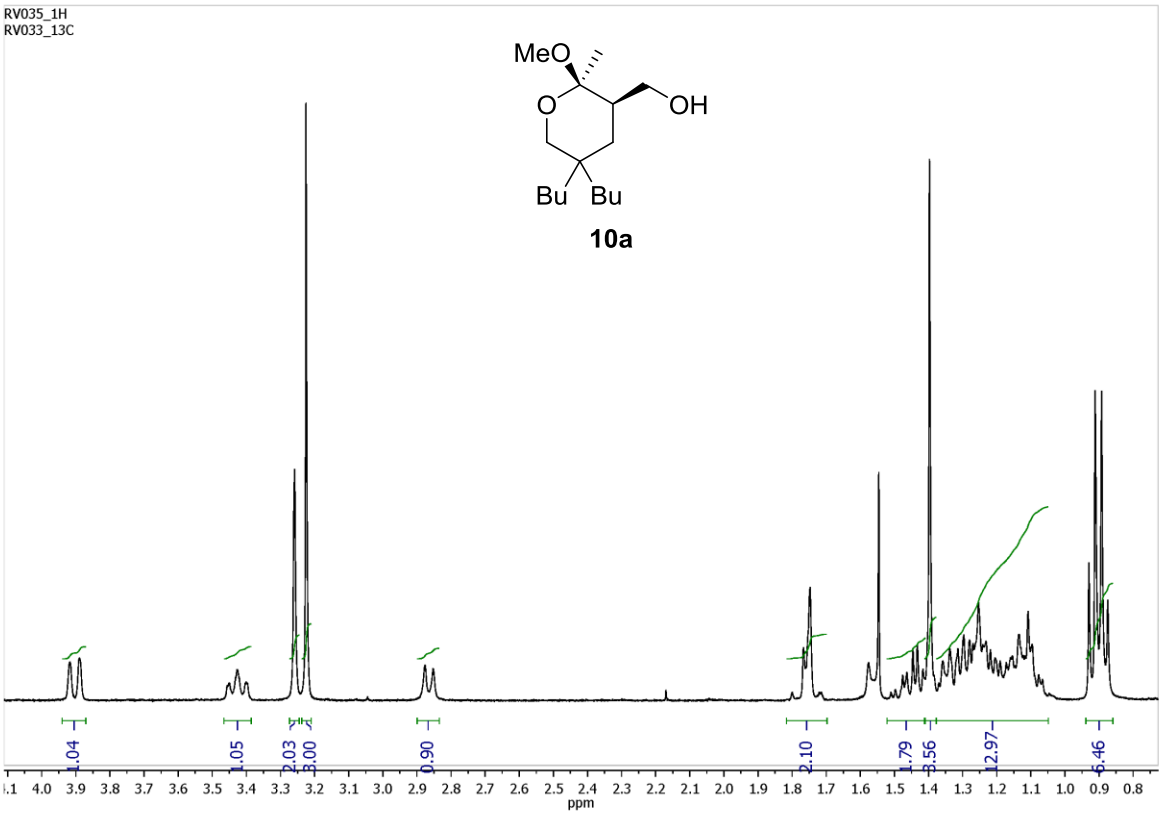
RV035_1H
RV033_13C
MeO
O
OH
Bu
Bu
10a
1.04
1.05
2.03
3.00
0.90
2.10
1.79
3.56
12.97
6.46
ppm

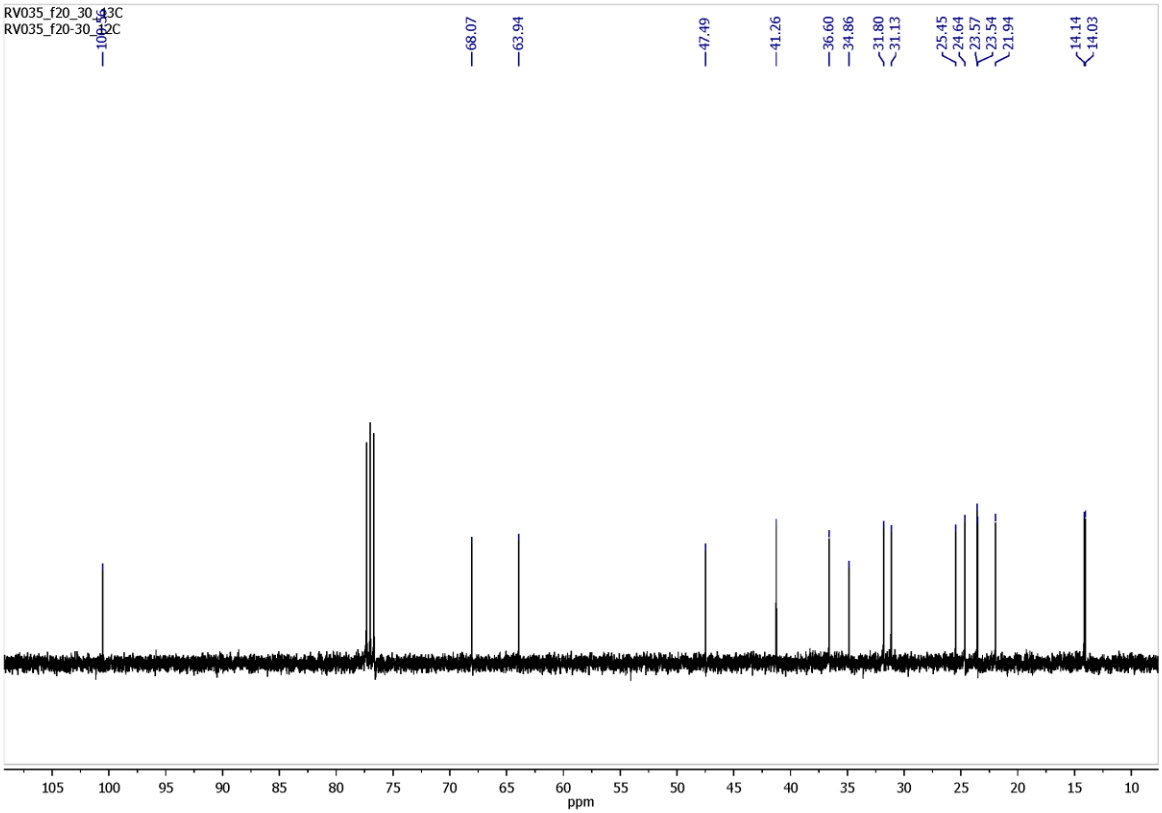
RV035_f20_30_13C
RV035_f20-30_12C
68.07
63.94
47.49
41.26
36.60
34.86
31.80
31.13
25.45
24.64
23.57
23.54
21.94
14.14
14.03
ppm

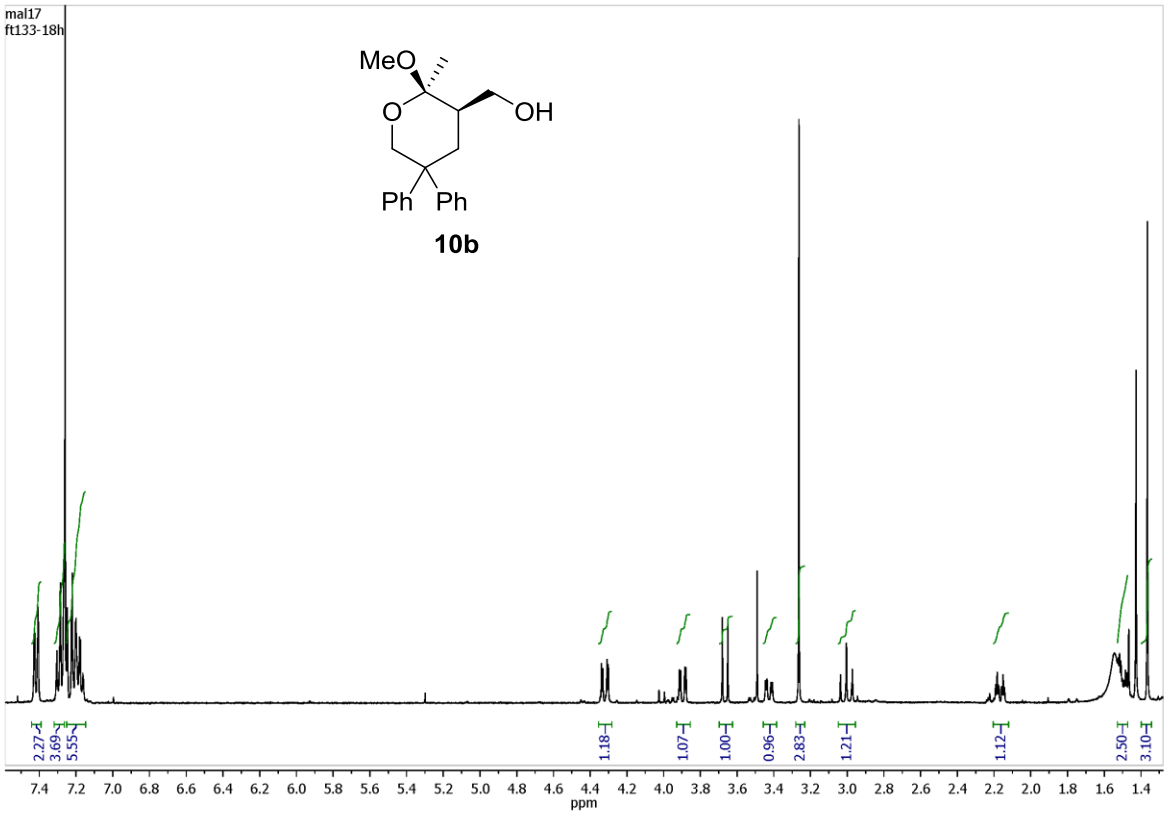
mal17
ft133-18h
MeO
O
OH
Ph
Ph
10b
2.27
3.69
5.55
1.18
1.07
1.00
0.96
2.83
1.21
1.12
2.50
3.10
7.4 7.2 7.0 6.8 6.6 6.4 6.2 6.0 5.8 5.6 5.4 5.2 5.0 4.8 4.6 4.4 4.2 4.0 3.8 3.6 3.4 3.2 3.0 2.8 2.6 2.4 2.2 2.0 1.8 1.6 1.4
ppm

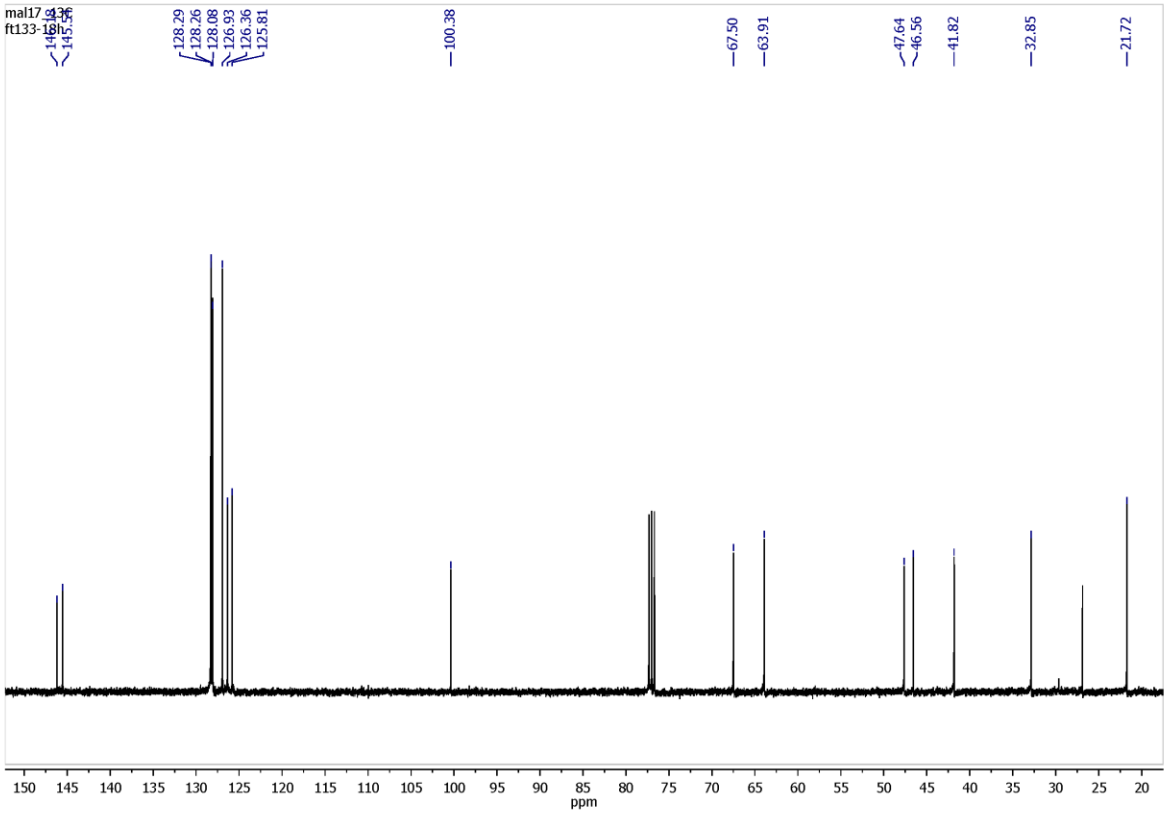
mal17
ft133-18h
145.36
145.15
128.29
128.26
128.08
126.93
126.36
125.81
100.38
67.50
63.91
47.64
46.56
41.82
32.85
21.72
150 145 140 135 130 125 120 115 110 105 100 95 90 85 80 75 70 65 60 55 50 45 40 35 30 25 20
ppm

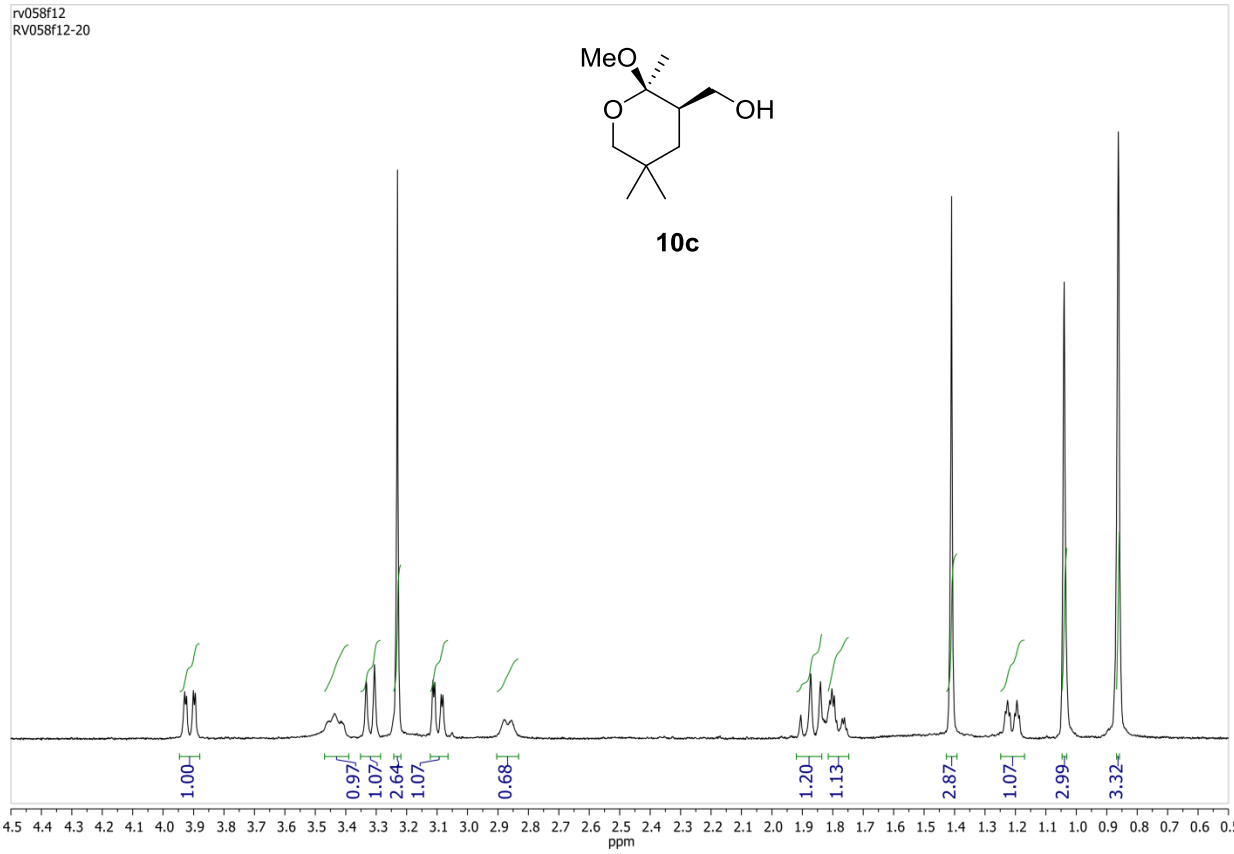
rv058f12
RV058f12-20
MeO
O
OH
10c
1.00
0.97
1.07
2.64
1.07
0.68
1.20
1.13
2.87
1.07
2.99
3.32
ppm

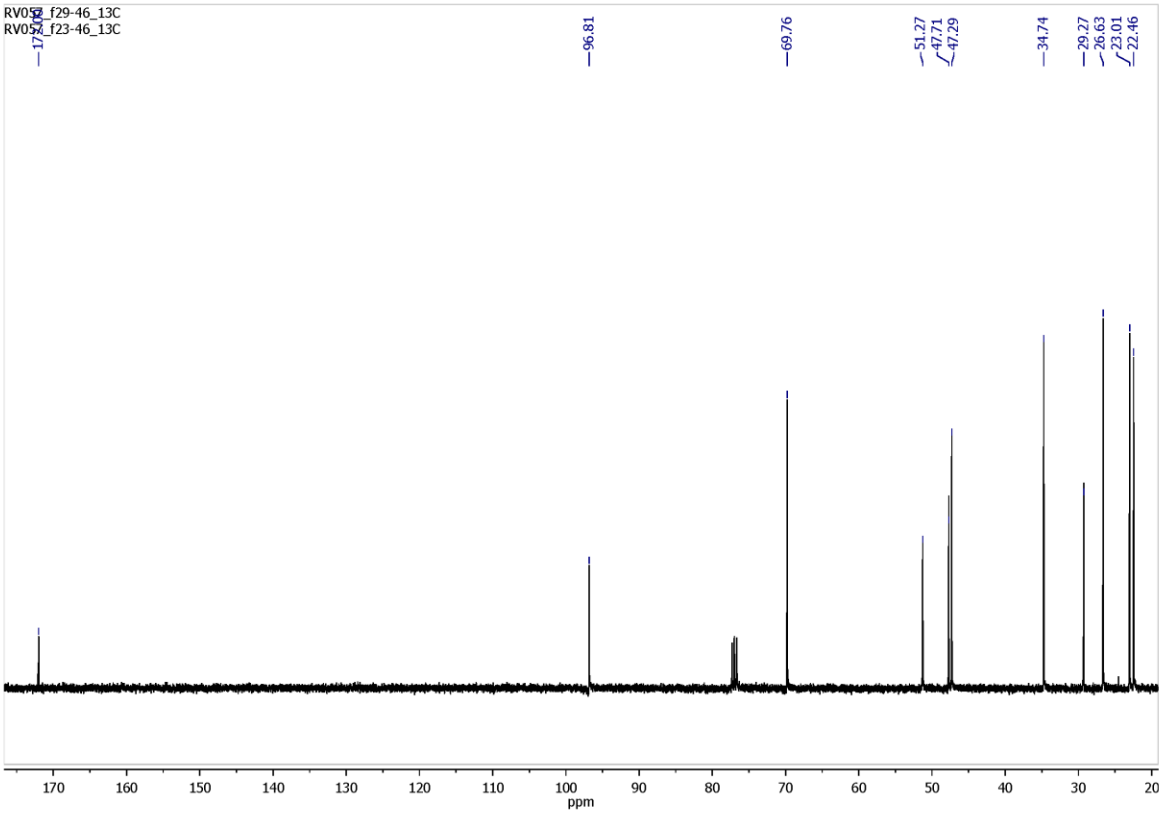
RV057_f29-46_13C
RV057_f23-46_13C
96.81
69.76
51.27
47.71
47.29
34.74
29.27
26.63
23.01
22.46
ppm

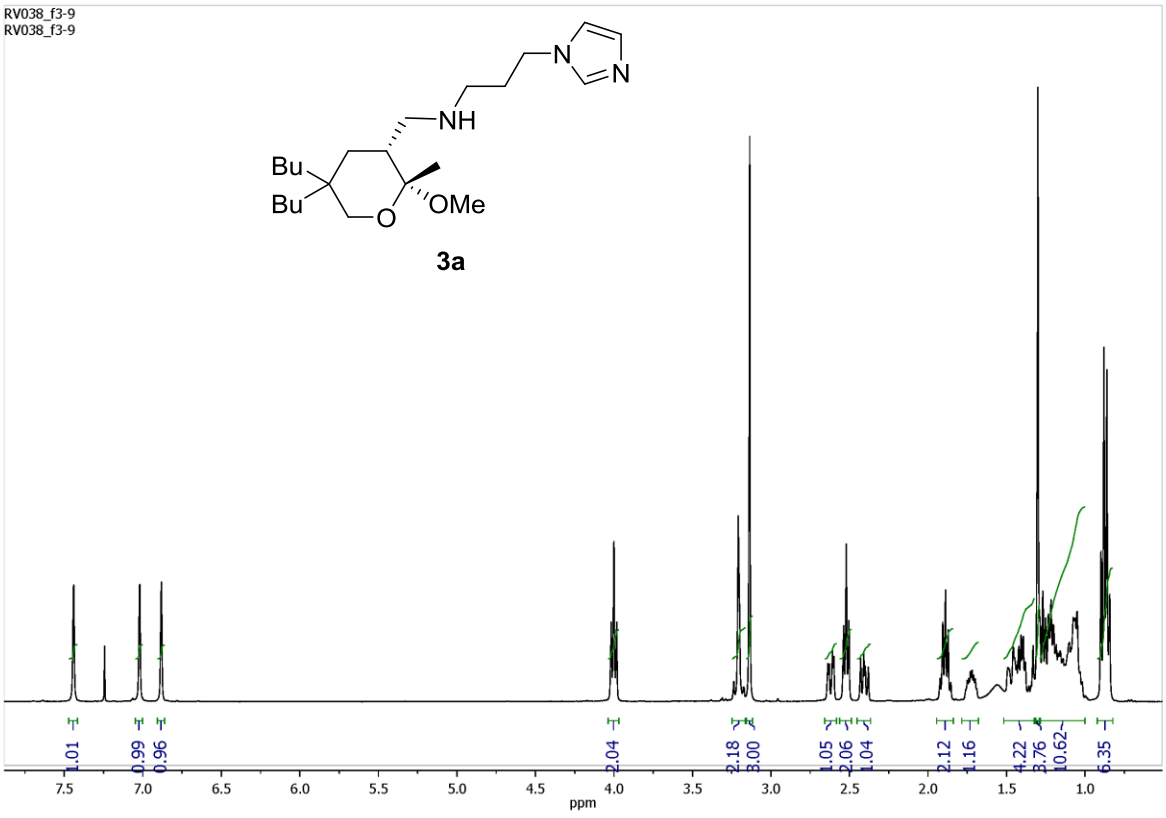
RV038_f3-9
RV038_f3-9
N
N
NH
Bu
Bu
O
OMe
1.01
0.99
0.96
2.04
2.18
3.00
1.05
2.06
1.04
2.12
1.16
4.22
3.76
10.62
6.35
7.5
7.0
6.5
6.0
5.5
5.0
4.5
4.0
3.5
3.0
2.5
2.0
1.5
1.0
ppm

3a

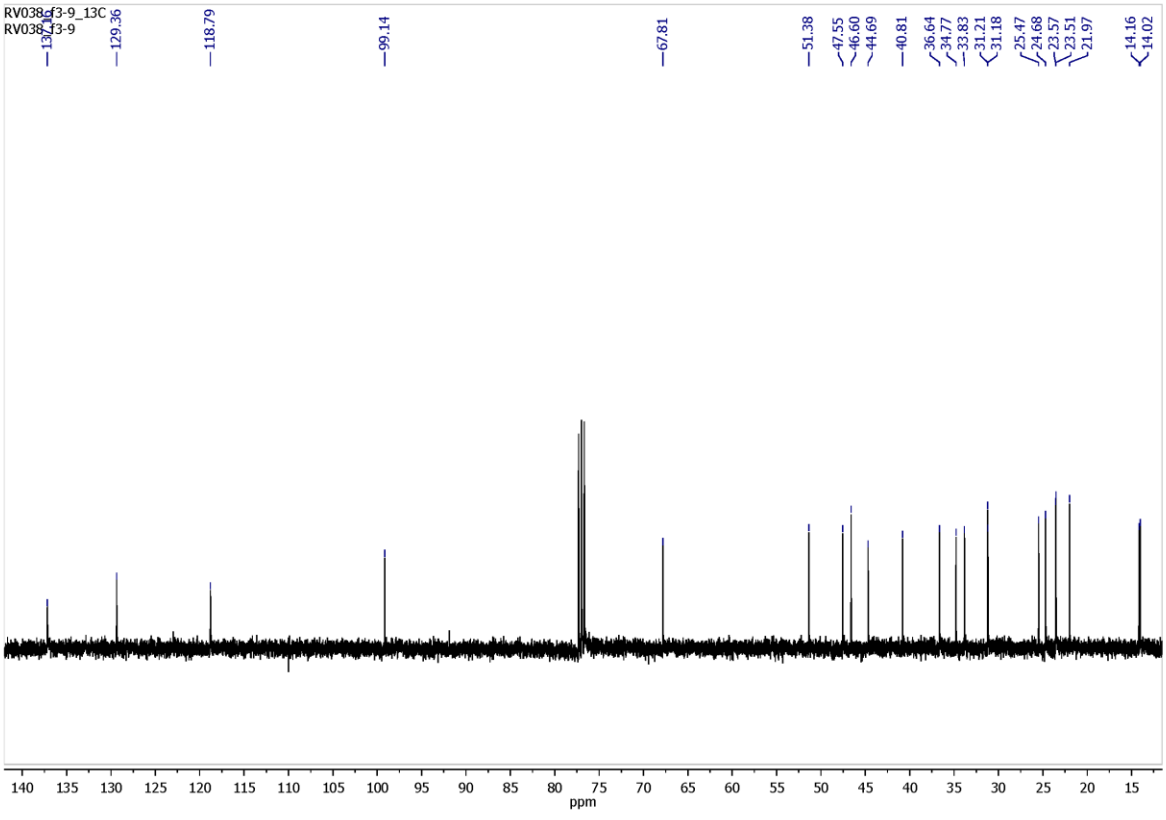
RV038_f3-9_13C
RV038_f3-9
129.36
118.79
99.14
67.81
51.38
47.55
46.60
44.69
40.81
36.64
34.77
33.83
31.21
31.18
25.47
24.68
23.57
23.51
21.97
14.16
14.02
140
135
130
125
120
115
110
105
100
95
90
85
80
75
70
65
60
55
50
45
40
35
30
25
20
15
ppm

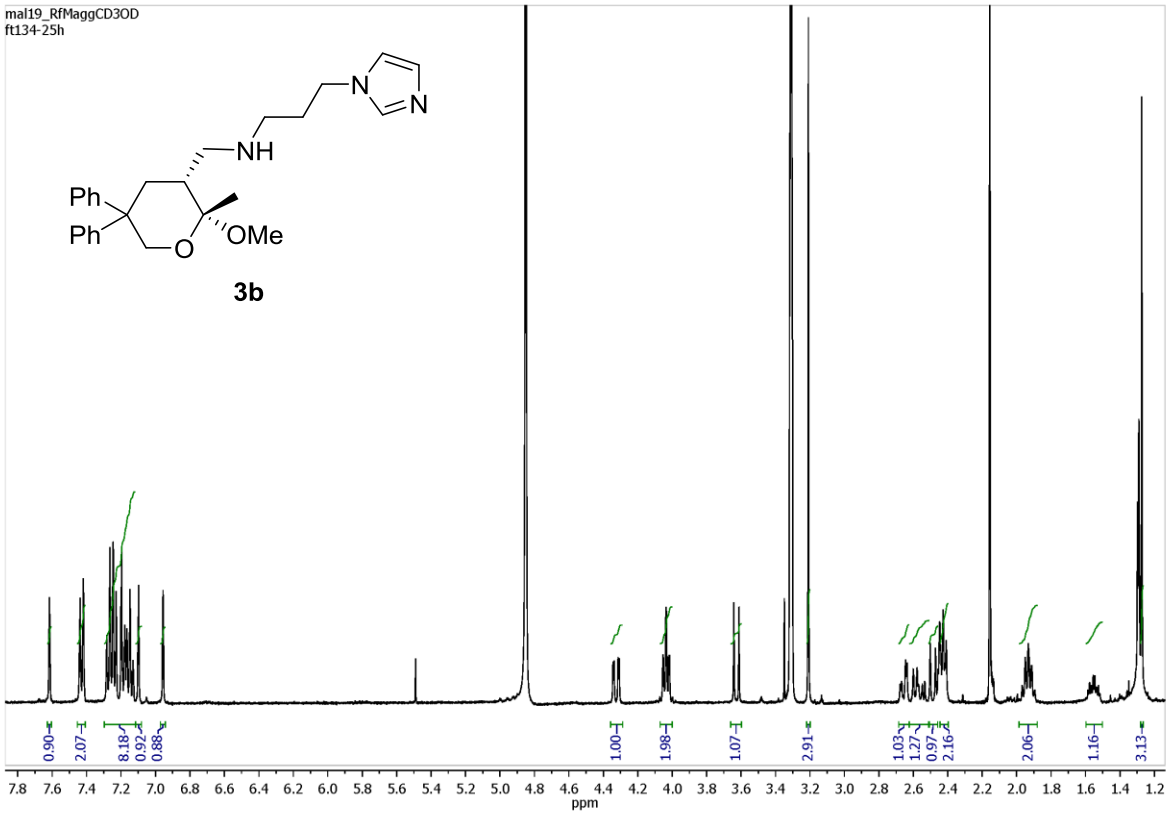
mal19_RfMaggCD3OD
ft134-25h
3b
ppm

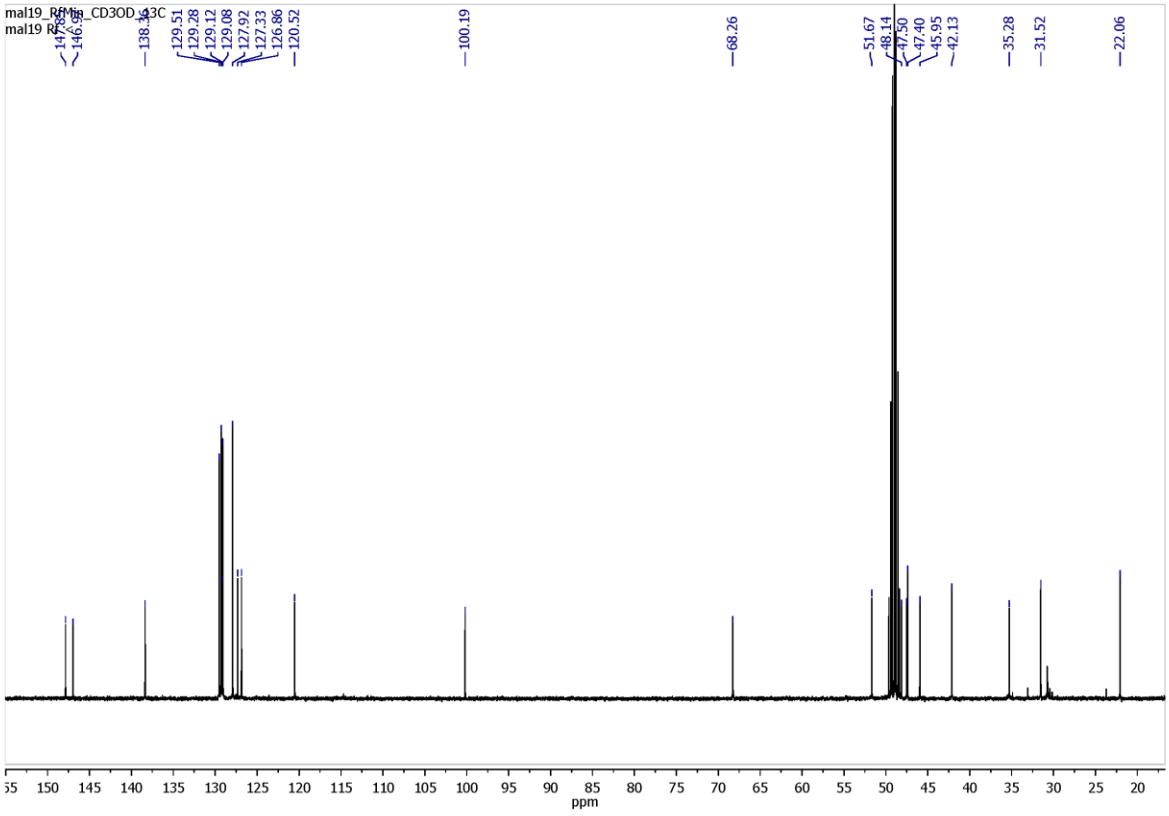
mal19_RfMin_CD3OD_13C
mal19 RF
ppm

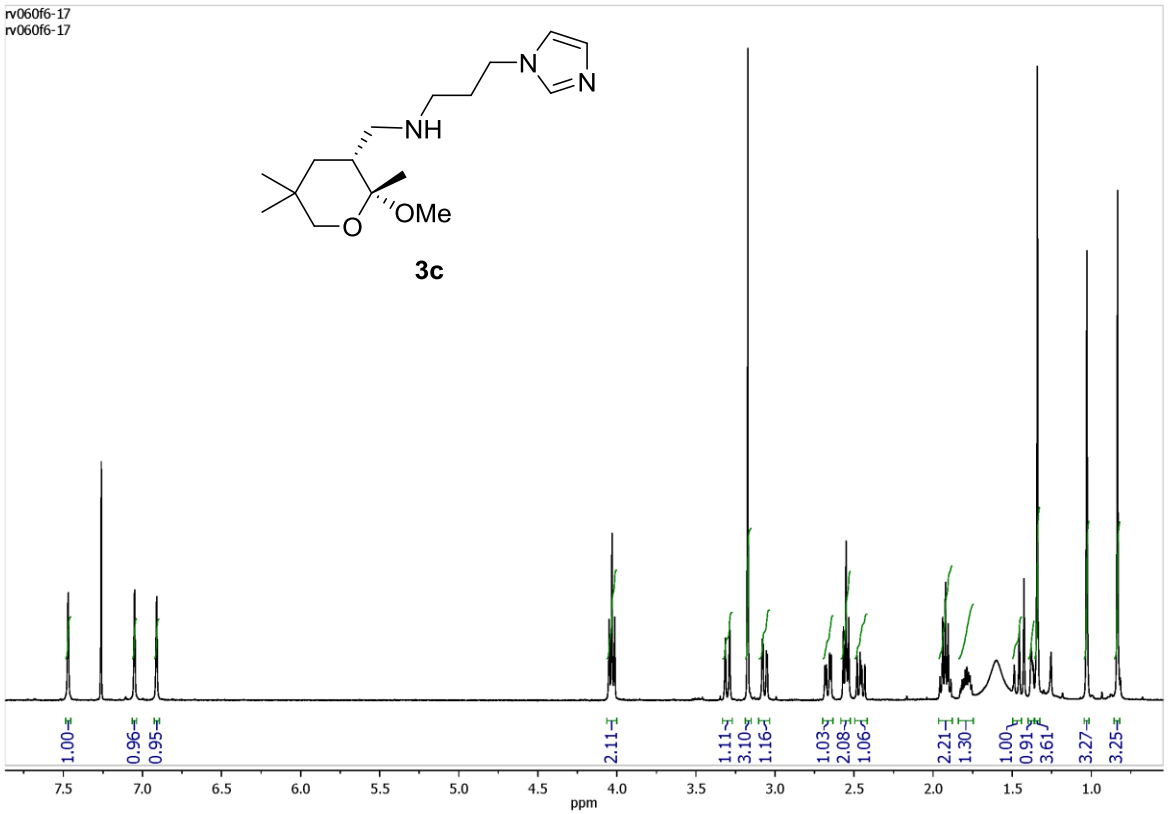
rv060f6-17
rv060f6-17
N
N
NH
O
OMe
1.00
0.96
0.95
2.11
1.11
3.10
1.16
1.03
2.08
1.06
2.21
1.30
1.00
0.91
3.61
3.27
3.25
7.5
7.0
6.5
6.0
5.5
5.0
4.5
4.0
3.5
3.0
2.5
2.0
1.5
1.0
ppm

3c

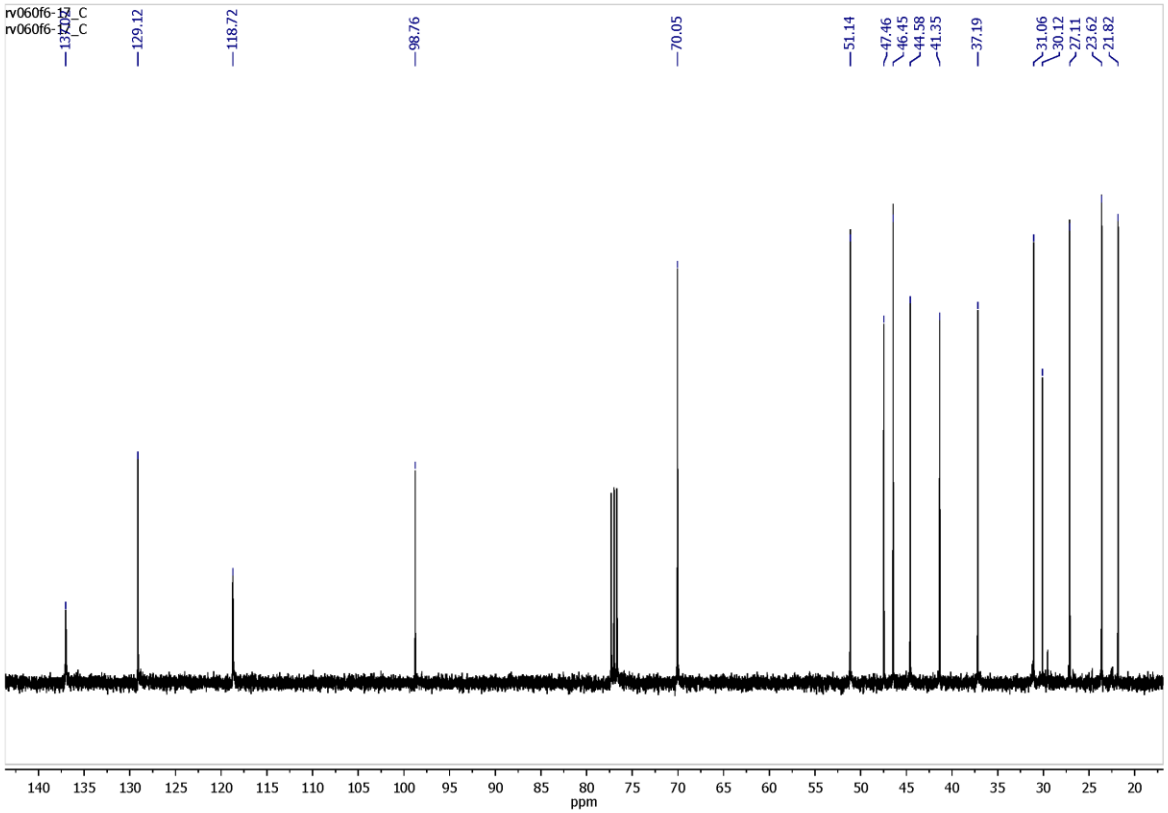
rv060f6-17_C
rv060f6-17_C
137.42
129.12
118.72
98.76
70.05
51.14
47.46
46.45
44.58
41.35
37.19
31.06
30.12
27.11
23.62
21.82
140
135
130
125
120
115
110
105
100
95
90
85
80
75
70
65
60
55
50
45
40
35
30
25
20
ppm

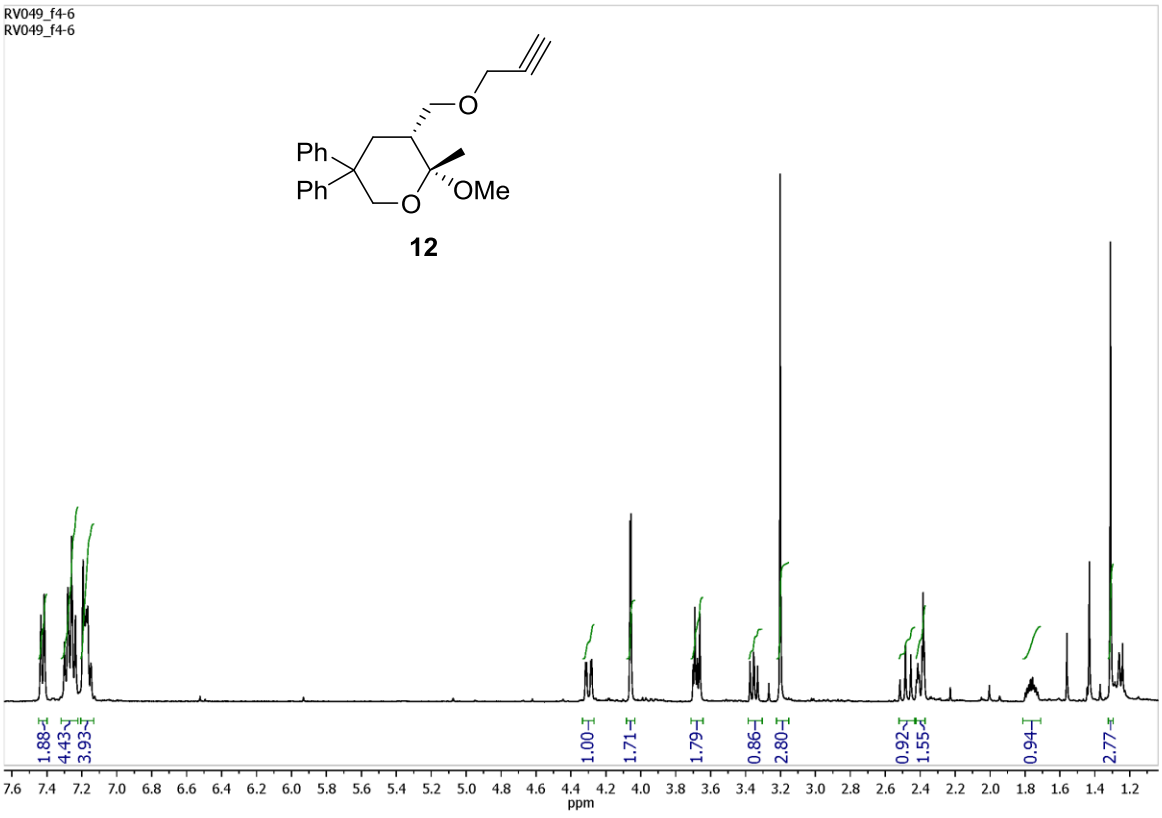
RV049_f4-6
RV049_f4-6
Ph
Ph
O
O
OMe
12
1.88
4.43
3.93
1.00
1.71
1.79
0.86
2.80
0.92
1.55
0.94
2.77
ppm

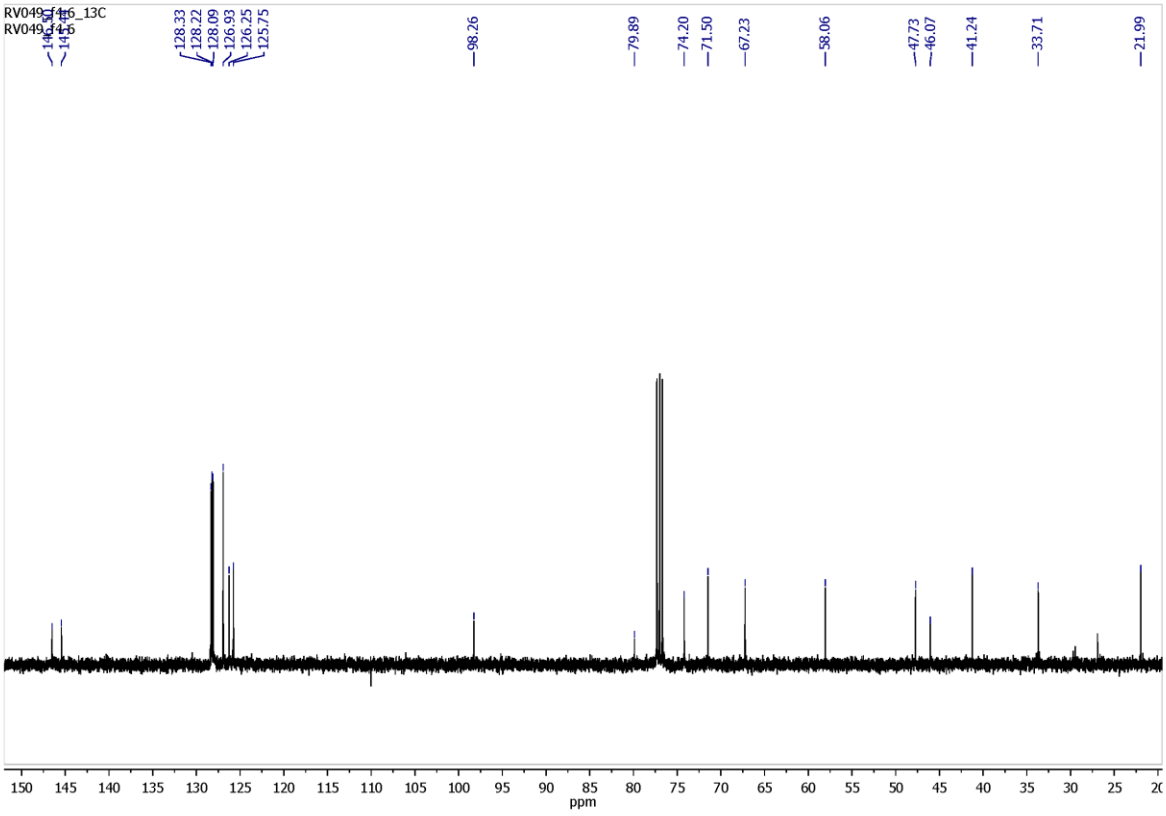
RV049_f4-6_13C
RV049_f4-6
128.33
128.22
128.09
126.93
126.25
125.75
98.26
79.89
74.20
71.50
67.23
58.06
47.73
46.07
41.24
33.71
21.99
ppm

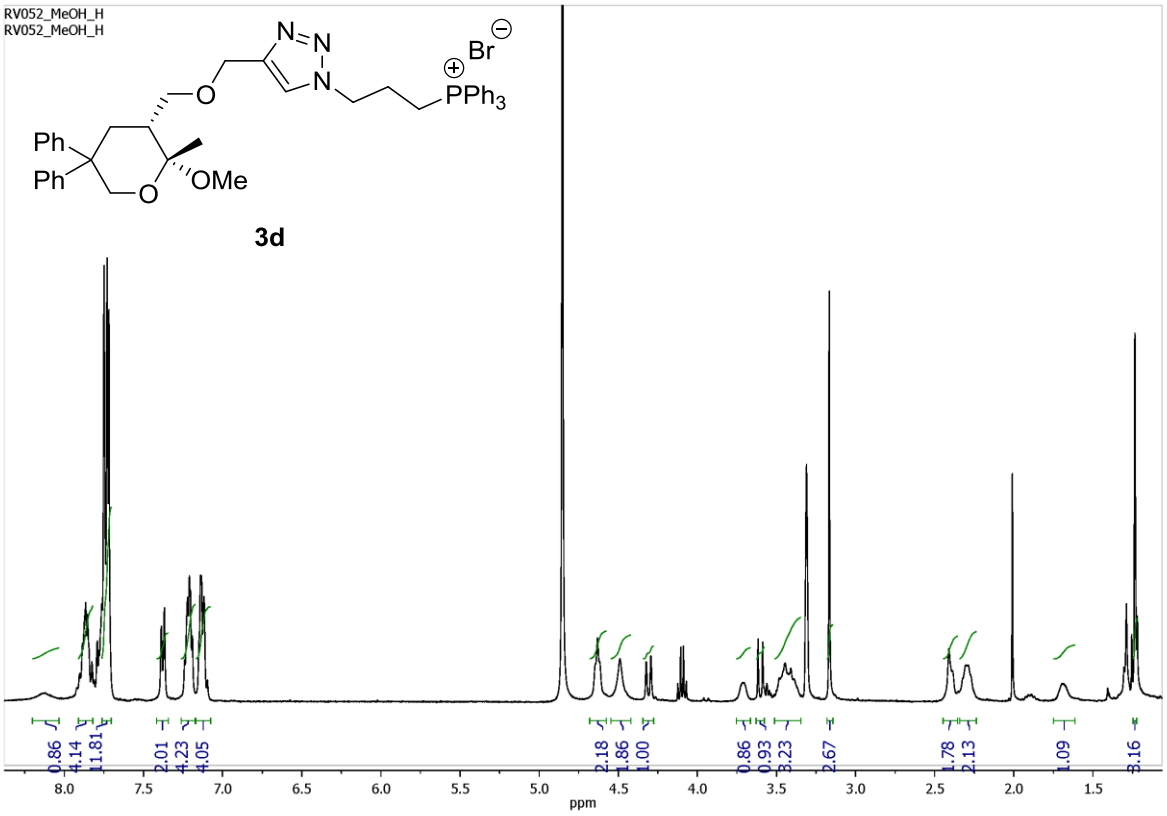
RV052_MeOH_H
RV052_MeOH_H
Br
PPh3
Ph
Ph
OMe
3d
0.86
4.14
11.81
2.01
4.23
4.05
2.18
1.86
1.00
0.86
0.93
3.23
2.67
1.78
2.13
1.09
3.16
ppm

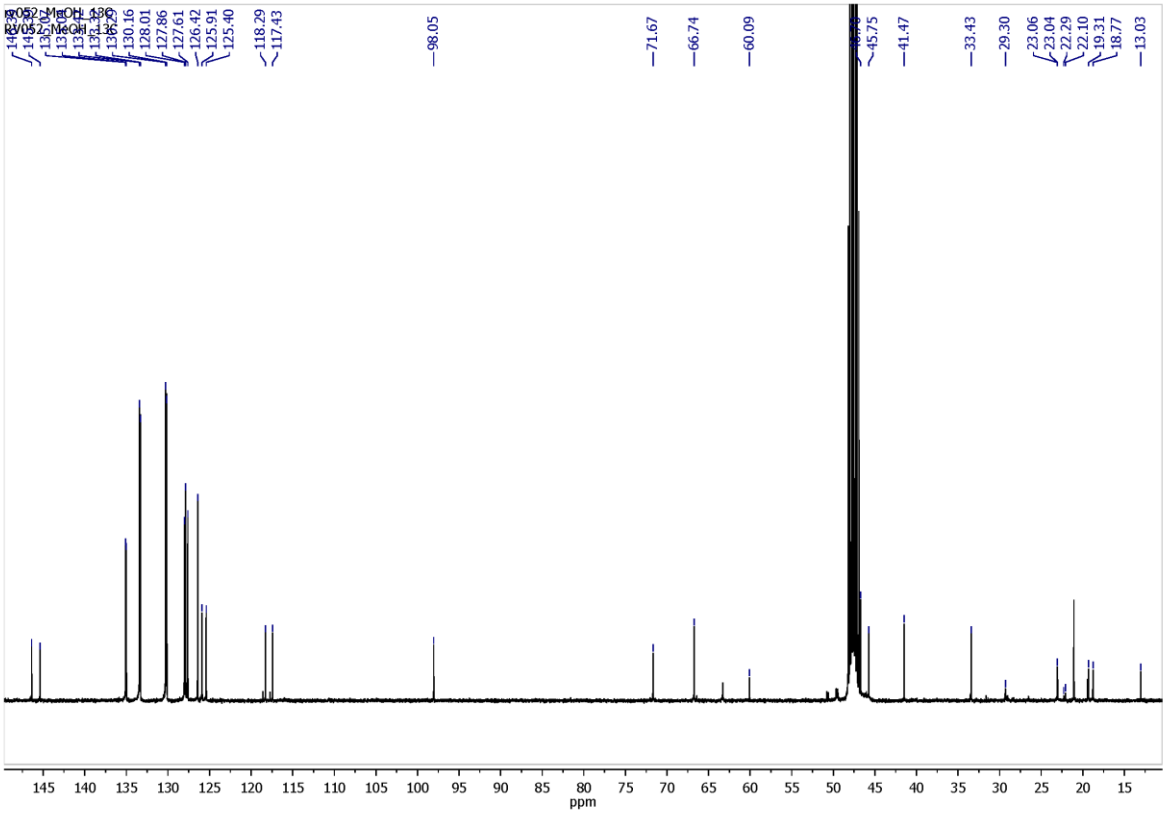
RV052_MeOH_13C
RV052_MeOH_13C
98.05
71.67
66.74
60.09
45.75
41.47
33.43
29.30
23.06
23.04
22.29
22.10
19.31
18.77
13.03
ppm

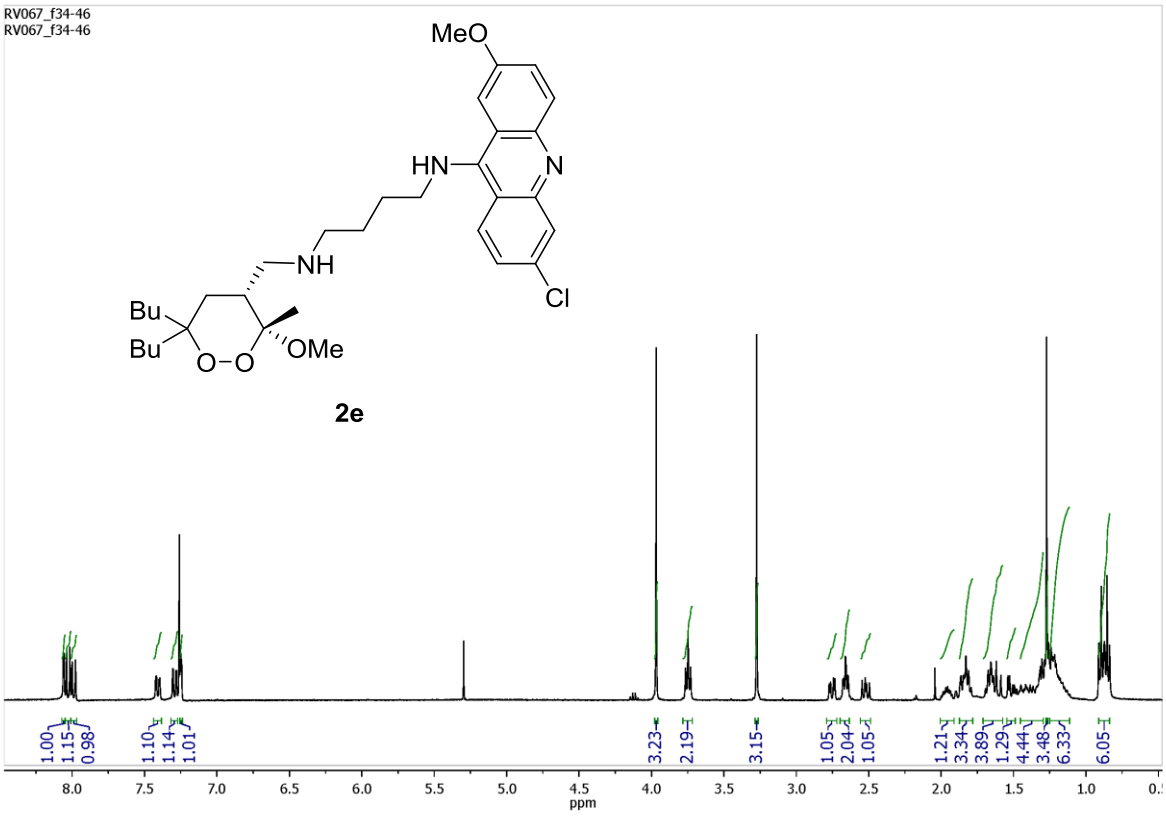
RV067_f34-46
RV067_f34-46
MeO
HN
N
NH
Cl
Bu
Bu
O–O
OMe
2e
1.00
1.15
0.98
1.10
1.14
1.01
3.23
2.19
3.15
1.05
2.04
1.05
1.21
3.34
3.89
1.29
4.44
3.48
6.33
6.05
8.0
7.5
7.0
6.5
6.0
5.5
5.0
4.5
4.0
3.5
3.0
2.5
2.0
1.5
1.0
ppm

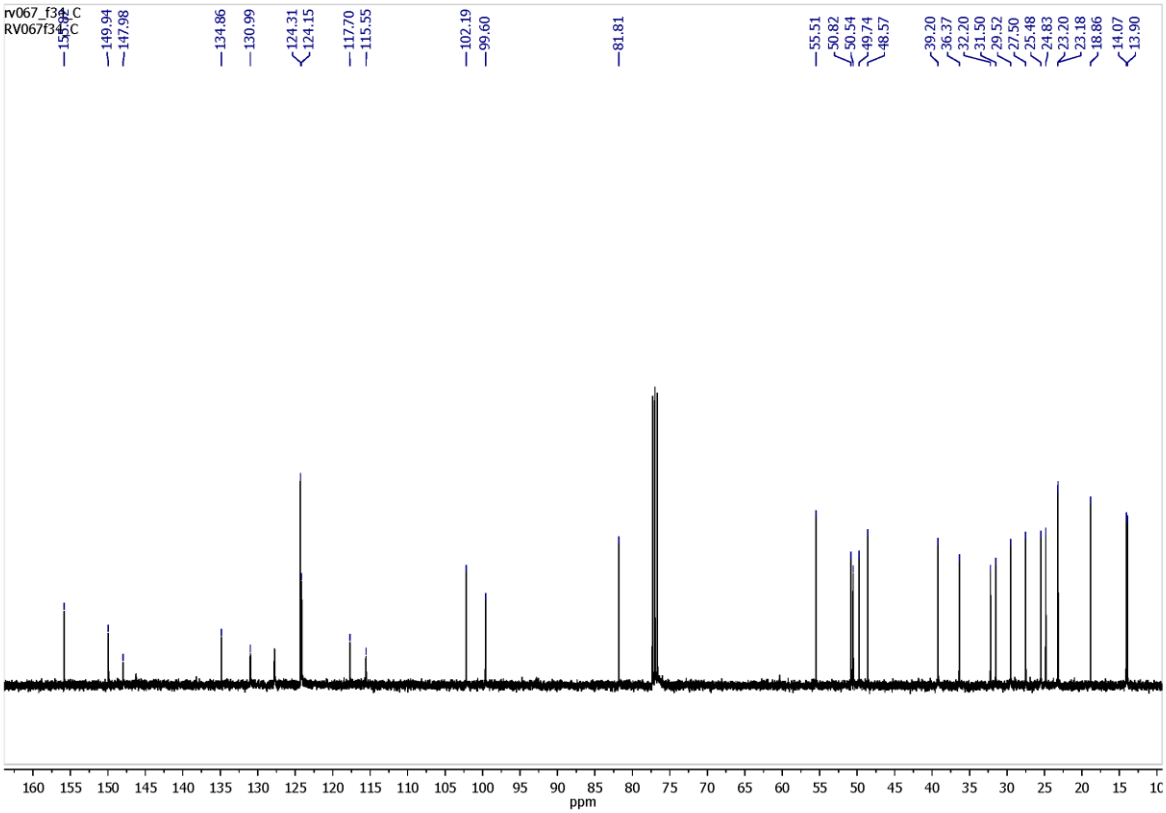
rv067_f34-C
RV067f34-C
155.42
149.94
147.98
134.86
130.99
124.31
124.15
117.70
115.55
102.19
99.60
81.81
55.51
50.82
50.54
49.74
48.57
39.20
36.37
32.20
31.50
29.52
27.50
25.48
24.83
23.20
23.18
18.86
14.07
13.90
160
155
150
145
140
135
130
125
120
115
110
105
100
95
90
85
80
75
70
65
60
55
50
45
40
35
30
25
20
15
ppm

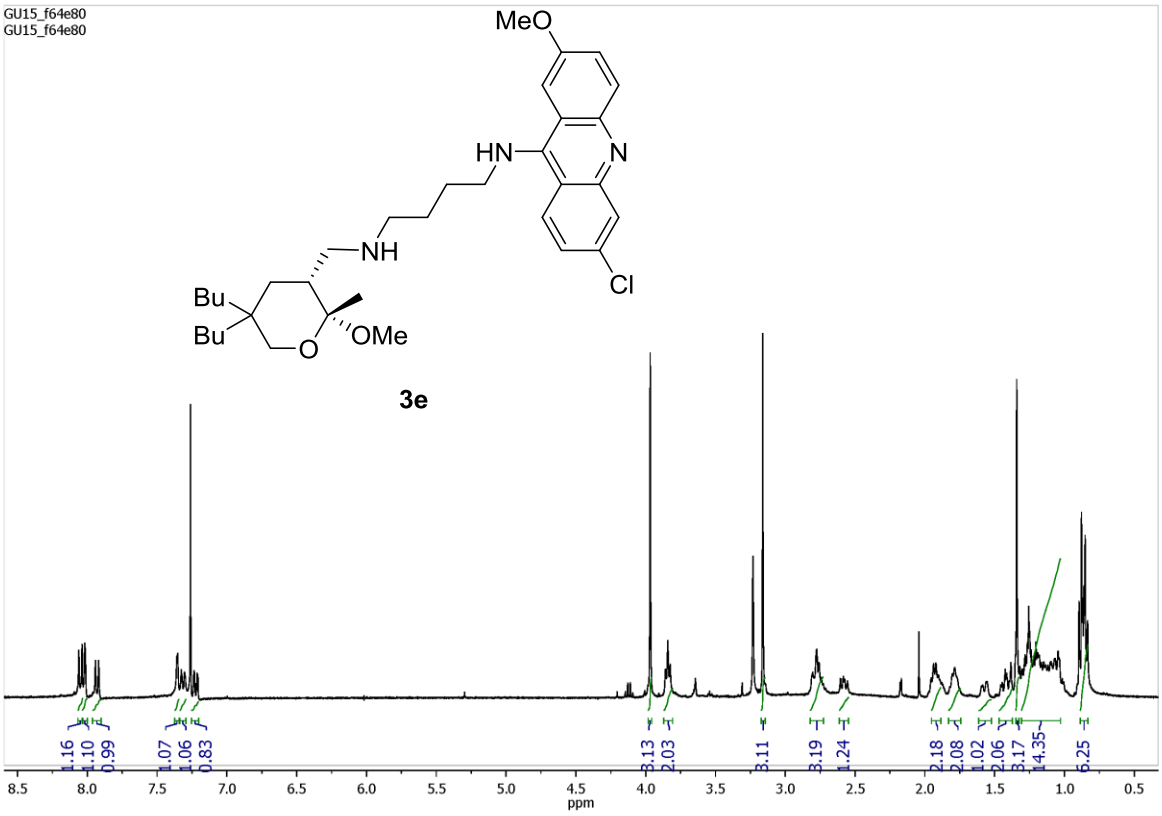
GU15_f64e80
GU15_f64e80
MeO
HN
N
NH
Cl
Bu
Bu
O
OMe
3e
1.16
1.10
0.99
1.07
1.06
0.83
3.13
2.03
3.11
3.19
1.24
2.18
2.08
1.02
2.06
3.17
14.35
6.25
ppm

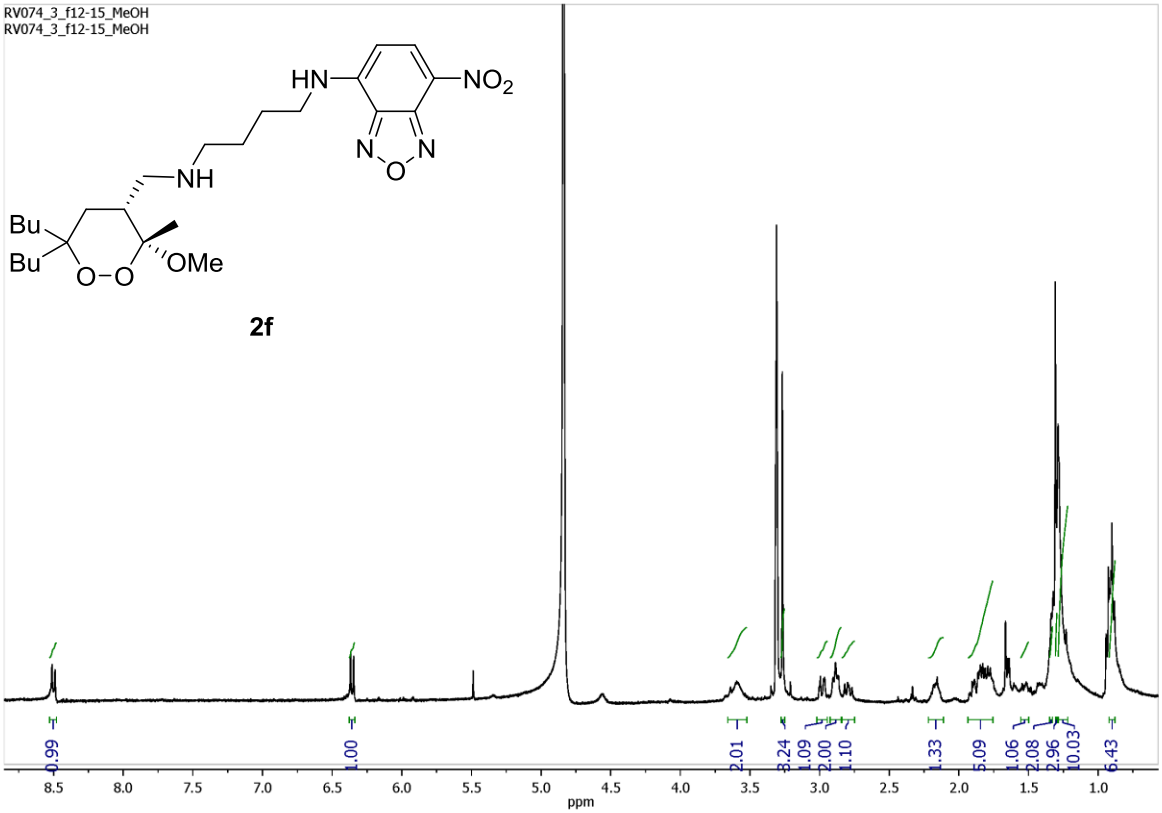
RV074_3_f12-15_MeOH
RV074_3_f12-15_MeOH
HN
NO2
N
O
N
NH
Bu
Bu
O
O
OMe
2f
0.99
1.00
2.01
3.24
1.09
2.00
1.10
1.33
5.09
1.06
2.08
2.96
10.03
6.43
ppm

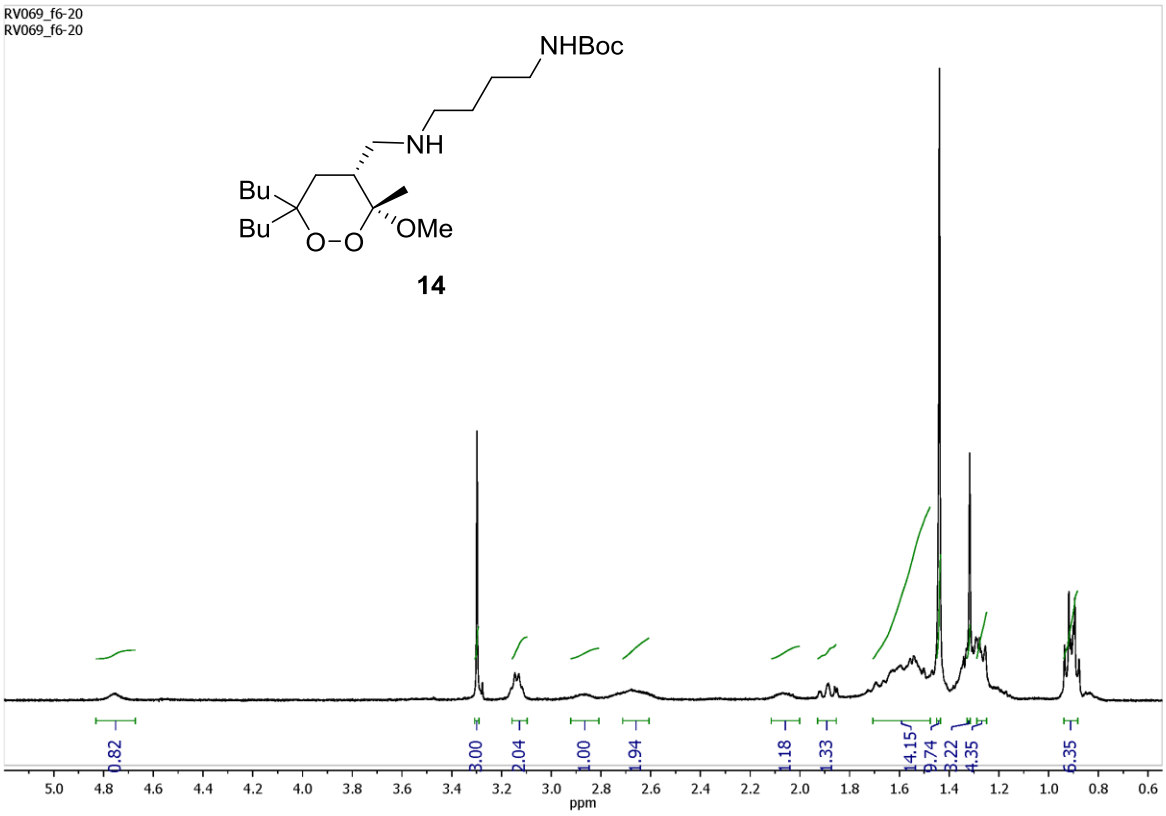
RV069_f6-20
RV069_f6-20
NHBoc
NH
Bu
Bu
O–O
OMe
14
0.82
3.00
2.04
1.00
1.94
1.18
1.33
14.15
9.74
3.22
4.35
6.35
ppm

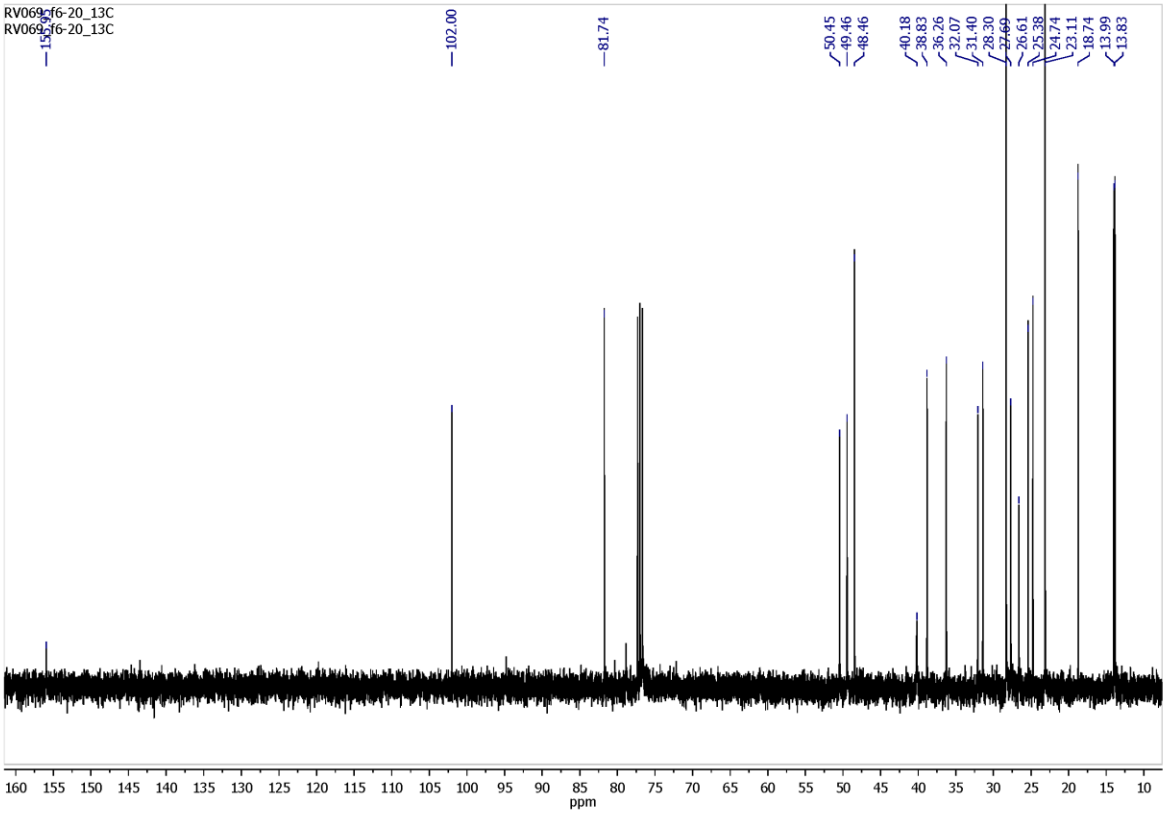
RV069_f6-20_13C
RV069_f6-20_13C
102.00
81.74
50.45
49.46
48.46
40.18
38.83
36.26
32.07
31.40
28.30
27.69
26.61
25.38
24.74
23.11
18.74
13.99
13.83
ppm

HPLC analyses

Compound **3a** (*method B*):

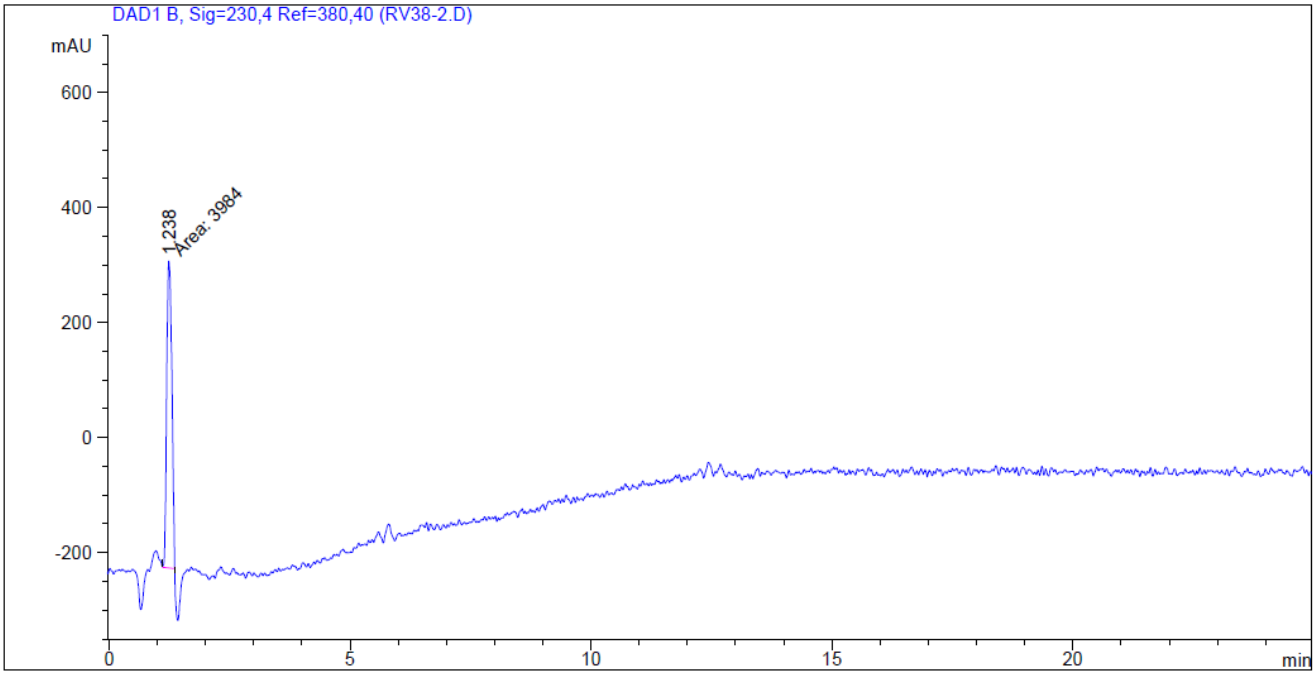


```
=====================================================================
                      Area Percent Report
=====================================================================

Sorted By             :      Signal
Multiplier            :      1.0000
Dilution              :      1.0000
Use Multiplier & Dilution Factor with ISTDs


Signal 1: DAD1 B, Sig=230,4 Ref=380,40

Peak RetTime Type  Width     Area      Height     Area
  #   [min]        [min]   [mAU*s]     [mAU]       %
----|-------|----|-------|----------|----------|--------|
   1   1.238 MM    0.1240 3983.99561  535.34558 100.0000
```

Compound **3b** (*method A*):

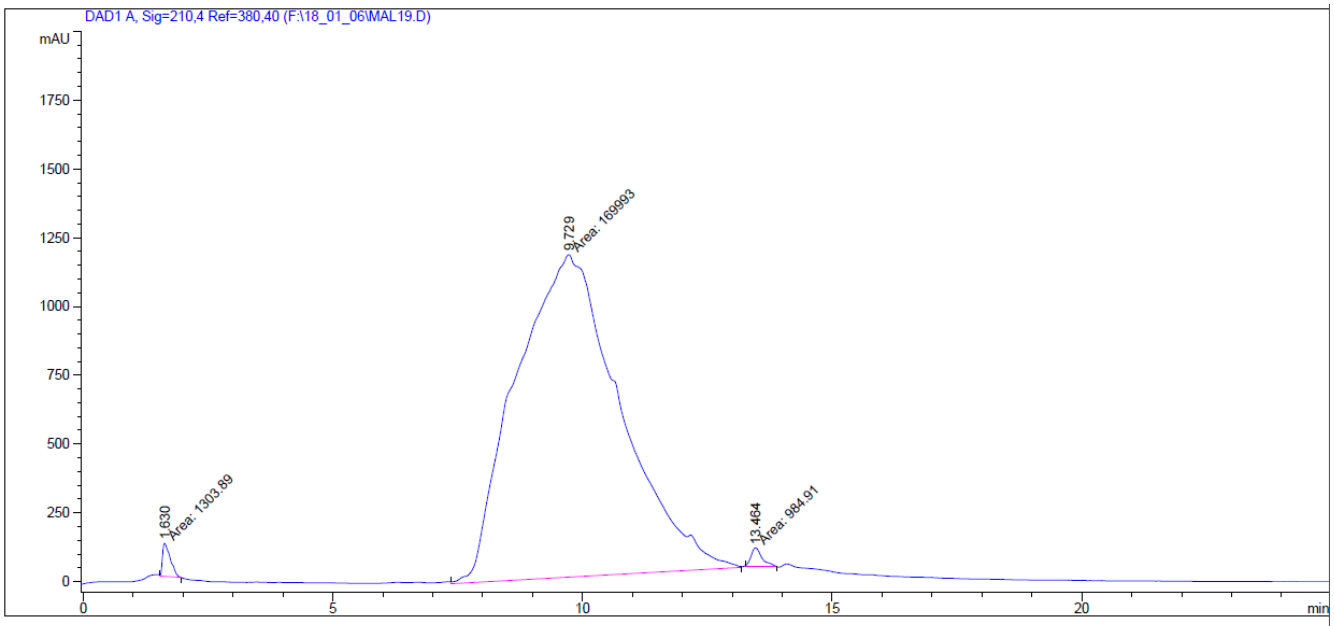


```
=====================================================================
                      Area Percent Report
=====================================================================

Sorted By             :      Signal
Multiplier            :      1.0000
Dilution              :      1.0000
Use Multiplier & Dilution Factor with ISTDs


Signal 1: DAD1 A, Sig=210,4 Ref=380,40

Peak RetTime Type  Width     Area      Height     Area
  #   [min]        [min]   [mAU*s]     [mAU]       %
----|-------|----|-------|----------|----------|--------|
   1   1.630 MM    0.1802 1303.88806  120.57082   0.7568
   2   9.729 MM    2.4164 1.69993e5  1172.46887  98.6715
   3  13.464 MM    0.2480  984.91028   66.19936   0.5717
```

Compound **3c** (*method B*):

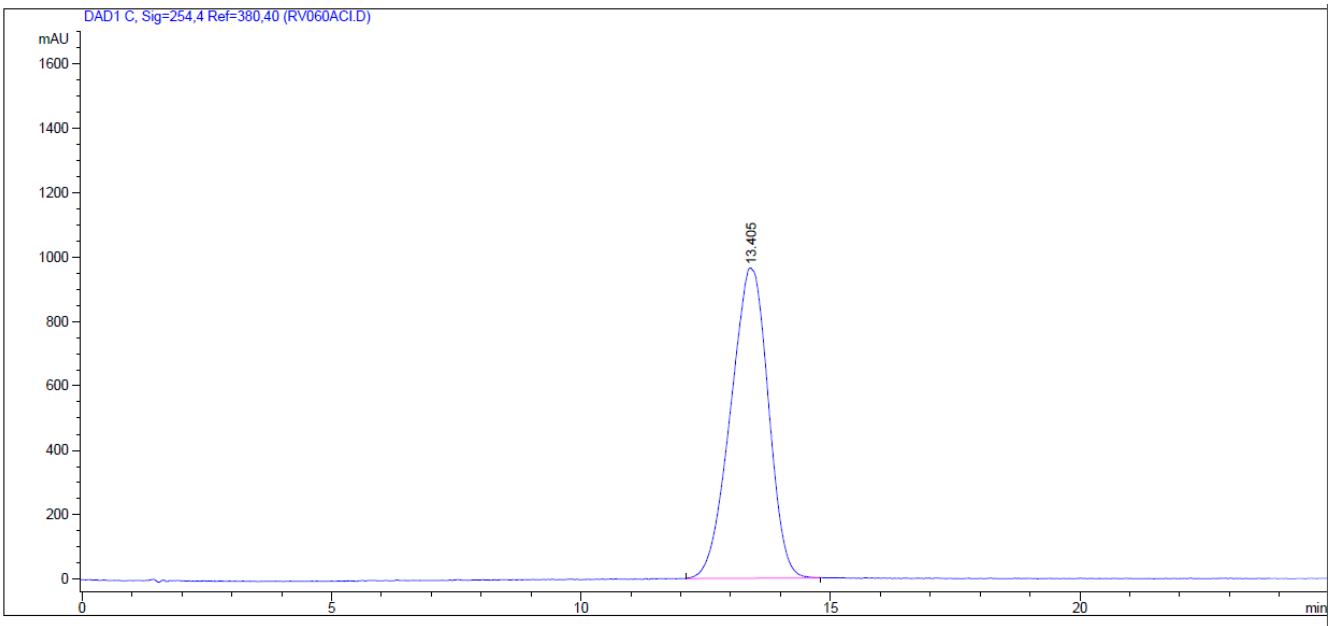


```
=====================================================================
                      Area Percent Report
=====================================================================

Sorted By             :      Signal
Multiplier            :      1.0000
Dilution              :      1.0000
Use Multiplier & Dilution Factor with ISTDs


Signal 1: DAD1 C, Sig=254,4 Ref=380,40

Peak RetTime Type  Width     Area      Height     Area
  #   [min]        [min]   [mAU*s]     [mAU]       %
----|-------|----|-------|----------|----------|--------|
   1  13.405 BB    0.6263 5.05425e4   963.09241 100.0000
```

Compound **3d** (*method B*):

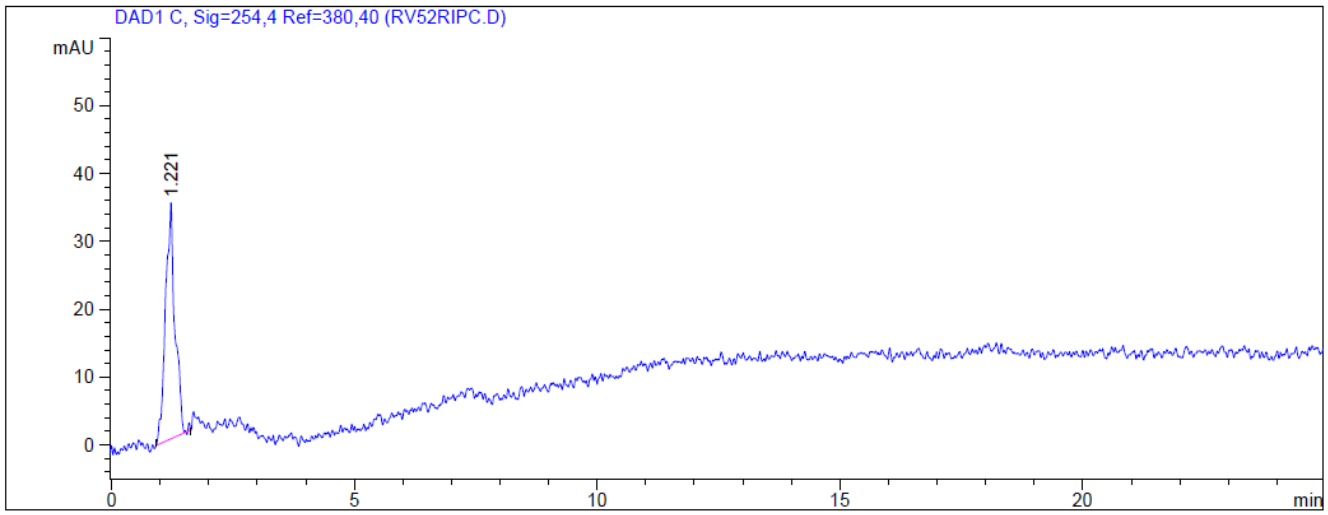


```
=====================================================================
                      Area Percent Report
=====================================================================

Sorted By             :      Signal
Multiplier            :      1.0000
Dilution              :      1.0000
Use Multiplier & Dilution Factor with ISTDs


Signal 1: DAD1 C, Sig=254,4 Ref=380,40

Peak RetTime Type  Width     Area      Height     Area
  #   [min]        [min]   [mAU*s]     [mAU]       %
----|-------|----|-------|----------|----------|--------|
   1   1.221 PB    0.1721  472.37149   34.84964 100.0000
```

Compound **3e** (*method A*):

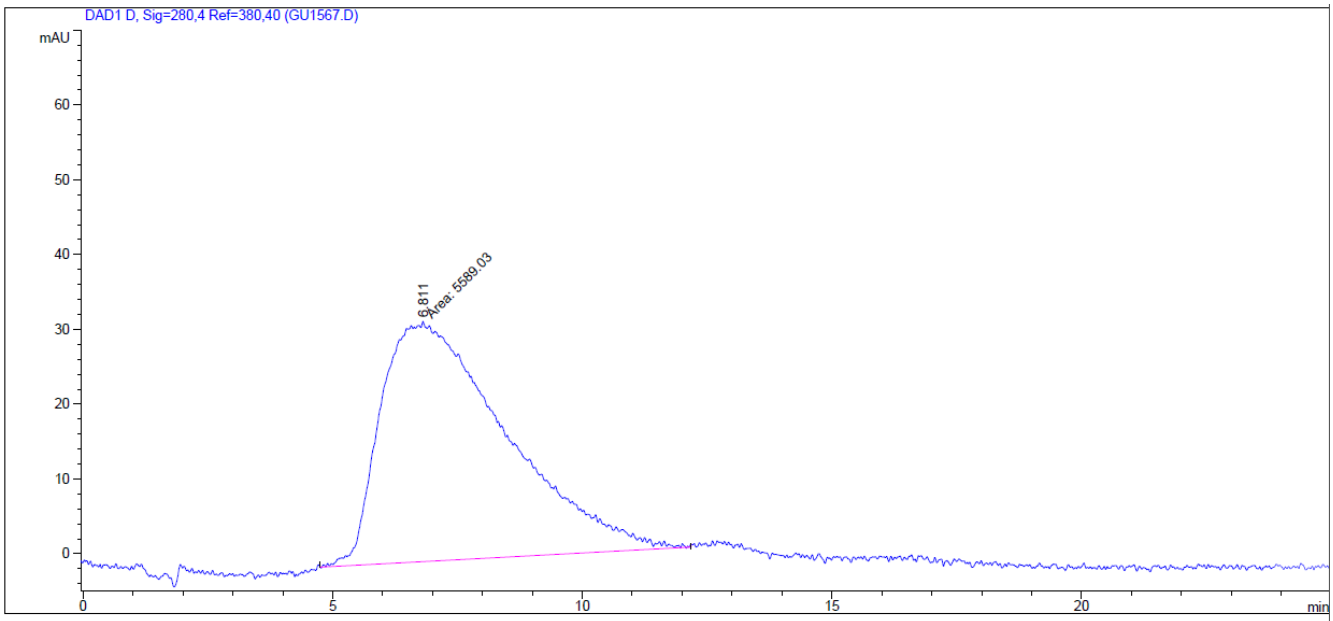


```
=====================================================================
                      Area Percent Report
=====================================================================

Sorted By             :      Signal
Multiplier            :      1.0000
Dilution              :      1.0000
Use Multiplier & Dilution Factor with ISTDs


Signal 1: DAD1 D, Sig=280,4 Ref=380,40

Peak RetTime Type  Width     Area      Height     Area
  #   [min]        [min]   [mAU*s]     [mAU]       %
----|-------|----|-------|----------|----------|--------|
   1   6.811 MM    2.8949 5589.02539   32.17752 100.0000
```

Compound **2e** (*method B*):

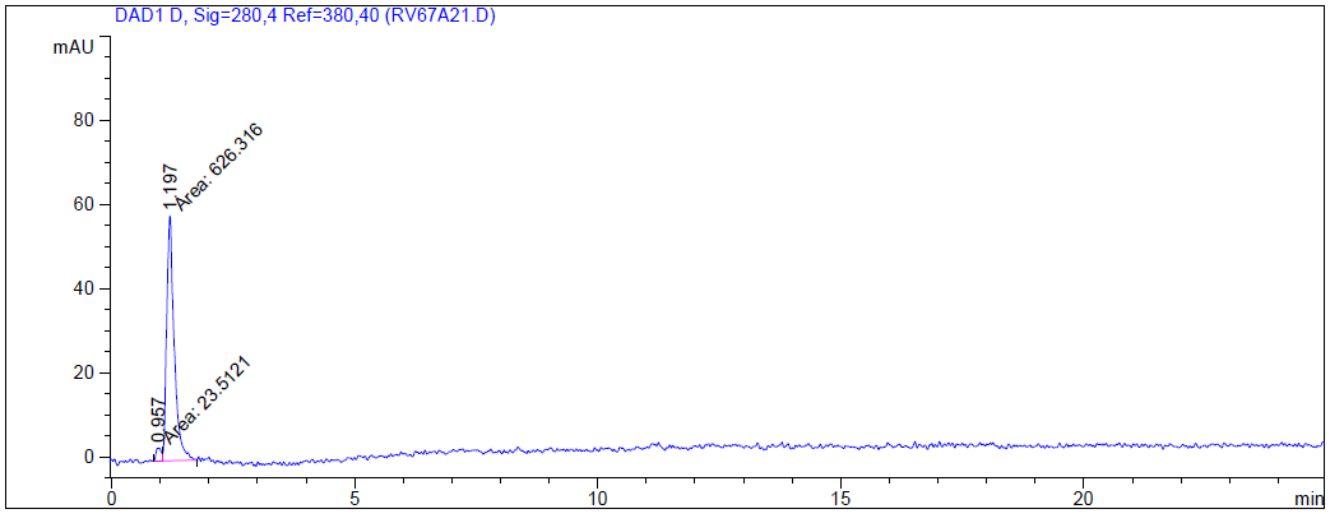


```
=====================================================================
                      Area Percent Report
=====================================================================

Sorted By             :      Signal
Multiplier            :      1.0000
Dilution              :      1.0000
Use Multiplier & Dilution Factor with ISTDs


Signal 1: DAD1 D, Sig=280,4 Ref=380,40

Peak RetTime Type  Width     Area      Height     Area
  #   [min]        [min]   [mAU*s]     [mAU]       %
----|-------|----|-------|----------|----------|--------|
   1   0.957 MF    0.1273   23.51208    3.07771   3.6182
   2   1.197 FM    0.1788  626.31610   58.39663  96.3818
```

Compound **2f** (*method B*):

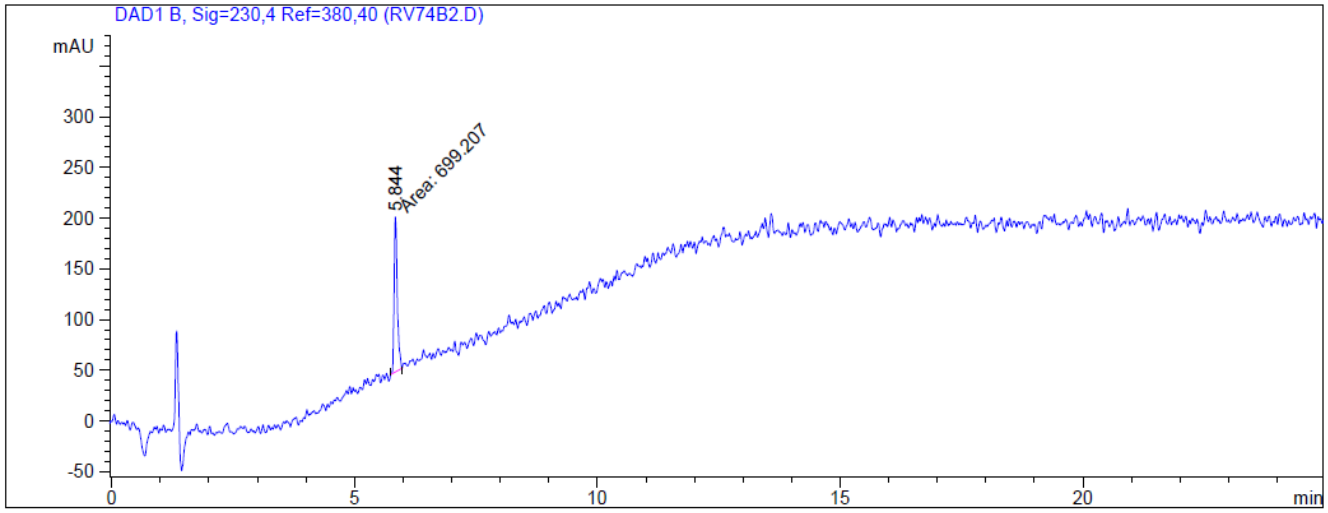


```
=====================================================================
                      Area Percent Report
=====================================================================

Sorted By             :      Signal
Multiplier            :      1.0000
Dilution              :      1.0000
Use Multiplier & Dilution Factor with ISTDs


Signal 1: DAD1 B, Sig=230,4 Ref=380,40

Peak RetTime Type  Width     Area      Height     Area
  #   [min]        [min]   [mAU*s]     [mAU]       %
----|-------|----|-------|----------|----------|--------|
   1   5.844 MM    0.0761  699.20667  153.15910 100.0000
```

References

(1) SMART & SAINT Software Reference Manuals, version 5.051 (Windows NT Version); Bruker Analytical X-ray Instruments Inc.: Madison, WI, **1998**.

(2) Sheldrick, G. M. *SADABS-2008/1 - Bruker AXS Area Detector Scaling and Absorption Correction*, Bruker AXS: Madison, Wisconsin, USA, 2008.

(3) Burla, M. C.; Caliandro, R.; Carrozzini, B.; Cascarano, G. L.; Cuocci, C.; Giacovazzo, C.; Mallamo, M.; Mazzone, A.; Polidori, G. *J. Appl. Cryst.* **2015**, *48*, 306-309.

(4) Sheldrick, G. M. *Acta Cryst C71***,** 2015, 3-8.

(5) Macrae, C. F.; Bruno, I. J.; Chisholm, J. A.; Edgington, P. R.; McCabe, P.; Pidcock, E.; Rodriguez-Monge, L.; Taylor, R.; van de Streek, J.; Wood, P. A. *J. Appl. Cryst.*, **2008**, *41*, 466-470.